電解重合導電性高分子の機能発現と高密度二次電池への応用

Function Creation of Electropolymerized Conductive Polymers and Their Application to High Energy Density Rechargeable Batteries

（０３６５０６６４）

平成３年度科学研究費補助金（一般研究Ｃ）研究成果報告

平成５年３月

研究代表者　　逢坂　哲彌
（早稲田大学理工学部応用化学科）

はしがき

本研究は導電性高分子薄膜を電解重合法で合成し、その膜自身の機能を発現させ、その機能発現評価を行うことを目的とし、特に高密度二次電池材料への応用を検討している。

（１）小型、高エネルギー密度リチウム二次電池のカソード電極材料として利用するためには、導電性高分子へのイオンのドーピング現象を利用するが、これらの材料は、リチウムアノードとの組み合せにより、３Ｖ級の高エネルギー密度電池として働くことが示されている。電極材料としてはポリアニリン／ポリピロール（ＰＰｙ）ポリマーを用いて両者の特徴を生かした積層カソードを作製し電池特性を評価して特徴ある機能材料化の可能性を明らかにしている。さらに、電解質として固体の高分子電解質ＰＥＯ（ポリエチレンオキシド）－$LiClO_4$型電解質を用いて全固体型リチウム／ポリピロール二次電池を試作し、その特性として溶液型のものと同等の特性を示すことを明らかにした。従って、全固体型はその薄膜化の可能性大なることから、今後薄膜化により、より高エネルギー密度の電池作製の可能性を示している。さらに、カソードとしてはＰＰｙ／ＰＳＳ（ポリスチレンスルフォネート）複合薄膜を作製し、Li^+が電荷を担うｎ型カソードポリマーが非水溶液中でリチウム二次電池カソードに利用できることを明らかにした。

（２）電解重合導電性高分子をそれ自身の導電性ではなく、絶縁性膜としての可能性を考え、液晶駆動用非線形型素子としてのＭＩＭ（メタル・インシュレータ・メタル）素子作製を試みた。特にこの応用のためには前者（１）の場合とは異なり、導電性が低く、ほとんど絶縁膜が得られる膜作製条件を探求し、ＮａＯＨ、$NaHCO_3$、Na_2CO_3等のアルカリ性溶液からポリピロール膜を重合すると、初期の膜作製後直ちに膜自身が不導体化してある厚さ（例えば０．２μm）までの成長で膜厚が停止する絶縁膜が作製できることを明らかにした。この膜はＭＩＭ素子として良好な対称的非線形スイッチング素子として働き、液晶素子を駆動させることを明らかにした。また、その時の非線形応答メカニズムはプールフレンケル機構によることを明らかにした。

（３）すでに（２）項において絶縁性膜が電解重合法で出来ＭＩＭ素子として働くことを明らかにしたが、このＭＩＭ素子構造を利用して絶縁部に微量溶液を滴下しうる極微小センサーの作製を試みた結果、絶縁性ポリピロール膜がOH^-イオンのみに応答することを明らかにし、ＭＩＭ素子と同じく金属電極部に電圧印加することによりアンペロメトリックな微小ｐＨセンサーが作製できることを明らかにした。

本報告書は，平成３年度および平成４年度文部省科学研究費補助金（一般研究Ｃ）の援助によって行われた研究の成果を述べたものである。

本研究の大部分は、すでに学会等において論文もしくは口頭発表で発表されているが、本報告書によりその全体像を把握され、関連分野の研究の資として頂ければ幸いである。

研究組織

研究代表者　：　逢坂　哲彌　　（早稲田大学理工学部教授）

研究分担者　：　中村　節子　　（日本女子大学理学部教授）

研究経費

平成　3年度	1，300千円
平成　4年度	600千円
計	1，900千円

学会誌等

1. Rechargeable Lithium/Polymer Cathode Batteries-Application of Electropolymerized Polymer Films to Lithium Batteries-.
T.Osaka, K.Shiota, T.Momma, Proc. of Third International Conference Batteries for Utility Energy Storage, P479 (1991).

2. Electroactive Polyaniline Film Deposited from Nonaqueous Media III. Effect of Mixed Organic Solvent on Polyaniline Deposition and Its Battery Performance.
T.Osaka, T.Nakajima, K.Shiota, T.Momma, J. Electrochem. Soc., 138, No.10, 2853 (1991).

3. Electropolymerization of Electroinactive Polypyrrole Film for a Nonlinear MIM Switching Device.
T.Osaka, T.Fukuda, K.Ouchi, T.Nakajima, Denki Kagaku, 59, No.12, 1019 (1991).

4. LCD Driving Characteristics of MIM Diode Using Electropolymerized Polypyrrole Thin Film as an Insulator.
T.Nakajima, F.Matsushima, T.Fukuda, T.Osaka, Denki Kagaku, 59, No.12, 1074 (1991).

5. ポリマー二次電池とその基礎特性評価法.
逢坂哲彌, 門間聰之, 電気化学, 60, No5, 369 (1992).

6. Electrochemical Aspects of Advanced Electronic Materials.
T.Osaka, Electrochimica Acta, vol.37, No.6, 989-995 (1992).

7. Conduction Mechanism in Indium Tin Oxide/Electroinactive Polypyrrole/ Indium Tin Oxide Sandwitch Structures.
T.Osaka, T.Fukuda, K.Ouchi, T.Momma, Thin Solid Films, 215, 200-202 (1992).

8. Electroactivity Change of Electropolymerized Polypyrrole/Polystyrenesulfonate Composite Film in Some Organic Electrolytes.
T.Osaka, T.Momma, K.Nishimura, Chem. Lett., 1992, 1787-1790 (1992).

9. Application of electroinactive polypyrrole film to the pH sensor electrode.
T.Osaka, T.Fukuda, H.Kanagawa, T.Momma, S.Yamauchi, Sensors and Actuators B, in press.

10. Electropolymerization Conditions for Producing Insulator Polypyrrole Films.
T.Osaka, T.Momma, H.Kanagawa, Chem. Lett., in press.

講　演　発　表

1. Rechargeable Lithium/Polymer Cathode Batteries-Application of Electropolymerized Polymer Films to Lithium Batteries.
T.Osaka, K.Shiota, T.Momma, Proc. of Third International Conference Batteries for Utility Energy Storage, P479, Kobe, (1991.3.20).

2. 二次電池正極材料を目的としたポリアニリン／ポリピロール積層膜の下地層の効果.
逢坂哲彌，塩田晃，門間聰之，中野多恵子，電気化学協会第58回大会講演要旨集，P154，野田，(1991.4.6).

3. 電解重合PPy/PSS 複合膜のPC電解液中における電気化学的挙動.
逢坂哲彌，門間聰之，西村賢，電気化学協会第58回大会講演要旨集，P156，野田，(1991.4.6).

4. MIM 素子への応用を目的とした電気化学的不活性ポリピロールの電解重合.
逢坂哲彌，大内潔，福田俊広，尾池啓子，中島俊貴，
電気化学協会第58回大会講演要旨集，P33，野田，(1991.4.7).

5. Electrochemical Aspects for Advanced Electronic Materials.
T.Osaka, International Society of Electrochemistry 42nd Meeting, KL2-1, Montreux, Switzerland (1991.8.26).

6. Application of Polyaniline/Polypyrrole Dual-Layer to Lithium Secondary Battery.
T.Osaka, K.Shiota, T.Momma, S.Nakamura,
International Society of Electrochemistry 42nd Meeting Abstracts, P3-52, Montreux, Switzerland (1991.8.27).

7. PC-DME系電解液中におけるLi電析形態II.
逢坂哲彌，門間聰之，西村賢，田鳴尚之，大崎隆久，高見則雄，
第32回電池討論会講演要旨集，P231，京都，(1991.9.19).

8. 電解重合ポリピロール／ポリスチレンスルフォネート複合膜のリチウム二次電池正極材料への応用.
逢坂哲彌，門間聰之，西村賢，近藤奈穂子，中村節子，
1991年電気化学協会電気化学秋季大会講演要旨集，P130，名古屋，(1991.10.13).

9. 電解重合ポリピロールの電気化学的活性度とMIM非線形素子への応用.
逢坂哲彌，福田俊広，金川姫子，杉山規子.
日本化学会第６３春期年会講演予稿集Ｉ，ｐ１０１０，大阪(1992.3.31)．

10. 電解重合ポリピロール／ポリスチレンスルフォネート複合膜の交流インピーダンス法による評価.
逢坂哲彌，門間聰之，西村賢，田嶋尚之，近藤奈穂子，中村節子.
電気化学協会第５９回大会講演要旨集，ｐ１５１，八王子(1992.4.4.).

11. Electrochemical Thin Film Formation for Advanced Electronic Materials.
T.Osaka, T.Homma, Abstracts of The First West Pacific Electrochemistry Symposium, P.21, Tokyo, Japan (May.25.1992).

12. In-Situ Photothermal Spectroscopy Method for Investigating the Surface Change of Electrode.
Z.Jiang, Y. Xiang, B.Qiau, C.Jin, T.Osaka, Abstracts of The First West Pacific Electrochemistry Symposium, P.111, Tokyo, Japan (May.26.1992).

13. Preparation of Electropolymerized Conducting Polymers for Rechargeable Lithium Battery Cathodes.
K.Nishimura, T.Momma, T.Osaka, Abstracts of The First West Pacific Electrochemistry Symposium, P.353, Tokyo, Japan (May.27.1992).

14. Impedance Analysis of Electropolymerized Conducting Polymers for Polymer Battery Cathodes.
T.Osaka, T.Momma, Extended Abstracts of Second International Symposium on Electrochemical Impedance Spectroscopy, Santa Barbara, U.S.A. (June.15.1992).

15. Application of Electroinactive Polypyrrole Film to the pH Sensor Electrode.
T.Osaka, T.Fukuda, H.Kanagawa, S.Yamauchi, Technical Digest of the Fourth International Meeting on Chemical Sensors, P.244, Tokyo, Japan (Sept.15.1992).

16. 高分子固体電解質を利用したLi/ポリピロール二次電池.
逢坂哲彌，門間聰之，西村賢，田嶋尚之，角田聡子，第３３回電池討論会講演要旨集，P.67，東京(1992.9.16).

17. 電解重合ppy/pss複合膜の酸化還元挙動とそのリチウム二次電池正極としての可能性.
逢坂哲彌，門間聰之，西村賢，田鳴尚之，臼居亜美，中村節子，第３３回電池討論会講演要旨集，P.69，東京(1992.9.16).

18. ＰＣ電解液中におけるLi負極の充放電特性に及ぼす電流密度の影響.
逢坂哲彌，門間聰之，西村賢，田鳴尚之，丹羽大也，高見則雄，大崎隆久，第３３回電池討論会講演要旨集,p.215，東京(1992.9.18).

19. Preparation and Evaluation of Electropolymerized Polymers for Lithium Battery.
T.Osaka, T.Momma, 43rd Meeting of International Society of Electrochemistry, Abst.p.115, Cordoba, Argentina (Sept.24.1992).

出版物

1. 電池便覧：〔執筆〕ポリマー電池 P.378　電池便覧編集委員会編，丸善，1990．8

2. 標準化学用語辞典：〔執筆〕，日本化学会編，丸善，1991.3

3. 湿式法を利用したエレクトロニクス高機能薄膜作成法：〔編集、執筆〕
   広信社，1992.10

Third International Conference

Batteries for Utility Energy Storage

NEDO
EPRI
BEWAG

PROCEEDINGS

March 18-22, 1991
Kobe, Japan
International Conference Center Kobe

Hosted by
New Energy and Industrial Technology
Development Organization
(NEDO)

RECHARGEABLE LITHIUM/POLYMER CATHODE BATTERIES - APPLICATION OF ELECTROPOLYMERIZED POLYMER FILMS TO LITHIUM BATTERIES -

Tetsuya OSAKA, Koh SHIOTA and Toshiyuki MOMMA

Department of Applied Chemistry,
School of Science and Engineering,
Waseda University,
Okubo, Shinjuku-ku, Tokyo 169, Japan

Abstract

Electropolymerized conducting polymers have been investigated for an application to a cathode material of Li secondary batteries for a load conditioner use, which have high energy density and flexibility of cell design. Properties of these polymers, polypyrrole, polyaniline, polyazulene and so on, are controlled via the select of electropolymerization conditions such as deposition potential, supporting electrolyte and solvent in the polymerization solutions in order to advance the properties of Li/polymer batteries. Moreover, conducting polymers doped with various polymer anions or redox systems are used for a cathode material for increase in capacity of Li secondary cells. We not only overview rechargeable Li/polymer batteries but also clarify the relationship between the properties of Li/polymer cathode batteries and the electropolymerization conditions of these polymers relating to the film properties.

INTRODUCTION

Lithium/polymer cathode batteries, having high energy density and flexibility of cell design, are one of the candidate for high energy load conditioner. Among electropolymerized conducting polymers, polyaniline(PAn), polypyrrole(PPy) and polyazulene (PAz) can be utilized as one of the promising candidates for cathode materials in future rechargeable lithium cell systems(1,2). The model of new secondary batteries utilizing electrochemically-formed conducting PPy is recently examined to gain a better understanding of such new batteries(3), and possibility and limit of the cell performance of polymer cathode systems are theoretically indicated(4). Many researchers have paid an attention to polyaniline as a cathode material of lithium batteries, because of its high reversibility of doping-undoping process, high energy density and also high power density. The Bridgestone Corp. and the Seiko Instrument Inc. group realized the coin type battery utilizing an electropolymerized PAn as the cathode material(5) although the cell capacity is small. The Li/n-type polyacene battery was proposed by CRIEPI and Kanebo Corp. as one of the higher energy density load conditioner(6). Ricoh Co. Ltd. and Sanyo Chem. Ltd. group presented all solid "card type" lithium/polyaniline battery(7).

Recently, in order to increase in battery capacity and energy density, conducting polymer films composited with various redox systems, *e.g.* anthraquinone-1-sulfonate, WO_3 and MnO_2, were investigated for the application to a cathode material of rechargeable Li/polymer batteries(8).

LITHIUM/POLYMER BATTERIES

The battery systems using polymers are schematically given in Fig. 1. Li/p-type polymer cell, as is seen in Fig. 1a), is the most common system because there are a lot of p-type conducting polymers. The system has a demerit to need larger electrolyte volume because of decrease in the concentration of supporting electrolyte during charge process. The system of Li/n-type polymer, however, can avoid this disadvantage because only Li^+ ion moves during charge-discharge process seen in Fig. 1b). Unfortunately, there are very little kinds of n-type polymer, but another combination such as p-type polymer with polymer anion works as the same behavior as shown in Fig. 1d). For example, the compos-

ite membrane of PPy with PSS^- (polystyrenesulfonate) has been examined, where only cation is the moving ion in appearance(9).

The candidates of cathode materials for rechargeable Li batteries at ambient temperature are inorganic intercalation compounds as well as organic conducting polymers. Figure 2 shows the battery capacities of representative lithium secondary batteries, where the possibility of Li/polymer battery is indicated. The capacity using polymer is inferior to that using inorganic compounds, however, the energy density becomes relatively higher because of its higher output voltage. Also, the polymer has higher power density because of its rapid kinetics of doping-undoping reaction. The most advantage of polymer batteries is that Li/polymer batteries have flexible form-free feature, as shown in Table 1, as well as higher voltage. Some demerits are also listed in Table 1.

Some samples of prototype or more advanced type batteries are shown in Fig. 3, where the coin type with PAn cathode is commercially available. The prototype of "cylinder type" has ca. 50 Wh kg^{-1} energy density per cell, and the prototype of "card type" has energy density per cell of 21Wh/l or 8.9Wh/kg(7). The most possible candidates of polymer cathode materials are listed in Fig. 4, and the feature of PAn and PPy films as the most possible materials, which are used in Fig. 3, is shown in Table 2. PAn film has high doping level to keep larger capacity, while the PPy film has stronger mechanical strength.

Polyacene semiconductor (PAS) has been investigated to application to a cathode material for lithium secondary battery for load conditioner use, because Li/PAS cell has the advantages of having substantial buffer capacity above and below the normal cutoff voltages(6). Table 3 shows a comparison of the battery performance between Li/PAS cell and other Li secondary batteries.

PPy(POLYPYRROLE) CATHODES

[1] ANION EFFECT OF PPy PREPARATION

Film properties of PPy are strongly dependent on the species of electrolyte anions in the polymerization solution, and they can be controlled by varying the anions at PPy polymerization(10). Figure 5 shows the relationship between the doping charge of ClO_4^- anion at the conditions of $LiClO_4$-PC (propylene carbonate) solution and the polymerization potential for PPy films formed with ClO_4^-, $CF_3SO_3^-$ or PF_6^- anions as a function of deposition charge.

When polymerizing with PF_6^- or $CF_3SO_3^-$ anion, the PPy films become to give higher doping charge of ClO_4^- dopant as is seen in Fig. 5. Battery performance of $Li/LiClO_4$-PC/PPy is given in Fig. 6. The battery assembled with the PPy cathode formed with PF_6^- keeps 100% coulombic yield up to the current density of 2.5 mA cm^{-2} at 20% doping charge level.

[2] PPy MORPHOLOGY MODIFICATION WITH NBR(NITRILE BUTADIENE RUBBER)

PPy preparation with the host polymer of NBR insulating film can make the structure rougher for accelerating anion diffusion in the film(11). A schematic image for the preparation procedure of NBR-aided grown PPy electrode (Pt/NBR/PPy) is illustrated in Fig. 7. A Pt substrate was first coated with a commercially available NBR host polymer and dried completely. The Pt electrode precoated with NBR was then immersed in the same polymerization solution used for the preparation of the Pt/PPy electrode. Thereafter, also on the Pt/NBR electrode, PPy was grown at 0.8V *vs.* Ag/Ag^+. After PPy was formed by passing 1 C cm^{-2}, the host polymer of NBR film was totally washed away with MEK (methylethylketone) and subsequently dried. By the SEM observation of the films, the NBR-aided grown PPy film becomes more porous and rougher conditions than those of PPy film directly grown on Pt electrode. The battery performance of $Li/LiClO_4$-PC/PPy grown with NBR is shown in Fig. 8. The battery performance is observed to be very much enhanced with regard to both charge-discharge current density and charge capacity, especially the current density becomes three times larger at low doping level(12).

PAn(POLYANILINE) CATHODES

An electroactive PAn film was successfully obtained by electropolymerization from non-aqueous solution of propylene carbonate(PC) containing CF_3COOH and $LiClO_4$(13). The battery performance of lithium battery using PAn film deposited from PC solution was similar to that of the cell using PAn cathode deposited from aqueous solution, as is seen in Fig. 9. The most important factor to form electroactive PAn film is proton from an organic acid and its acidity strongly affects the activity and reversibility of anion doping-undoping process. The effect of acid content at the polymerization was clearly given and the PAn film formed with

the conditions of 4:1 ratio (acid:aniline) finally gave the excellent battery performance as seen in Fig. 10(14).

PPy/PSS⁻(POLYSTYRENESULFONATE) CATHODES

Electroactive PPy/PSS⁻ composite films electropolymerized from aqueous solutions containing pyrrole and poly(sodium styrenesulfonate)(PSSNa) had a good electroactivity in organic solution, *e.g.* dimetylsulfoxide(DMSO), as in aqueous solution(15). These composite films can be used as a pseudo-cathodic doping material for a cathode of rechargeable lithium battery. The optimum of electropolymerization conditions was that the film was polymerized at 0.625V *vs.* Ag/AgCl and in solution of 0.25 mol dm^{-3} pyrrole and 0.5N PSSNa. Figure 11a) shows a charge-discharge curve of $Li/LiClO_4$-DMSO/(PPy/PSS⁻) cells and Fig. 11b) shows an effect of charge-discharge current density on coulombic yield. As is seen in Fig. 11b), Li/(PPy/PSS⁻) cells show higher coulombic yield at high charge-discharge current density region than Li/PPy cells, probably because cation is undoped and doped into PPy/PSS⁻ films with oxidation and reduction of PPy films.

CONCLUSION

The most advantage of Li/polymer batteries is form-free feature, moreover, the some disadvantages can be overcome by morphology control or development of morphology at preparation process as is discussed in the text. The control of morphology gives the higher current density and also an increase of energy density per cathode materials.

As for future targets, the following three are the most attractive items to be developed in future in the field of Li/polymer batteries.

*R&D for solid polymer electrolyte with higher conductivity.
*R&D for p-type polymer with polymer anion.
*R&D for new material of n-type polymer.

REFERENCES

1. T.Osaka, T.Nakajima, K.Shiota and B.B.Owens, *Ext. Abst. of the 176th ECS Meeting (Hollywood, Florida)*, 89-2, Abst. No.61 (1989); *Proc. of Symp. on Rechargeable Lithium Batteries*, S.Subbarao, V.R.Koch, B.B.Owens and W.H.Smyrl, ed by, p.170, Electrochem. Soc. Inc., NJ (1990).
2. T.Osaka and K.Ueyama, *Kagaku-Kogyo (Chemical Industry)*, March Issue, p.31 (1989).
3. T.Yeu and R.E.White, *J. Electrochem. Soc.*, 137, 1327 (1990).
4. K.Naoi, B.B.Owens and W.H.Smyrl, *Ext. Abst. of the 176th ECS Meeting (Hollywood, Florida)*, 89-2, Abst. No.63 (1989); *Proc. of Symp. on Rechargeable Lithium Batteries*, S.Subbarao, V.R.Koch, B.B.Owens and W.H.Smyrl, ed by, p.170, Electrochem. Soc. Inc., NJ (1990).
5. M.Ogawa, T.Fuse, T.Kida, T.Kawagoe and T.Matsunaga, *Proc. of the 27th Battery Symp. Jpn.*, p.197 (1986).
6. K.Ishihara, T.Iwahori, T.Tanaka, S.Yata, H.Kinoshita and M.Komori, *Proc. of the 31st Battery Symp. Jpn.*, p.29 (1990).
7. T.Kabata, O.Kimura, S.Yoneyama, T.Ohsawa and T.Samura, *ibid.*, p.37 (1990).
8. S.Kuwabata, Y.Ii and H.Yoneyama, *ibid.*, p.5 (1990); S.Hirao, S.Kuwabata and H.Yoneyama, *ibid.*, p.7 (1990); A.Kishimoto, S.Kuwabata and H.Yoneyama, *ibid.*, p.9 (1990).
9. T.Iyoda, A.Ohtani, T.Shimizu and K.Honda, *Synthetic Metals*, 18, 747 (1987).
10. T.Osaka, K.Naoi and S.Ogano, *J. Electrochem. Soc.*, 135, 1071 (1988).
11. K.Naoi and T.Osaka, *J. Electrochem. Soc.*, 134, 2479 (1987).
12. T.Osaka and K.Ueyama, *"Practical Lithium Batteries"*, p.114, JES Press, Ohio (1987).
13. T.Osaka, S.Ogano, K.Naoi and N.Oyama, *J. Electrochem. Soc.*, 136, 306 (1989).
14. T.Osaka, T.Nakajima, K.Naoi and B.B.Owens, *J. Electrochem. Soc.*, 137, 2139 (1990).
15. T.Osaka, K.Shiota, T.Momma and K.Nishimura, *Proc. of the 31st Battery Symp. Jpn.*, p.27 (1990).

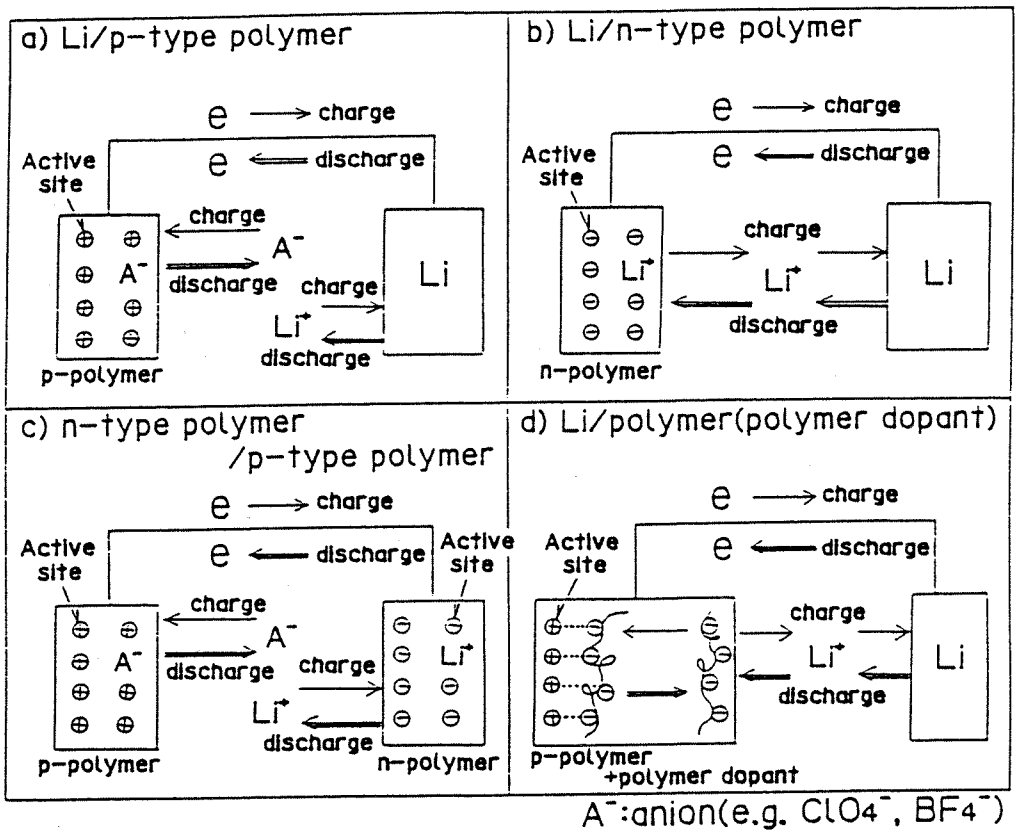

Fig.1 Various types of lithium/polymer batteries.

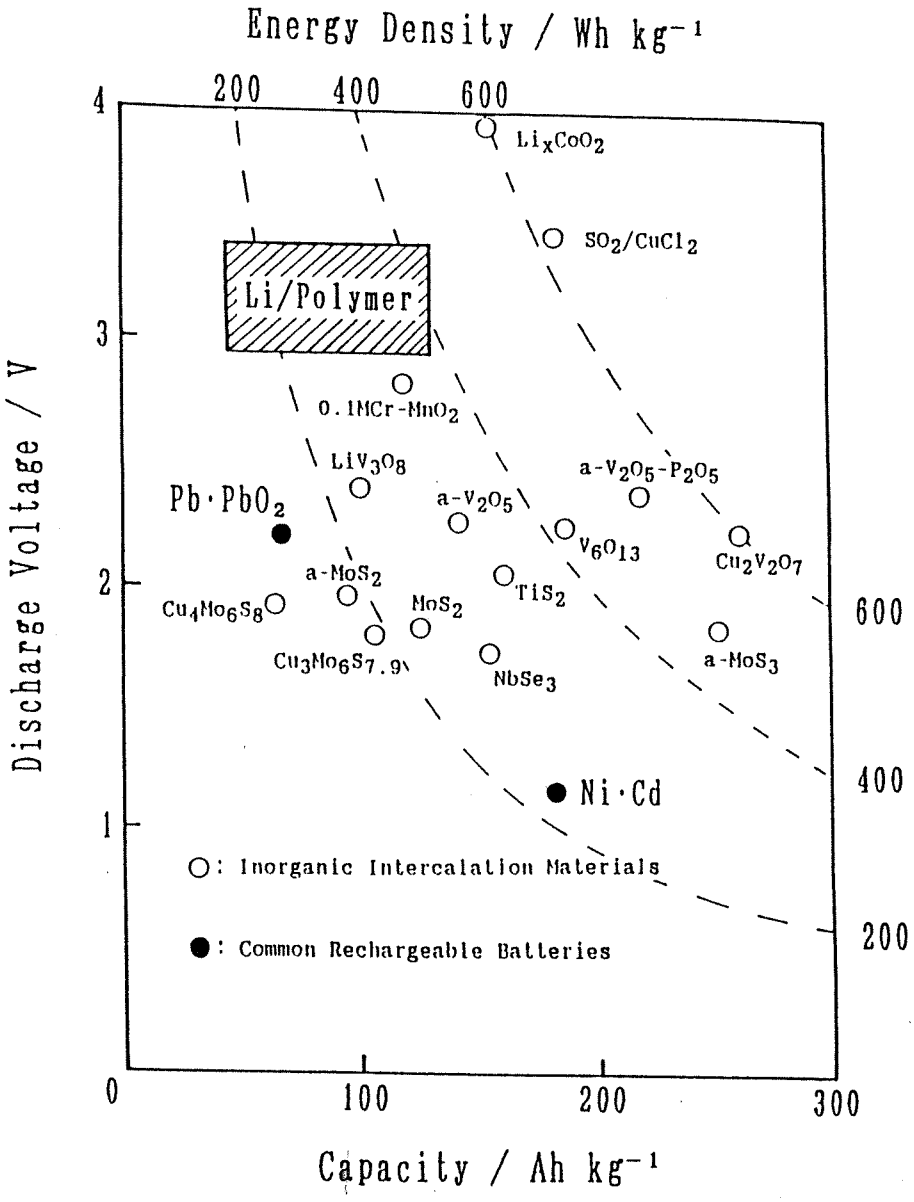

Fig.2 Performances of various rechargeable lithium batteries.

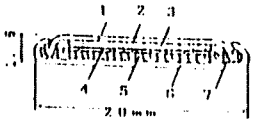

1. Anode Case 2. Current collector
3. Anode 4.Separator
5. Cathode 6. Cathode Case
7. Gasket

a) Coin type Li/PAn battery
(Bridgestone Corp., Seiko I)

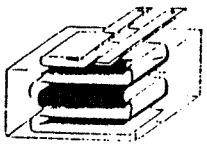

b) Li/PPy multilayer
type battery (BASF/BARTA)

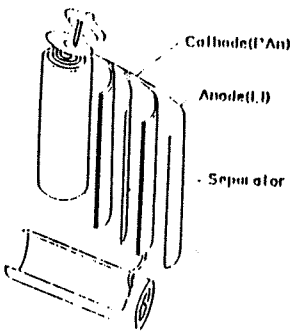

c) Cylinder type Li/PAn battery
(Furukawa Electric, Tokyo Electric Power)

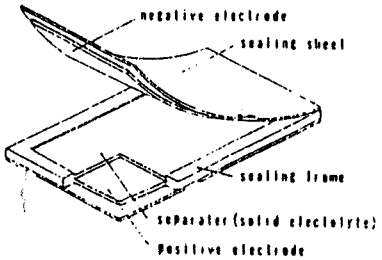

d) Rechargeable card type battery
(Ricoh Company, Ltd.,
Sanyo Chemical Industries, Ltd.)

Fig.3 Prototype and more advanced type Li/polymer batteries using conducting polymers.

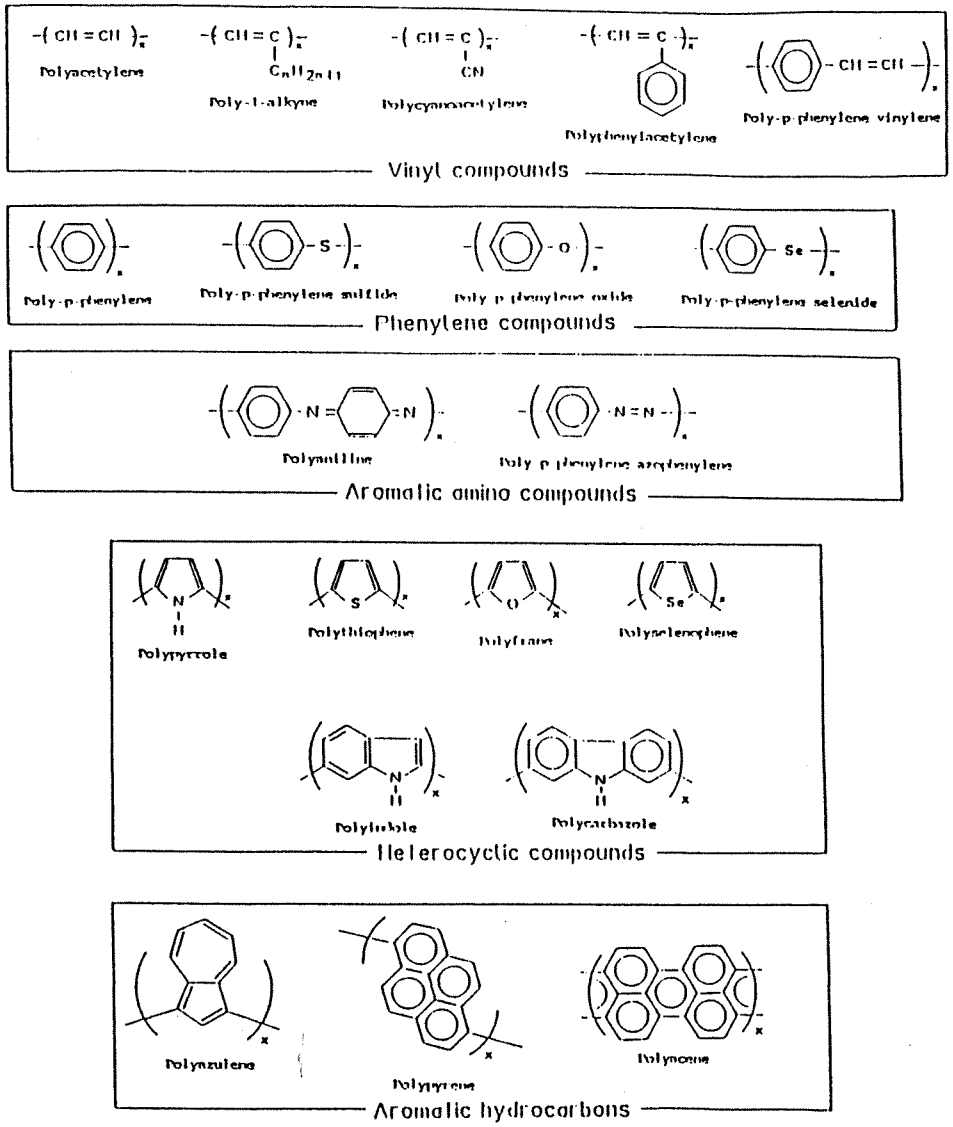

Fig.4 Classification of organic conducting polymers in terms of the chemical structure.

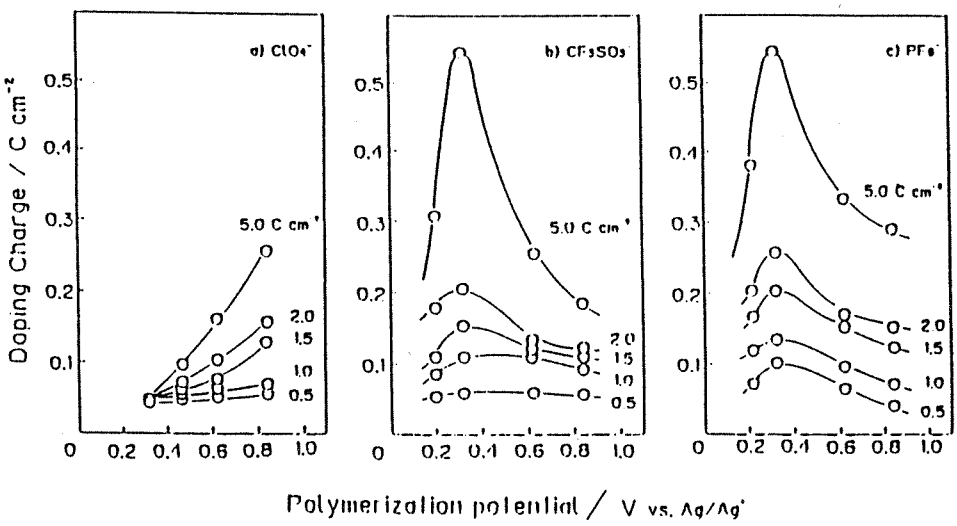

Fig.5 Dependence of polymerization potential on the dopoing charge of PPy films deposited with various supporting anions of a)ClO_4^-, b)$CF_3SO_3^-$ and c)PF_6^- as a function of the film thickness.

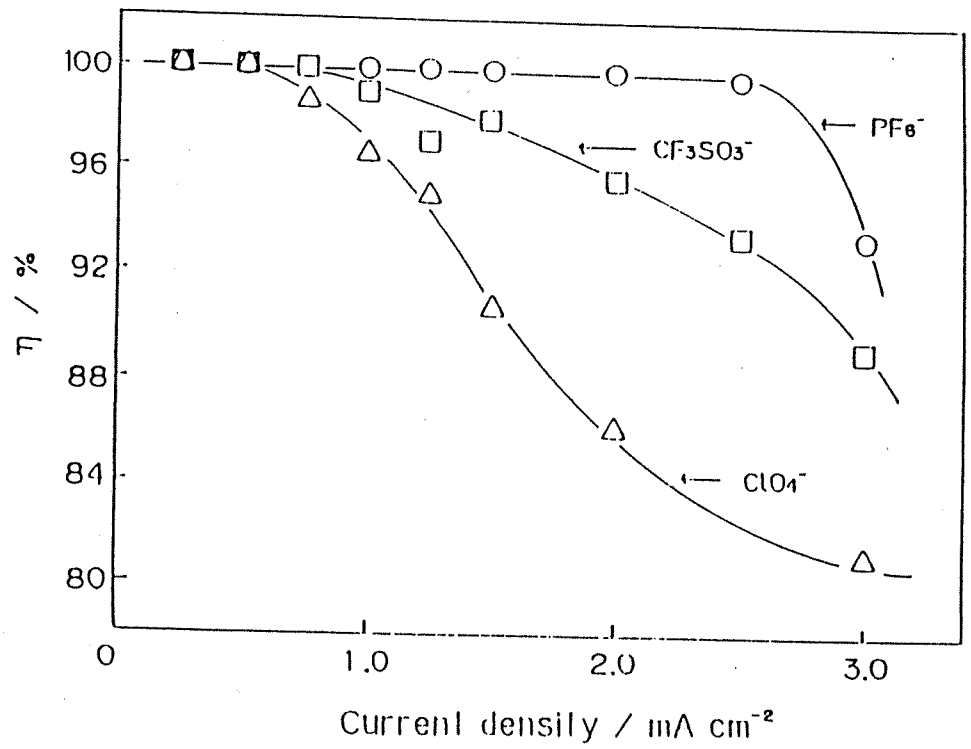

Fig.6 Dependence of current density on the coulombic efficiency of $Li/LiClO_4$-PC/PPy(5 C cm^{-2}) batteries; charge depth=20% of doping level.

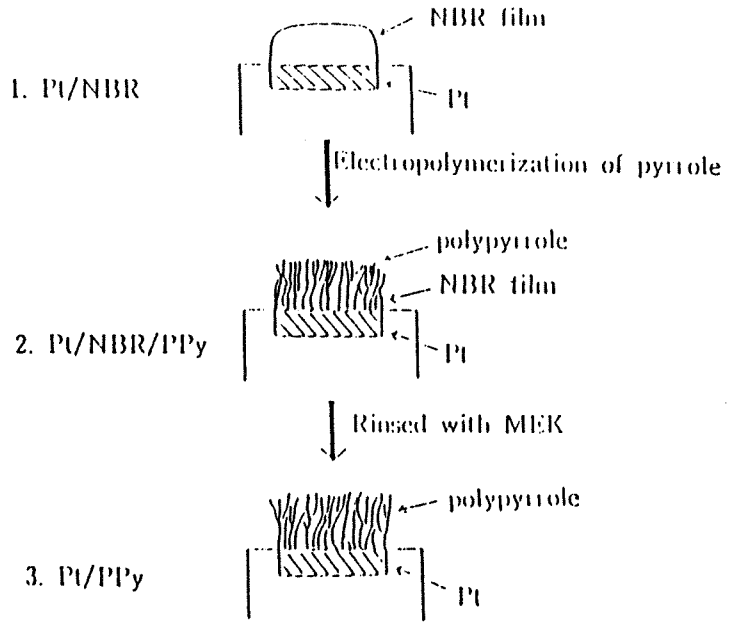

Fig.7 Preparation procedure of NBR/PPy(NBR-guided grown PPy) film.

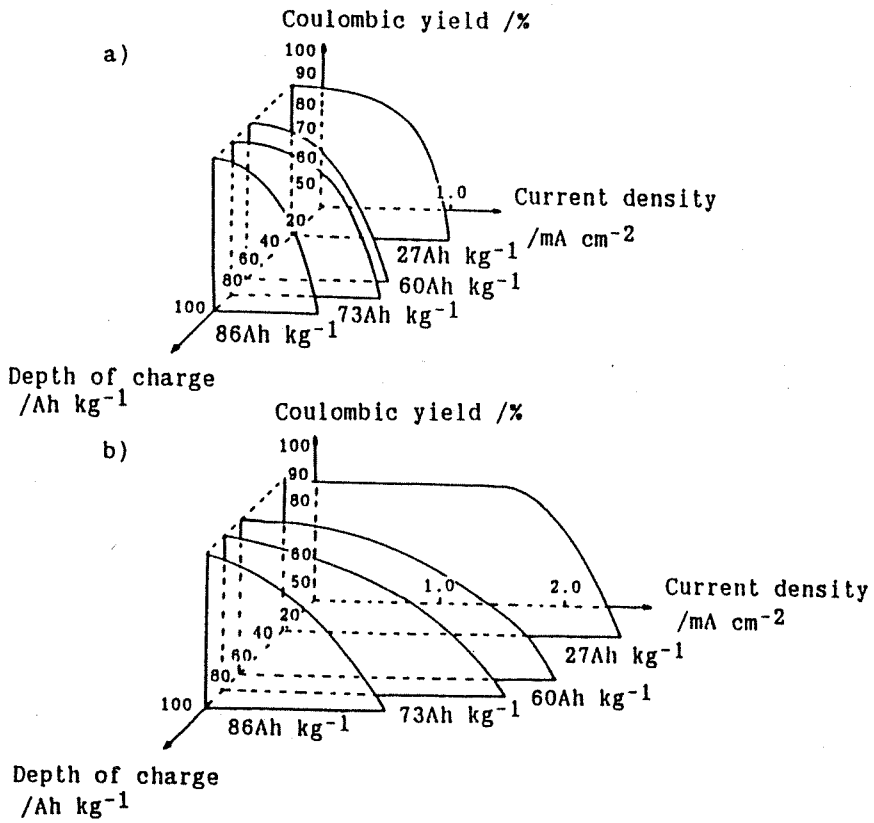

Fig.8 Comparison of charge-discharge performance of a)Li/$LiClO_4$-PC/(Pt/PPy) and b)Li/$LiClO_4$-PC/(Pt/NBR/PPy) batteries.

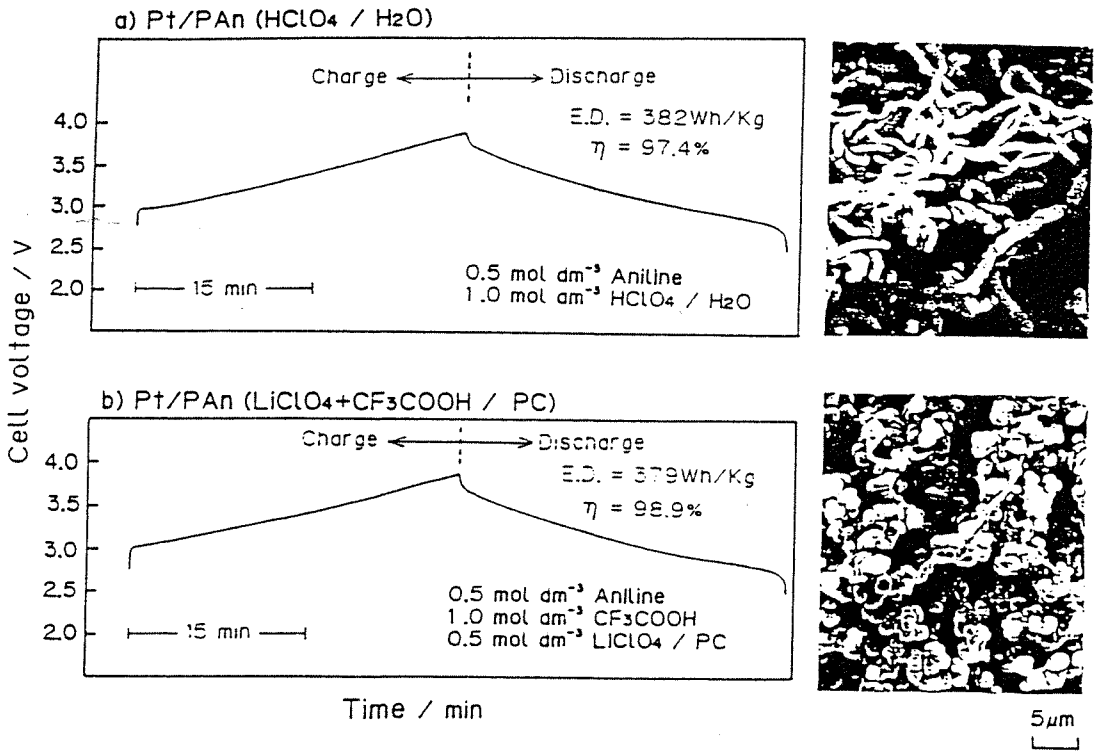

Fig.9 Charge-discharge curves of $Li/LiClO_4$-PC/PAn batteries at a constant current density of 2.0 mA cm^{-2} and SEM micrographs of PAn films deposited from a)aqueous solution and b)PC solution.

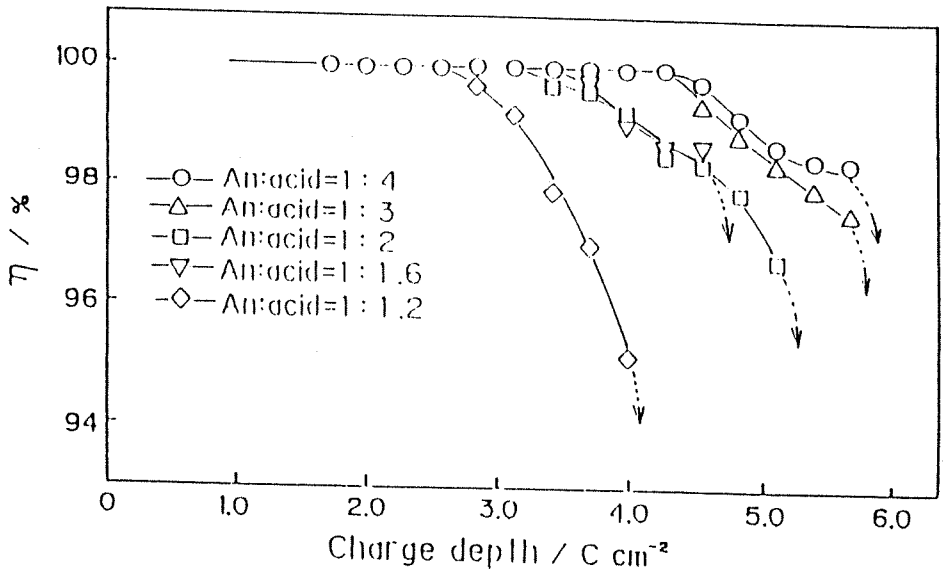

Fig.10 Effect of charge depth on the coulombic efficiency for Li/$LiClO_4$-PC/PAn batteries as a function of aniline:acid ratio in polymerization solution. The current density at charge-discharge test was 8 mA cm^{-2}.

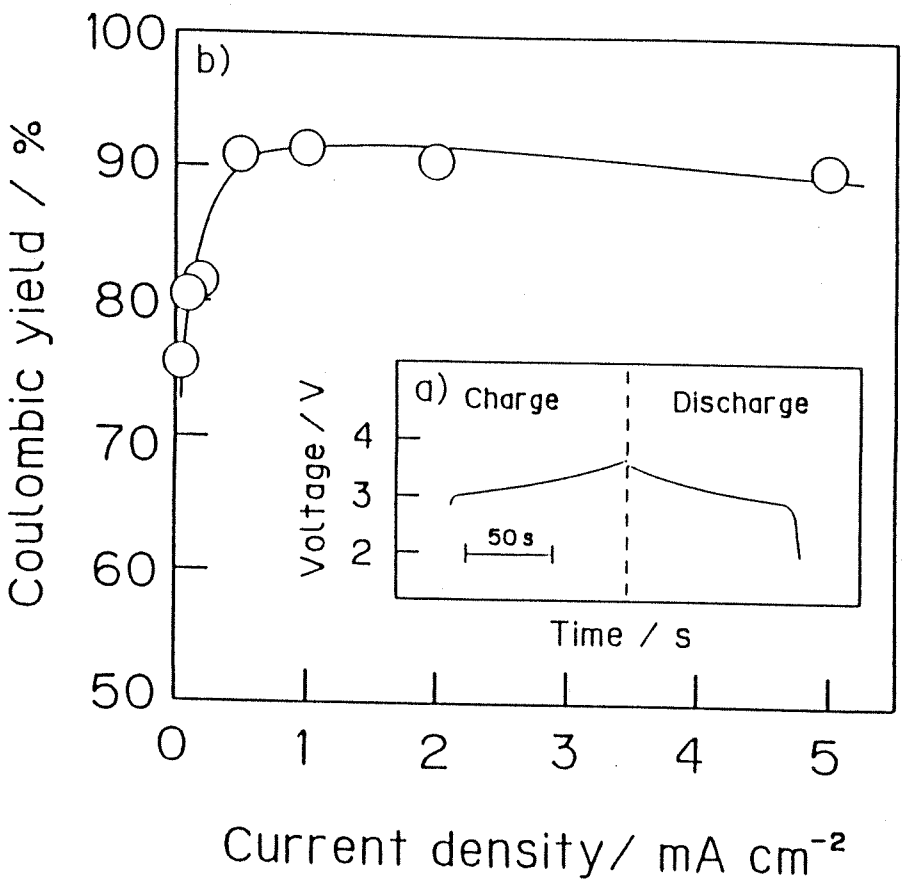

Fig.11 a) Charge-discharge curve of lithium/(PPy/PSS$^-$) cells. Charge-discharge current density was 0.5 mA cm^{-2}. b)Effect of charge-discharge current density on coulombic yield of Li/(PPy/PSS$^-$) cells.

Table 1. Merits and demerits of Li/Polymer batteries.

Merit

1. Form-free
2. High Energy Density and Capacity / Weight
   (~ 400 Wh/kg, 100 ~ 150 Ah/kg)
3. High Power Density / Weight

Demerit

1. Chemical and Physical Stability of Polymer Cathodes
2. Stability of Non-aqueous Electrolyte due to higher voltage
3. Self-dischargeability of Li/Polymer Batteries

Common problem for Li batteries
Li anode cycleability and safety

Table 2. Comparison between PPy and PAn.

ITEMS	PPy	PAn
Structure	π-conjugated polymer	Ionic polymer
Mechanical strength	Strong	Low
Conductivity	High (max. 10^{3} S cm^{-1})	Relatively high (max. 5S cm^{-1})
Doping level	~ 45%	50 - 60%
Voltage	2.8 - 3.2V	3.0 - 3.2V
Preparation method	many variation	low variation

Table 3 Comparison of battery performances between Li/PAS and other Li secondary batteries.(6)

	Cutoff Voltage [V]	Mean Disch. Voltage [V]	Discharged Capacity *1 [Ah/kg]	Discharged Energy *1 [Wh/kg]
Li/PAS	4 / 2	2.88	102	291
	(4.2/1.6)	(2.61)	(152)	(402)
Li/PAn *2	4/2.5	3.35	87	292
Li/β-MoS_2 *3	2.2/1.3	1.75	97	170

*1 Based on active materials

*2 Basic unit : PAn $0.2ClO_4$, Doping : $0.55ClO_4^-$ /unit

*3 Basic unit : $Li_{0.2}MoS_2$, Intercalation : 0.6 Li^+ /unit (MOLICEL)

Electroactive Polyaniline Film Deposited from Nonaqueous Media

III. Effect of Mixed Organic Solvent on Polyaniline Deposition and Its Battery Performance

Tetsuya Osaka,* Toshiki Nakajima, Koh Shiota, and Toshiyuki Momma

Department of Applied Chemistry, School of Science and Engineering, Waseda University, 3-4-1 Okubo, Shinjuku-ku, Tokyo 169, Japan

ABSTRACT

Electroactive polyaniline (PAn) films were deposited from PC (propylene carbonate)-EC (ethylene carbonate) and PC-DME (1,2-dimethoxyethane) mixed polymerization solutions containing aniline, CF_3COOH, and $LiClO_4$. Higher dielectric constant solvents are necessary to deposit the PAn film where protons, dissociated from the acid, initiate the polymerization of aniline. Various PAn films deposited in the PC, the PC-EC (50 mole percent), and the PC-DME (50 volume percent) solutions were used for the cathode materials of the rechargeable lithium batteries. Charge capacity and discharge ability of the Li/PAn batteries in the PC-$LiClO_4$ electrolyte solution are almost the same, regardless of the polymerization solvents, such as PC ≈ PC-EC ≥ PC-DME and PC-EC ≥ PC-DME ≈ PC. The mixed solvent electrolyte solution effect on the Li/PAn (polymerized in the PC solution) batteries becomes much larger such as PC-DME > PC-EC > PC. Moreover, the electrochemical kinetic factors of the PAn films deposited in the various mixed polymerization solutions and also in the different electrolytes were experimentally determined by measuring the ac impedance. The results of the ac impedance analysis of each PAn film correlate well with the battery performances of Li/PAn cells.

Electropolymerized conductive polymer films have been extensively investigated in recent years (1). Among these polymers, polyaniline (PAn) (2-7), polypyrrole (PPy) (8-11), and polyazulene (PAz) (12-16) are promising candidates for the cathode materials for future rechargeable lithium cell systems (17). Recently, a new secondary battery model, utilizing electrochemically conductive PPy, was examined to gain a better understanding of these new batteries (18), and the cell performances of the polymer cathode systems were theoretically calculated (19). Many researchers have investigated polyaniline for the material of a lithium battery cathode, because of its high energy density (Wh/kg), chemical stability, and highly reversible doping-undoping process. Recently, the Bridgestone Corporation and the Seiko Instruments Incorporated group developed a coin battery utilizing electropolymerized PAn as the cathode material (20). However the capacity density of these cells was small.

In our previous investigations (6, 7), the PAn film deposited from a nonaqueous solution with an organic acid (CF_3COOH) containing electrolyte $LiClO_4$ showed electroactive properties as well as those of PAn film deposited from an acidic aqueous solution. The PAn film deposition from a nonaqueous organic solution has the advantage of not requiring a film drying process that is needed when the deposition is done from an aqueous solution. It increases the possibility of selecting a solution for PAn polymerization.

The properties of many nonaqueous, dipolar-aprotic organic solvents have been examined by many researchers (21-25). In particular, the solvent systems of propylene carbonate (PC) can be blended to continuously vary the physical properties so as to change the dielectric constants and viscosities. For example, in the PC-DME (1,2-dimethoxyethane) system (24), the ionic transport becomes faster because of a decrease in the solution viscosity; in the PC-EC (ethylene carbonate) system (25), the ionic dissociation and conductivity are enhanced by an increase in the dielectric constant.

In this paper, we investigate the electropolymerization conditions of PAn in mixed solvent systems, furthermore, the effects of mixed solvent electrolytes on the cell performance of lithium/PAn batteries are also reported.

Experimental

Solutions and film preparation.—Reagent-grade propylene carbonate (PC) was used as the principal solvent. Reagent-grade 1,2-dimethoxyethane (DME) and ethylene carbonate (EC) were used to blend with the PC. The ratios of DME and EC for PC-DME and PC-EC were 0, 25, 50, 75, and 100 volume percent (v/o) and 0, 25, 50, and 75 mole percent (m/o), respectively. Mole percent is used in PC-EC system because EC is in a solid state at ambient temperatures and volume percent is used in PC-DME system because DME is in a liquid state. The properties of PC, DME, and EC at 25°C are as follows: dielectric constant (ϵ) = 64.4, 7.20, and 89.6 (40°C); viscosity (η) = 2.530, 0.455, and 1.86 (40°C) cP; and donor number = 15.1, 24, and 16.4.

Polymerization solutions of PAn contained 0.5 mol dm^{-3} aniline monomer, 2.0 mol dm^{-1} CF_3COOH, 1.0 mol dm^{-3} $LiClO_4$, and the various solvents described above. Molecular sieves were added to remove water in the solutions.

PAn films were deposited on Pt substrates in a three-electrode cell in an argon gas atmosphere. A Pt wire or plate was used as a counterelectrode. All potentials were referred to an Ag/Ag^+ (0.01 mol dm^{-3} $AgNO_3$/the same solvent as polymerization solution) reference electrode. The electro-oxidative method of polymerization was either via a scanned potential between −0.6 and 0.6 V (*vs.* Ag/Ag^+) at 10 mV s^{-1}, or a constant current of 0.5 mA cm^{-2}. The scanned potential method was used to monitor the polymerization reaction while the constant current was used for forming films for battery cathodes.

Electrochemical measurements.—Cyclic voltammetric and ac impedance measurements of the PAn films were performed in the 1.0 mol dm^{-3} $LiClO_4$/PC electrolyte solution using the same three-electrode cell, except that a Li/Li^+ reference electrode was used for the ac impedance measurements. PAn films were prepared by galvanostatic electropolymerization with a loading of up to 1 and/or 5 C cm^{-2}. The voltammetric apparatus included a potentiostat (Hokuto HA-501) and a function generator (Hokuto HB-111) coupled to a digital coulometer (Hokuto HF-201). AC impedance measurements were taken with the same apparatus coupled to a frequency response analyzer (NF FRA-5020) and a computer (NEC PC-9801RX). The amplitude of the signal applied to the samples was 10 mV and the frequency range covered extended from 10 mHz to 20 kHz.

A Li/PAn battery was assembled with a PAn-coated electrode as the cathode and a Li anode mounted on a Ni-expanded mesh. PAn films were prepared in the various solutions described above at 0.5 mA cm^{-2}, and only a loading of up to 5 C cm^{-2} was used for this purpose. Electrolyte solutions used in the Li/PAn cells were PC, PC-DME (50 v/o), and PC-EC (50 m/o) containing 1.0 mol dm^{-3} $LiClO_4$. All charge-discharge tests were performed at a constant current density of 1 ~ 20 mA cm^{-2}. Discharge of the cell was terminated when the cell voltage reached 2.0 V.

* Electrochemical Society Active Member.

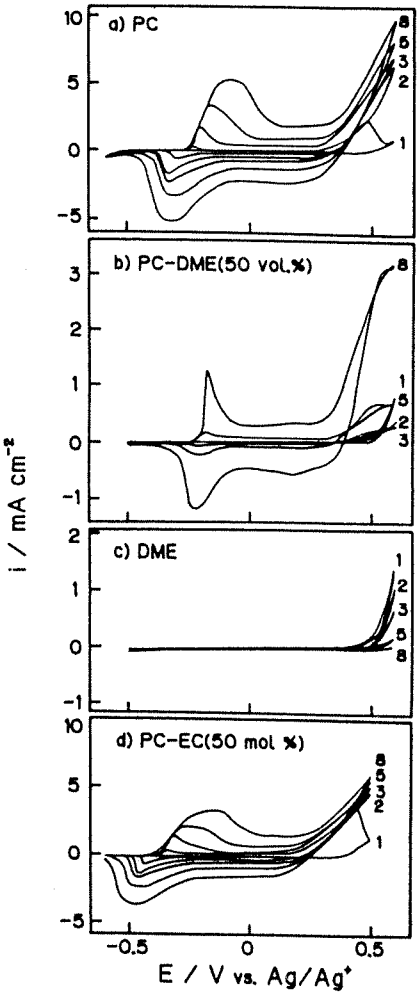

Fig. 1. Cyclic voltammograms for polymerization of aniline in various solutions at 10 mV s^{-1}. Polymerization solutions: 0.5 mol dm^{-3} aniline, 2.0 mol dm^{-3} CF_3COOH, 1.0 mol dm^{-3} $LiClO_4$/various solvents. Numbers in the figure show the cycle numbers.

SEM and infrared spectroscopy observations.—The morphology of the PAn films was inspected by scanning electron microscopy. Fourier-transform IR absorption spectroscopy (JEOL FT-IR 5M) was used to identify the films formed in the various solutions.

Results and Discussion

Polymerization of polyaniline in various mixed solvent systems.—Polymerization of PAn.—In our previous investigations (6, 7), an electroactive polyaniline film was observed to be formed from nonaqueous solutions with trifluoroacetic acid. Figure 1 shows the cyclic voltammograms at 10 mV s^{-1} in PC, PC-DME, and PC-EC solutions containing an aniline monomer, supporting electrolyte ($LiClO_4$), and the organic acid (CF_3COOH). In PC solutions as shown in Fig. 1a, there are the polymerization current at around 0.4 V (*vs.* Ag/Ag^+) (5) and the doping-undoping peaks at around −0.4 V to 0 V, suggesting the polymerization of the electroactive PAn film. In the DME solution shown in Fig. 1c, there is no redox peak and only the anodic polymerization current, suggesting the deposit of a nonactive film. In the blended solution of PC-DME (50 v/o shown in Fig. 1b), the polymerization current decreases for the first two scans, but it increases after the third cycle. This indicates that the initial deposition of PAn in the PC-DME (50 v/o) solution is difficult, but that after the initial film forms the deposition of PAn proceeds easily. In the solution of PC-EC (50 m/o) as shown in Fig. 1d, an electroactive PAn film, similar to that in a PC solution, is formed.

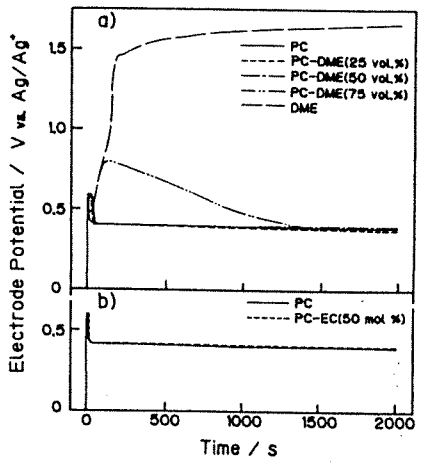

Fig. 2. Potential-time curves during galvanostatic polymerization (0.5 mA cm^{-2}) in solutions: 0.5 mol dm^{-3} aniline, 2.0 mol dm^{-3} CF_3COOH, 1.0 mol dm^{-3} $LiClO_4$/various solvents. (a) PC-DME and (b) PC-EC mixed solvents system.

The potential-time curves at constant-current polymerization are shown in Fig. 2. In PC-DME solutions, the polymerization potential stays constant at the *ca.* 0.4 V region in the region between 0 and 50 v/o DME electrolyte solutions. The electrode potential, however, shifts to a very high potential during the initial time in electrolyte solutions containing over 75 v/o DME. An electroactive PAn deposit was observed on the Pt substrate, but at the same time, a large amount of an oligomer dissolved into the solution, which was detected by the dark green solution color.

In contrast to the PC-DME system, the polymerization potential curves in various PC-EC mixed solutions looked the same as that in the pure PC solution, as shown in Fig. 2b. Therefore, the PAn films deposited in the PC-EC mixed solutions are thought to be the same as those obtained in the PC solution.

Electrochemical characteristics of PAn.—The ion doping ability can be compared as the amount of doping charge, Q_d, that is estimated from the anodic current peak of the cyclic voltammogram at 5 mV s^{-1}. Figure 3 shows the Q_d value of PAn films as a function of mixed ratio of solvents for the polymerization solution. For PC-DME mixed solutions, Q_d keeps more than 90% of its maximum value until a 50 v/o DME content, then it dramatically decreases to 8 mC cm^{-2} at a 75 v/o DME content. In the region between 0 and 50 v/o DME, the coulombic efficiency of constant-current polymerization, as checked by the measurements of the film weight, decreases slightly. However, for more than 50 v/o DME, it decreases drastically and a soluble product is detected by the dark green solution color. Therefore, the PC-DME blended solvent system is unsuitable for the formation of electroactive PAn films at high DME content. Then, only the PAn film deposited from PC-DME (50 v/o) solution was used for the comparison of the others. For PC-EC mixed solutions, the Q_d values are a constant value of *ca.* 148 mC cm^{-2}, regardless of the solvent ratio. Since the Q_d value reflects the battery capacity, the PAn films formed in the PC-EC (50 m/o) mixed solution system were used for the remaining experiments.

IR observations.—The IR spectra for various PAn films are shown in Fig. 4. These measurements were done in order to clear the solution effects on the PAn. The comparison of the IR spectra was done with *ca.* 20 μm thick films deposited by passing 1 C cm^{-2}. The absorption peaks of PAn are common to all three films. A strong absorption

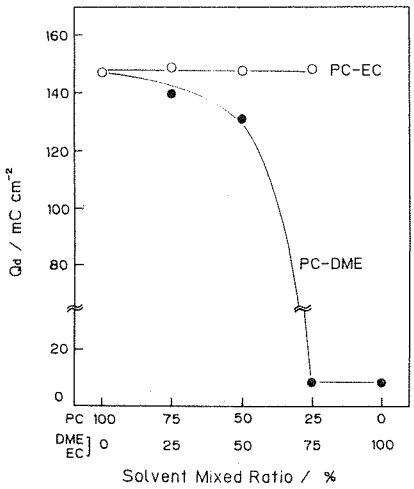

Fig. 3. Dependence of solvent blended ratio on the doping charge (Q_d) of PAn electrode (1 C cm^{-2}) deposited in various PC-DME and PC-EC blended solutions. The Q_d values were estimated from cyclic voltammograms at 5 mV s^{-1}.

peak at 810 cm^{-1} from C—H out-of-plane bending is clearly observed in the spectra of all three films. This absorption peak suggests that the electrochemical polymerization in the PC, the PC-DME, and the PC-EC solutions all occurs through the coupling of the phenyl nuclei at the *para*-position with respect to the amino group.

The effect of the organic solvent of the physical properties is thought to be as follows. For the PC-DME solvent system, the dielectric constant of the solvent decreases with the increase in the DME content, while the viscosity decreases. Thus the dissociation of ions decreases, but the mobility of the species increases. Since the electrochemical polymerization of aniline is initiated by aromatic radical cations and proceeds via the radical cation intermediate (26-28), the increase in DME retards on the initiation of the polymerization. This appears to outweigh the benefit of lower viscosity. In contrast, the PC-EC solvent has a high enough dielectric constant to form good PAn films throughout the range of EC content studied.

SEM observation.—Figure 5 shows SEM images for PAn films prepared in the various solutions. The PAn films formed in PC and PC-EC solutions (Fig. 5a, c) have a grainy structure of *ca.* 1 μm diam, as previously reported (6). In contrast, the PAn film deposited from PC-DME solution (Fig. 5b) has mixed regions of grainy and fibrous structures. The diameter of the grainy structure is one third that observed in other solutions.

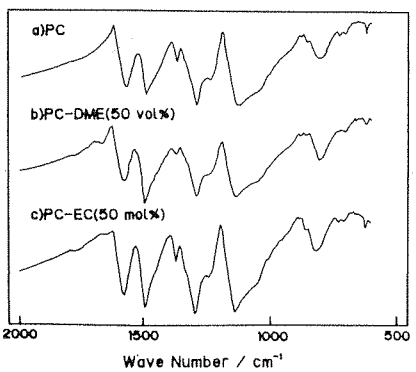

Fig. 4. IR spectra of PAn films deposited from (a) PC, (b) PC-DME (50 v/o), and (c) PC-EC (50 m/o) solutions.

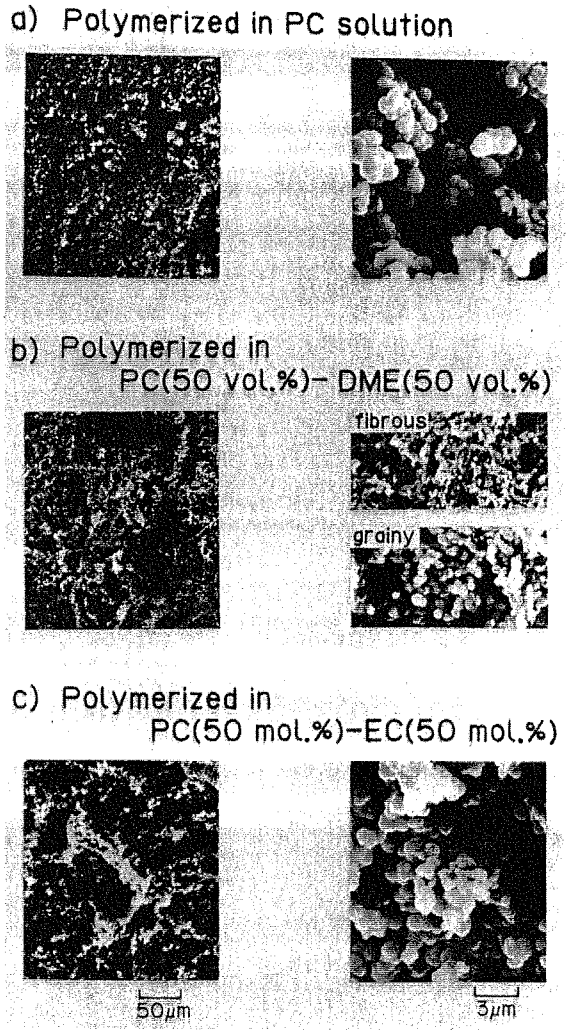

Fig. 5. SEM images for the top views of PAn films (5 C cm^{-2}) polymerized at various conditions.

Performance of Li/PAn batteries.—Charge-discharge performance of Li/PAn cathode (prepared from various polymerization solutions) batteries.—We assembled Li/PAn cells using the PC electrolyte containing 1.0 mol dm^{-3} $LiClO_4$. The PAn films were 5 C cm^{-2} thick. Figure 6a shows the dependence of the coulombic efficiency on the charge depth at the current density of 2 mA cm^{-2} for both charge and discharge. Figure 6b shows this efficiency against the current density at the charge depth of 800 mC cm^{-2}. In Fig. 6a, a large difference is not observed until the capacity reaches 1200 mC cm^{-2} (*ca.* 140 Ah kg^{-1}). The coulombic efficiency estimated from the charge-discharge curve is nearly 100%. However, over 1200 mC cm^{-2}, there appear detectable differences between the batteries from the PC-DME solutions and those from the PC. This seems to be caused by the small decrease in the redox active sites of the films deposited from the PC-DME solutions. In Fig. 6b, the charge-discharge current density also is not large (PC-EC ≥ PC-DME ≈ PC).

Charge-discharge performance of Li/PAn (prepared from PC) batteries in various electrolyte solutions.—We investigated the Li/PAn (prepared from PC) cells with several electrolyte solutions containing 1.0 mol dm^{-3} $LiClO_4$. Figures 7a and b show the dependence of the coulombic efficiencies on the charge depth and on the charge-discharge

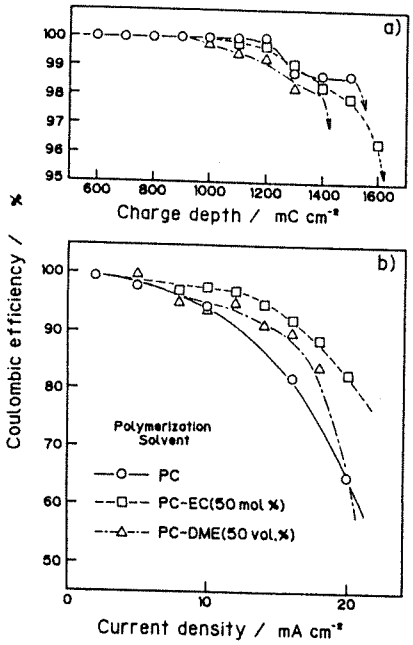

Fig. 6. Dependence of coulombic yield on charge depth (a) and on current density (b) of Li/$LiClO_4$-PC/PAn (5 C cm^{-2}) batteries, as a function of PAn films deposited from various polymerization solutions.

current density, respectively. In Fig. 7a, the coulombic efficiency is more than 98% up to a charge depth of 1200 mC cm^{-2}, however, the coulombic efficiency in PC-DME electrolyte solution decreases dramatically in the higher cell loading region. This is probably due to two causes. The first is the interaction between DME molecules and active

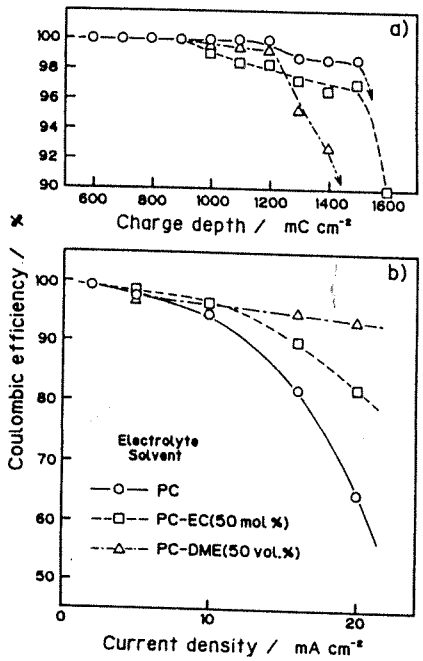

Fig. 7. Dependence of coulombic yield on charge depth (a) and on current density (b) of Li/$LiClO_4$-mixed solvent/PAn (5 C cm^{-2}) batteries as a function of mix solvent electrolytes. Polyaniline films were deposited from PC solution.

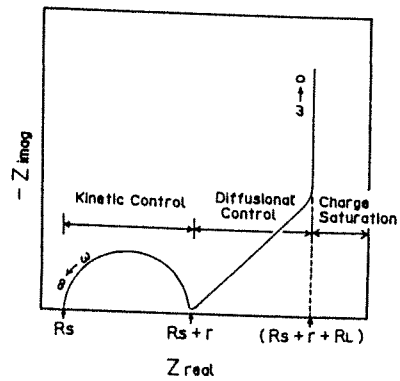

Fig. 8. Schematic representation of complex impedance behavior for the electroactive polymers.

sites in the PAn chains. The DME molecules stabilize the radical cations and restrain the ClO_4^- ions from interaction with the radical cations. The second is the decomposition of DME at potentials over 4.0 V.

The effect of the current density on the coulombic efficiency is shown in Fig. 7b. The coulombic efficiency using PC electrolytes decreases dramatically and becomes 65% at 20 mA cm^{-2}. However, by blending EC or DME, the coulombic efficiency can be maintained at a high value, up to 10 ~ 15 mA cm^{-2}.

Impedance analysis of PAn films.—Determination of reaction resistance of PAn films.—PAn films were measured by means of an ac impedance method to investigate and compare the film properties more precisely. Figure 8 shows ideal behavior in the form of Cole-Cole plots. There appear three regions: the semicircle at high frequencies, the linear relation with a 45° inclination at medium frequencies, and the vertical line at low frequencies. The three regions correspond to the rate-determining regions of charge-transfer, the ion diffusion, and the limitation of an ion diffusion in the film. The data for various preparation solutions and the electrolyte solutions are shown in Fig. 9 and 10. The values of R_s (solution resistance) and r (reaction resistance) are tabulated in Tables I and II. In Fig. 9, the PAn films polymerized from the PC, the PC-DME (50 v/o), and the PC-EC (50 m/o) polymerization solutions were measured in a 1.0 mol dm^{-3} $LiClO_4$/PC electrolyte solution at 3.55 V *vs.* Li/Li^+. In Fig. 10, the PAn film prepared from the PC polymerization solution was measured at the same potential of 3.55 V (*vs.* Li/Li^+) in the PC, the PC-DME (50 v/o), and the PC-EC (50 m/o) electrolyte solutions containing 1.0 mol dm^{-3} $LiClO_4$.

In Fig. 9 (see Table I), the reciprocal value of r (reaction rate) of PAn deposited in the PC-EC solution is larger than those in the PC-DME and the PC solutions (PC-EC > PC-DME ≥ PC), suggesting that the rate of charge-transfer in the PAn film prepared in the PC-EC solution is faster than the films prepared in other solutions. In Fig. 10 (see Table II), the reciprocal value of r (reaction rate) clearly shows the order of PC-DME > PC-EC > PC, which corresponds exactly to the dependence of battery performance on the charge-discharge current density shown in Fig. 7b.

The redox capacitance and the diffusion coefficient for PAn films determined from "finite diffusion" region.—Ho *et al.* (29) applied a model called the "finite diffusion model" to ac impedance analysis. Hunter *et al.* also applied the model to polymer film systems (30). In this model, the impedance is nearly purely capacitive, reflecting the charge saturation limit set by the finite polymer thickness. For thin film samples in the low-frequency range, $\omega << L^2/D$, where ω, L, and D are the frequency, the film thickness, and the diffusion coefficient of doping ions into the film, respectively. The phase angle approaches $\pi/2$ and C_L is given by

$$C_L^{-1} = d(-Z_i)/d(\omega^{-1}) \quad [1]$$

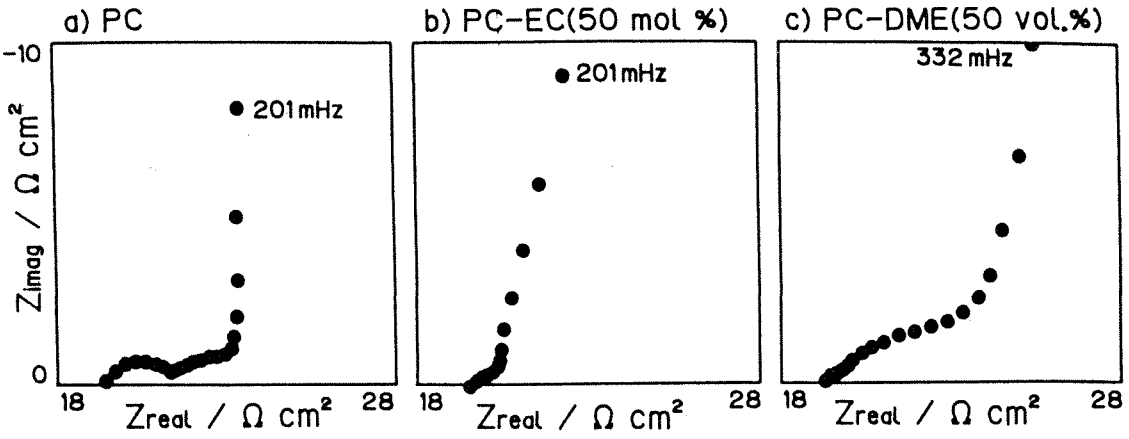

Fig. 9. Cole-Cole plots of PAn films (1 C cm^{-2}) polymerized from various polymerization solutions containing 0.5 mol cm^{-3} aniline, 2.0 mol dm^{-3} CF_3COOH, 1.0 mol dm^{-3} $LiClO_4$ and blended solvents. The impedance was measured in 1.0 mol dm^{-3} $LiClO_4$/PC electrolyte solution at 3.55 V *vs.* Li/Li^+.

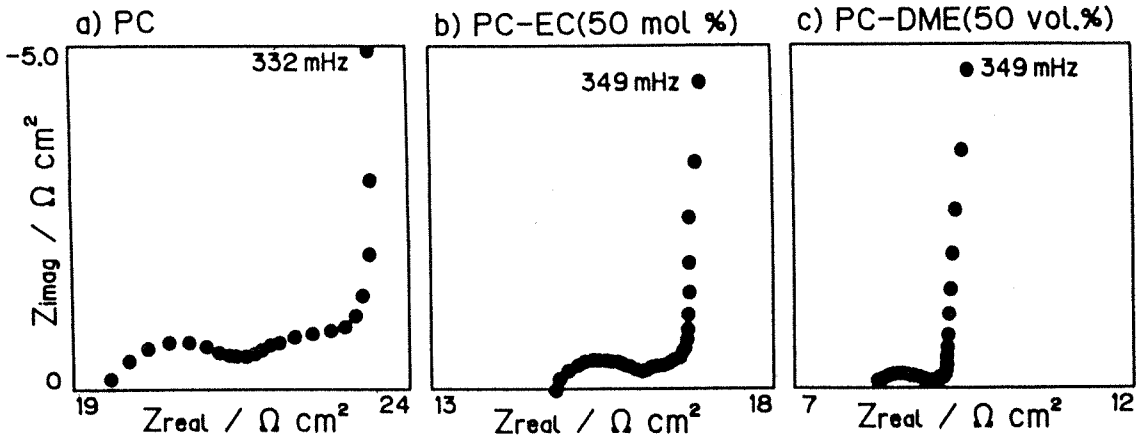

Fig. 10. Cole-Cole plots of PAn films (1 C cm^{-2}) measured in various electrolyte solutions containing 1.0 mol dm^{-3} $LiClO_4$, and blended solvents. PAn films were deposited from PC polymerization solution. The impedance was measured at 3.55 V *vs.* Li/Li^+.

where C_L is the low-frequency redox capacitance of the film. The low-frequency resistance R_L is related to the redox capacitance and the diffusional relaxation time, L^2/D is obtained by extrapolating the low frequency data to the x axis, as explained in Fig. 8

$$R_L = (1/C_L) \cdot L^2/3D \qquad [2]$$

From expression [2] plus the sample thickness, we can deduce the diffusion coefficient, D. Using the expressions [1] and [2], some D values were calculated for conducting polymers (*e.g.*, polyvinylferrocene) (30-35). However, in the case of a highly porous electrode as a PAn electrode, the effective length for the ion motion is not well defined and does not correspond to the sample thickness. The D value

Table I. Experimentally determined values from the rate-determining region of the charge-transfer and the finite diffusion region for PAn films (1 C cm^{-2}) deposited from various solutions, measured in PC electrolyte solution containing 1.0 mol dm^{-3} $LiClO_4$.

Polymerization solutions	Electrolyte solutions	R_s/Ω cm²	r/Ω cm²	$C_L \cdot 10^2$/F cm^{-2}	R_L/Ω cm²	$D \cdot 10^9/cm^2\ s^{-1}$
PC	PC	19.6	2.24	10.5	2.66	7.64
PC-EC	PC	19.5	0.98	11.2	2.32	8.21
PC-DME	PC	19.2	2.08	7.31	4.82	6.05

Table II. Experimentally determined values from the rate-determining region of the charge-transfer and the finite diffusion region for PAn films (1 C cm^{-2}) deposited from PC polymerization solution, measured at various conditions.

Polymerization solutions	Electrolyte solutions	R_s/Ω cm²	r/Ω cm²	$C_L \cdot 10^2$/F cm^{-2}	R_L/Ω cm²	$D \cdot 10^9/cm^2\ s^{-1}$
PC	PC	19.6	2.24	10.5	2.66	7.64
PC	PC-EC	14.7	1.60	10.9	0.90	21.7
PC	PC-DME	8.10	1.04	11.6	0.56	32.8

for this system found from using L which equals the film thickness results in estimates of D about 10^{-5} cm^2 s^{-1}. This value is too large. Mermilliod *et al.* (33) already discussed this effect and used the polymer chain size for the L value instead of the film thickness. We considered such results and discussion, and adopted the average particle size, *ca.* 0.8 μm, of the polymers observed by SEM, as the effective length for the ion motion, assuming the movement of doping ions in small domains of particle size.

The values of C_L, R_L, and D, using the above assumption, are tabulated in Tables I and II. The calculated D values are reasonable, on the order of $10^{-9} \sim 10^{-8}$ cm^2 s^{-1}, suggesting that particle size is a suitable limit for the diffusion length, L. The D values of PAn films deposited in various solutions (Table I) show the order of PC-EC ≥ PC ≥ PC-DME and the battery performance from Fig. 6b seems to correspond to this order of D values. In Table II, the order of the calculated D values, PC-DME > PC-EC > PC, corresponds exactly to the behavior of the charge-discharge current density shown in Fig. 7b.

The relationship between the electrochemical properties of PAn films is linked to the battery performance of the Li/PAn cells. Changing the polymerization solvent changes the electroactivity and the diffusion coefficient of PAn films. The values of r and D, of course, correlate with the corresponding battery's capacity (concerned with r^{-1}) and also the current density dependence (concerned with D) in the high-current density region.

Conclusion

Our investigation of the electropolymerization conditions on PAn films shows that a high dielectric solution is necessary to deposit an electroactive PAn film. The PAn films formed from the PC, PC-EC, and PC-DME mixed solvent systems all have the same basic structure, but the electrochemical activity of the films are influenced by the physical properties of these solvents. Battery performance is consistent with the electroactivity and morphology of the PAn films.

Acknowledgments

This work was financially supported in part by the Grant-in-Aid for Scientific Research, the Ministry of Education Science and Culture, and also in part by the General Sekiyu Research and Development Foundation.

Manuscript submitted Oct. 11, 1990; revised manuscript received April 16, 1991.

Waseda University assisted in meeting the publication costs of this article.

REFERENCES

1. T. Osaka, T. Nakajima, K. Shiota, and B. B. Owens, in "Rechargeable Lithium Batteries," S. Subbarao, V. R. Koch, B. B. Owens, and W. H. Smyrl, Editors, PV 90-5, p. 170, The Electrochemical Society Softbound Proceedings Series, Pennington, NJ (1990).
2. A. F. Diaz and J. A. Logan, *J. Electroanal. Chem.*, **111**, 111 (1980).
3. A. Volkov, G. Tourillon, P. C. Lacaze, and J. E. Dubois, *ibid.*, **115**, 279 (1980).
4. A. G. MacDiarmid, J. C. Chiang, M. Halpern, W. S. Huang, S. L. Mu, N. L. D. Somasiri, W. Wu, and S. I. Yaniger, *Mol. Cryst. Liq. Cryst.*, **121**, 173 (1985).
5. T. Ohsaka, Y. Onuki, N. Oyama, G. Katagiri, and K. Kamimoto, *J. Electroanal. Chem.*, **161**, 399 (1984).
6. T. Osaka, S. Ogano, K. Naoi, and N. Oyama, *This Journal*, **136**, 306 (1989).
7. T. Osaka, T. Nakajima, K. Naoi, and B. B. Owens, *ibid.*, **137**, 2139 (1990).
8. A. F. Diaz and K. K. Kanazawa, *JCS Chem. Commun.*, 635 (1979).
9. A. F. Diaz and J. I. Castillo, *ibid.*, 397 (1980).
10. K. Naoi and T. Osaka, *This Journal*, **134**, 2479 (1987).
11. T. Osaka, K. Naoi, and S. Ogano, *This Journal*, **135**, 1071 (1988).
12. J. Bargon, S. Mohmand, and R. J. Waltman, *Mol. Cryst. Liq. Cryst.*, **93**, 279 (1984).
13. R. J. Waltman, A. F. Diaz, and J. Bargon, *This Journal*, **131**, 1452 (1984).
14. G. Tourillon and F. Gamier, *J. Electroanal. Chem.*, **135**, 173 (1982).
15. T. Hirabayashi, K. Naoi, and T. Osaka, *This Journal*, **134**, 758 (1987).
16. T. Osaka, K. Naoi, and T. Hirabayashi, *ibid.*, **134**, 2645 (1987).
17. T. Osaka and K. Ueyama, *Kagaku-Kogyo (Chemical Industry)*, **40**, 231 (1989).
18. T. Yeu and R. E. White, *This Journal*, **137**, 1327 (1990).
19. K. Naoi, B. B. Owens, and W. H. Smyrl, in "Rechargeable Lithium Batteries," S. Subbarao, V. R. Koch, B. B. Owens, and W. H. Smyrl, Editors, PV 90-5, p. 194, The Electrochemical Society Softbound Proceedings Series, Pennington, NJ (1990).
20. M. Ogawa, T. Fuse, T. Kida, T. Kawagoe, and T. Matsunaga, in "Proceedings of Battery Meeting of Japan, p. 197 (1986).
21. J. P. Gabano, "Lithium Batteries," p. 13, Academic Press, Ltd., London (1983).
22. Y. Matsuda, "Practical Lithium Batteries," p. 13, JES Press, Cleveland, OH (1987).
23. S. Tobishima and T. Okada, *Electrochim. Acta*, **30**, 1715 (1985).
24. K. Imanishi, M. Satoh, Y. Yasuda, and R. Tsushima, *J. Electroanal. Chem.*, **242**, 203 (1988).
25. V. Gutmann, "The Donor-Acceptor Approach to Molecular Interactions," Plenum Press, New York (1978).
26. E. M. Genies, A. A. Syed, and C. Taintavis, *Mol. Cryst. Liq. Cryst.*, **121**, 181 (1985).
27. E. M. Genies and M. Lapkowski, *J. Electroanal. Chem.*, **236**, 189 (1987).
28. G. Zotti, S. Cattarin, and N. Comisso, *ibid.*, **239**, 387 (1988).
29. C. Ho, I. D. Raistrick, and R. A. Huggins, *This Journal*, **127**, 343 (1980).
30. T. B. Hunter, P. S. Tyler, W. H. Smyrl, and H. S. White, *ibid.*, **134**, 2198 (1987).
31. R. M. Penner and C. R. Martin, *J. Phys. Chem.*, **93**, 984 (1989).
32. S. Panero, P. Prosperi, S. Passerini, B. Scrosati, and D. D. Perlmutter, *This Journal*, **136**, 3729 (1989).
33. N. Mermilliod, J. Tanguy, and F. Petiot, *ibid.*, **133**, 1073 (1986).
34. S. H. Glarum and J. H. Marshall, *ibid.*, **134**, 142 (1987).
35. P. Fiordiponti and G. Pistoia, *Electrochim. Acta*, **34**, 215 (1989).

Reprinted from JOURNAL OF THE ELECTROCHEMICAL SOCIETY
Vol. 138, No. 10, October 1991
Printed in U.S.A.

Electropolymerization of Electroinactive Polypyrrole Film for a Nonlinear MIM Switching Device

Tetsuya OSAKA*, Toshihiro FUKUDA, Kiyoshi OUCHI and Toshiki NAKAJIMA†

Received June 13, 1991; Accepted August 22, 1991

Thin films of electroinactive polypyrrole (PPy) were electropolymerized in NaOH aqueous solutions on ITO (indium tin oxide) electrodes for the purpose of constructing nonlinear MIM (metal-insulator-metal) switching devices for large scale flat panel displays. Electroactivity and morphology of PPy films were greatly affected by the NaOH concentration. Highly anodic potential (1.5 V vs. Ag/AgCl) electrolysis in NaOH solution produced carbonyl groups in the PPy chain, so that electroinactive PPy was nonconducting in as-prepared conditions. The MIM structure of ITO/PPy/ITO was fabricated by ITO sputtering onto the PPy film. The device using the PPy film prepared from 0.01 mol dm^{-3} NaOH aqueous solution showed nonlinear and symmetric current-voltage (I-V) characteristics. In spite of using the nonconductive PPy, a dependence of I-V characteristics on polymerization time was observed, and a proper polymerization time was required to produce an MIM device.

1 INTRODUCTION

Electropolymerized films are insensitive to air. They are able to be prepared highly conductng, semiconducting and insulating materials when varying their polymerized conditions. Highly conducting or semiconducting polymers, formed by electropolymerization, have been extensively investigated from a practical point of view for electronic device application. Indeed, Schottky junction-type diodes[1] and field-effect transistors (FETs)[2] have been demonstrated using, e.g., a copolymer of pyrrole and N-methylpyrrole units, and polythiophene respectively. An application of electroinactive or nonconducting polymers formed with a electropolymerization technique, however, has scarcely been tried in this field. We have fabricated an MIM (metal-insulator-metal) device using an electropolymerized nonconducting film as an insulator[3,4].

The MIM device is a nonlinear, two terminal device, and its structure is simpler than that of a TFT (thin film transistor). An application of it to the switching element for the multiplexed liquid crystal (LC) display is expected[5]. The insulator of the MIM switching device is practically used with a Ta_2O_5 layer formed by anodizing a sputtered Ta film. Its fabricating process is still complex, and a simplified fabricating-process is required in order to realize a large area LC panel. On the basis of this requirement, some insulating organic films, such as polyimide formed using a Langmuir-Blodgett method[6], polyfuran using plasma polymerization[7], and polyethylene using an evaporated method[8] have been reported. We have already reported an MIM device using undoped poly-N-methylpyrrole (PMPy) film as an insulator[3]. An electropolymerization method is highly suitable for larger area fabrication, but the undoped PMPy film reported in ref. 3 is very sensitive to its anion undoping process, so that the stability of electric characteristics of this element must be developed.

In this paper, we try to use directly formed nonconducting polypyrrole (PPy) as an insulator[4], instead of undoped polymers, and report and discuss the nonlinear properties of the MIM device using the electroinactive PPy insulator.

Department of Applied Chemistry, School of Science and Engineering, Waseda University (3-4-1 Okubo, Shinjuku-ku, Tokyo 169)
†SEIKO EPSON Co. (17-1 Tsukahara 1-Chome, Chino-shi, Nagano 391)
Key Words: Electroinactive polypyrrole, Highly anodic electrolysis, Nucleophilic hydroxide ion, Nonlinear MIM device

2 EXPERIMENTAL

2.1 Chemicals and solutions

Reagent grade pyrrole (Tokyo Kasei Co.,Ltd.), $NaClO_4$ (Kanto Chemical Co., Inc.) and NaOH (Kokusan Chemical Works Ltd.) were used without further purification. Photoresists OMR-83 and OFPR-800 (Tokyo Ohka Kogyo Co., Ltd.) were used for ITO (indium tin oxide) glass substrate preparation and for etching the upper ITO electrode respectively. Aqueous solutions containing 0.25 mol dm^{-3} pyrrole monomer and 0.05, 0.01, and 0.001 mol dm^{-3} NaOH electrolyte salts were used for the preparation of PPy films. They were deaerated by argon gas before use.

2.2 Film preparation and electrochemical measurements

For the electropolymerization and electrochemical measurements, the cell was assembled with an ITO working electrode, a Pt counter electrode, and an Ag/AgCl reference electrode. Cyclic voltammetry at 10 mV s^{-1} was employed for surveying both electropolymerization behavior and the redox process. PPy films were formed by constant potential electrolysis at 1.5 V vs. Ag/AgCl with varying electrolysis time. Electroactive PPy for Fourier-transformed infrared (FT-IR) and visible (Vis) spectroscopic measurements were formed by constant potential electrolysis at 0.65 V vs. Ag/AgCl from an aqueous solution containing 0.2 mol dm^{-3} pyrrole monomer and 0.1 mol dm^{-3} $NaClO_4$ electrolyte salt.

2.3 Fabrication and current-voltage (I-V) characteristics measurement of an MIM device

Device fabrication was performed as previously reported[3,4]. A schematic representation of the MIM device is shown in Fig. 1. The holes for deposited polypyrrole layer were prepared on the ITO (ca. 400 nm thick) glass substrate using a photolithographic technique. The hole sizes were 100, 300, 500, 700, 1000 μm in diameter. PPy films formed by constant potential electrolysis at 1.5 V vs. Ag/AgCl were used for fabrication of the device. After a rinse in water and drying by a stream of argon gas of the PPy coated electrode, the upper ITO electrodes (ca. 60 nm thick) were prepared by using sputtering and etching technique. I-V characteristics of the device were measured between ± 10 V by 0.5 V steps in the dark.

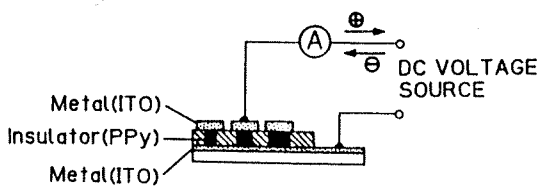

Fig. 1. Schematic representation of the MIM device structure.

2.4 Apparatus

The microscopic FT-IR spectroscopic measurement was carried out by a JEOL JIR-5500. Vis spectra were recorded on a HITACHI U-3200 spectrophotometer. The morphology of PPy films was observed with a JEOL JSM-T20 scanning electron microscope (SEM). Film thickness was measured using a contact profile meter (Alpha-step 200 TENCOR INSTRUMENTS). For the film preparation, the Potentio/galvanostat HA-301 (Hokuto Denko Co., Ltd) was employed. I-V characteristics were measured using a YOKOGAWA HEWLETT-PACKARD 4140B pA meter / dc voltage source.

3 RESULTS and DISCUSSION

3.1 Selection of the polymerization solution

Electropolymerization of insulating PPy has already been reported briefly by Murthy et al.[9], but details of the polymerization condition have scarcely been described. We prepared three polymerization solutions containing 0.001, 0.01, and 0.05 mol dm^{-3} NaOH, and surveyed electropolymerization behavior and the redox process of PPy films with cyclic voltammetry in polymerization solutions. Cyclic voltammograms over the range between -0.3 V and 1.8 V vs. Ag/AgCl for each solution are shown in Fig. 2. For the lower NaOH concentration (Fig. 2-(a)), anodic current for polymerization is shown at the first cycle and then the redox process is observed. This means that the PPy film obtained in 0.001 mol dm^{-3} NaOH solution is somewhat electroactive and its conductivity is not very low. The PPy film formed from this polymerization solution is considered to be unsuitable for use in an MIM device. On the other hand, anodic currents for polymerization are also observed in both Figs. 2-(b) and 2-(c), however, the redox process is not shown. This indicates that PPy films obtained from these solutions are electroinactive and the conductivities are very low. For polyaniline[10] and polyphenol[11], it was reported that the electroinactive and low conducting films are obtained in high pH solutions. But Li et al. reported that, even in NaOH electrolyte solution, electroactive PPy film showed the redox process with a decrease in

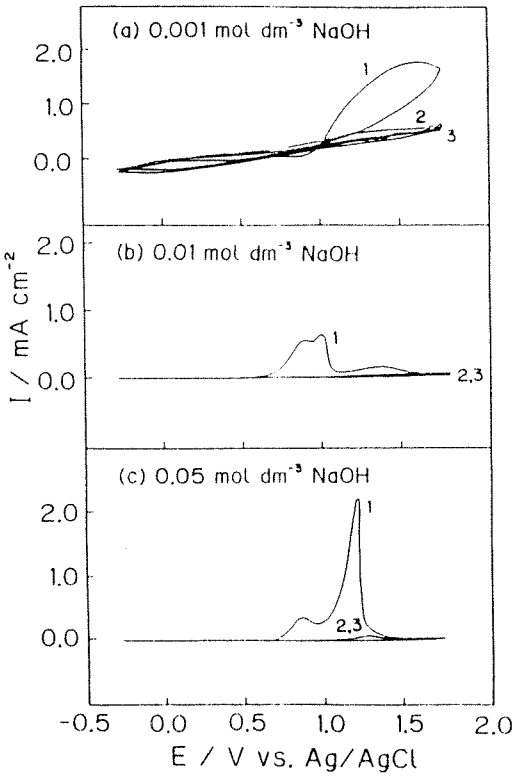

Fig. 2. Cyclic voltammograms at 10 mV s^{-1} in various NaOH aqueous solutions containing 0.25 mol dm^{-3} pyrrole: (a) 0.001 mol dm^{-3}, (b) 0.01 mol dm^{-3}, and (c) 0.05 mol dm^{-3} NaOH. Figures indicate the cycle numbers.

conductivity when an adequate scan range was selected, and that it became electroinactive when the anodic scan went to a higher anodic potential[12]. Judging from these reports, the electroinactivity of the PPy films obtained from 0.01 and 0.05 mol dm^{-3} NaOH solution is considered to be affected by highly anodic potential electrolysis rather than high pH value. Highly anodic potential (1.5 V vs. Ag/AgCl) electrolysis was employed for film preparation.

Next, we tried to electropolymerize PPy films for MIM devices in 0.01 and 0.05 mol dm^{-3} NaOH polymerization solutions by constant potential electrolysis at 1.5 V vs. Ag/AgCl. The surface morphology, the film thickness and the adherence to the ITO electrode are considered to affect I-V characteristics of the device significantly. The surface morphology of electroinactive PPy films were observed and are shown in Fig. 3, indicating the SEM images of PPy films obtained from 0.01 and 0.05 mol dm^{-3}

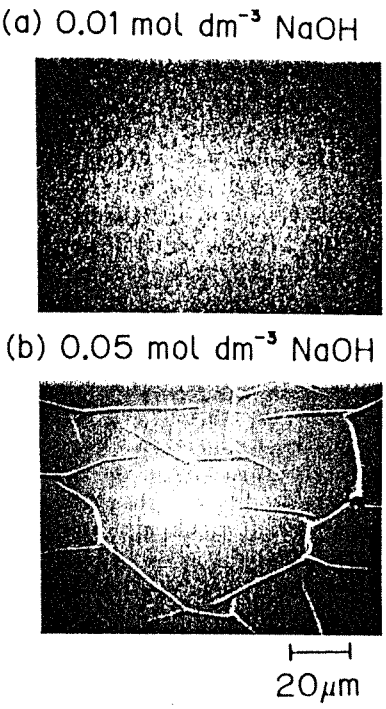

Fig. 3. SEM images of PPy films electropolymerized at 1.5 V vs. Ag/AgCl from polymerization solutions (a) 0.01mol dm^{-3} and (b) 0.05 mol dm^{-3} NaOH. Each solution contains 0.25 mol dm^{-3} pyrrole.

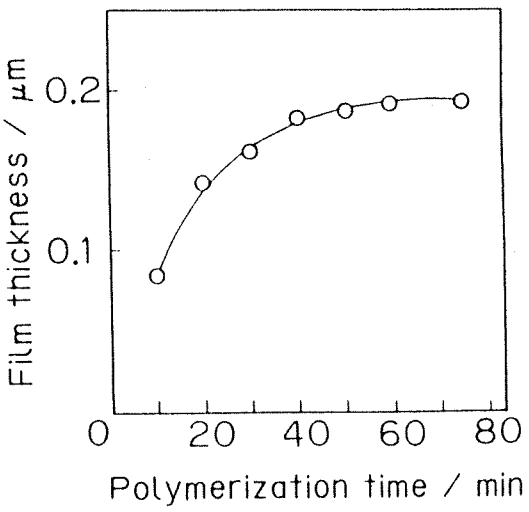

Fig. 4. The relationship between film thickness and electrolysis time at 1.5 V vs. Ag/AgCl from 0.01 mol dm^{-3} NaOH polymerization solution containing 0.25 mol dm^{-3} pyrrole.

NaOH polymerization solutions. In Fig. 3-(a), the PPy film obtained from 0.01 mol dm^{-3} NaOH solution is thin (ca. 0.2μm thick) and very smooth, so it would be free of the pin-hole defects. On the other hand, in Fig. 3-(b), the PPy film from 0.05 mol dm^{-3} NaOH solution is thicker than that from 0.01 mol dm^{-3} NaOH. However, wrinkles are observed, so the adherence of this film to the ITO electrode is found to be very low. Therefore, we selected the PPy film obtained from 0.01 mol dm^{-3} NaOH polymerization solution for an MIM device because of its low conductivity and good adherence to the ITO electrode.

Figure 4 shows the dependence of the film thickness on polymerization time when the PPy films were electropolymerized at 1.5 V vs. Ag/AgCl. Electroinactive PPy has low conductivity in as-prepared conditions, so the film thickness shows a rapid rate of increase at the start of polymerization and the deposition rate of the film slows down with a proceeding of deposition. The thickness of the PPy film is found to be saturated at ca. 0.2 μm.

3.2 Vis and IR spectra

The Vis spectra of electro-active and -inactive PPy films are shown in Fig. 5. Curve (a) in Fig. 5 shows the spectrum of the electroactive PPy film formed from polymerization solution containing $NaClO_4$ as an electrolyte at 0.65 V vs. Ag/AgCl. The spectrum contains broad absorption of more than 600 nm, originating from what is called the bipolaron absorption[13]. But such a bipolaron absorption is not observed in the electroinactive PPy film formed from 0.01 mol dm^{-3} NaOH polymerization solution at 1.5 V vs. Ag/AgCl for 60 min even in as-prepared conditions (curve (b)). Li et al. reported a similar spectrum in undoped and low conducting PPy by in situ spectrum measurement[12]. These facts imply that the electroinactive PPy is not in a bipolaron state and also that it is very low conducting in as-prepared conditions.

Figure 6 shows the FT-IR spectra of electro-active and -inactive PPy film species. Both in electro-active (curve(a)) and -inactive (curve(b)) PPy films, the absorption peaks assigned to pyrrole rings (ca. 860, 1017, 1162, 1524, and 3218 cm^{-1}) are demonstrated. A strong absorption peak at 1697 cm^{-1} is clearly observed in curve (b), not so clear in curve (a). This peak can be attributed to the C=O stretching vibration, indicating that the carbonyl (C=O) groups exist in the electroinactive PPy chain. The carbonyl groups may be intro-

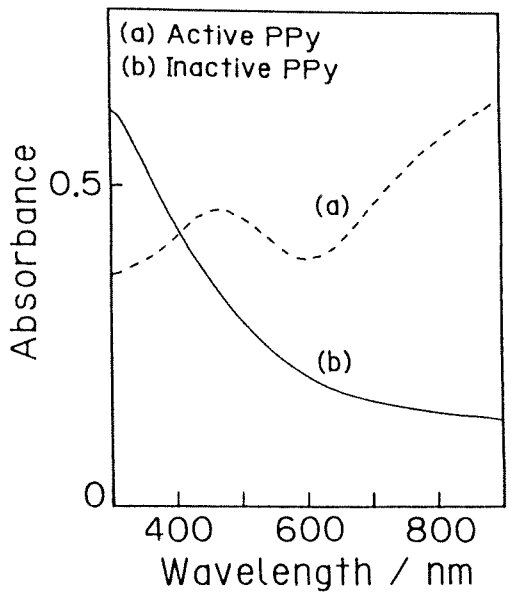

Fig. 5. Vis spectra of electro-active and -inactive PPy films: (a) electroactive PPy film formed at 0.65 V vs. Ag/AgCl from an aqueous solution containing 0.1 mol dm^{-3} pyrrole and 0.2 mol dm^{-3} $NaClO_4$, (b) electroinactive PPy film formed at 1.5 V vs. Ag/AgCl for 60 min from an aqueous solution containing 0.25 mol dm^{-3} pyrrole and 0.01 mol dm^{-3} NaOH.

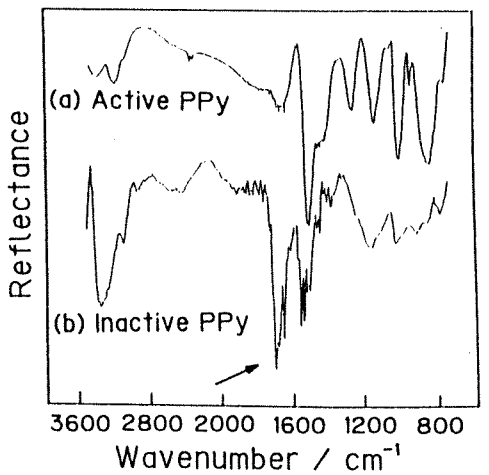

Fig. 6. FT-IR reflection spectra of electro-active and -inactive PPy films: (a) electroactive PPy film formed at 0.65 V vs. Ag/AgCl from an aqueous solution containing 0.1 mol dm^{-3} pyrrole and 0.2 mol dm^{-3} $NaClO_4$, (b) electroinactive PPy film formed at 1.5 V vs. Ag/AgCl for 60 min from an aqueous solution containing 0.25 mol dm^{-3} pyrrole and 0.01 mol dm^{-3} NaOH.

duced by highly anodic potential electrolysis (1.5 V vs. Ag/AgCl). The possibility of attacks of nucleophilic hydroxide anions from the NaOH electrolyte to α- or β- carbons is shown in scheme 1.

(a) Hydroxide ion attack at α-carbon

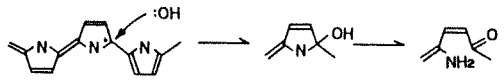

(b) Hydroxide ion attack at β-carbon

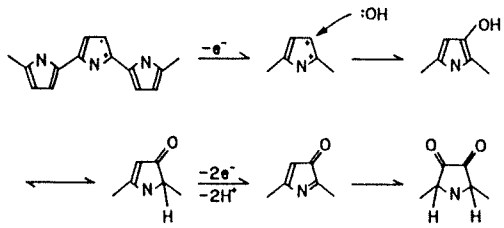

Scheme 1

The positive charged sites in PPy chain would exist in π-conjugated systems, so these two reactions shown in (a) and (b) are considered to occur simultaneously. Similar carbonyl group formation was reported as an irreversible overoxidation reaction which changed an electroactive polypyrrole[14] or polythiophene[15] to an electroinactive and low conducting state. The nucleophilic reactions would occur at electrophilic sites of the positive charged bipolarons and lead to shortening of π-conjugated length of the PPy chain. Such reaction makes the PPy films electroinactive and low conducting in as-prepared conditions, and this film preparation method probably consists of both the polymerization and the irreversible overoxidation reaction.

3.3 I-V characteristics of the MIM device

Figure 7 shows I-V characteristics of the MIM device using the PPy film formed from 0.01 mol dm^{-3} NaOH polymerization solution at 1.5 V vs. Ag/AgCl for 60 min. The positive and negative directions in Fig. 7-(a) and (b) correspond to a positive and negative bias in the ITO glass substrate respectively. The symmetric and nonlinear I-V responses and increases in currents, ca. 5 orders of magnitude(Fig. 7-(a)), are reproducibly observed, and the switching behavior of threshold voltage at ca. ± 5 V is obtained as shown in Fig. 7-(b). A number of measurements also confirmed the stability of the electric properties of it. The hole size did not influence I-V characteristics. As for the reproducibility and no necessity of undoping process, this device is superior to that using the undoped PMPy film reported previously[3]. Thus the electroinactive PPy films were found to be

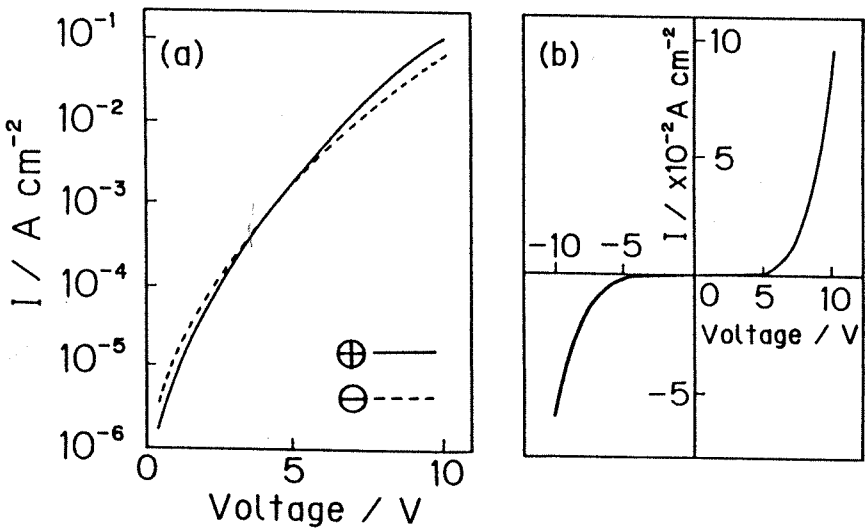

Fig. 7. I-V characteristics of the MIM device using the electroinactive PPy film formed at 1.5 V vs. Ag/AgCl for 60 min from aqueous solution containing 0.25 mol dm^{-3} pyrrole and 0.01mol dm^{-3} NaOH: (a) log I-V, (b) I-V.

suitable for an insulator of the MIM device from a practical point of view.

Next, we tried to fabricate the devices with varying polymerization time. When polymerization time is shorter than 30 min, high applied-voltage caused the breakdown of the I-V characteristics. On the other hand, polymerization for more than 30min confirmed the stability of them. Figure 8 shows the typical I-V characteristics of the devices using PPy film deposited for 30 and 60 min. The resistance and threshold voltages are found to increase with the passage of polymerization time. These phenomena can be explained as follows.

(1) An increase in the film thickness lowers the electric field of the PPy film, improving the resistance value.

(2) The structural change which improves the resistivity value proceeds during polymerization.

The former is easily confirmed by the results in Fig. 4. The latter is suggested by the relationship between PPy film conductivity and polymerization time. Figure 9 shows the relationship between polymerization time and the conductivity, $\sigma_{0.5}$, of PPy films measured at currents of +0.5 V. The $\sigma_{0.5}$ value is found to clearly decrease with polymerization time. This is probably caused by the structural change of the PPy film. The Vis spectra of PPy films were measured with varying polymerization time. The Vis spectra of the PPy film of different polymerization time are shown in Fig. 10. With the passage of polymerization time, the bipolaron peak, which is slightly observed

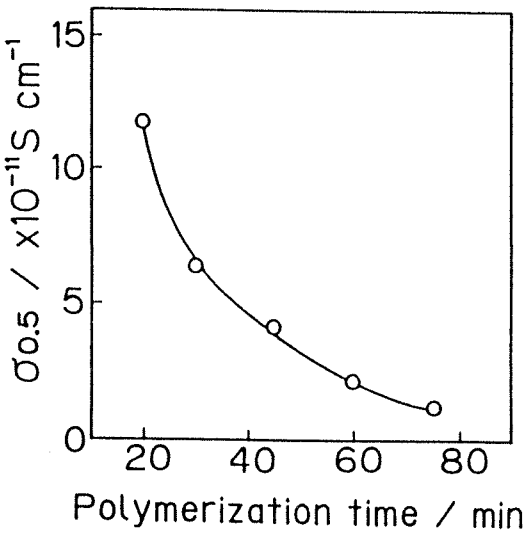

Fig. 9. The dependence of the conductivity, $\sigma_{0.5}$, in electroinactive PPy films measured at 0.5 V on polymerization time.

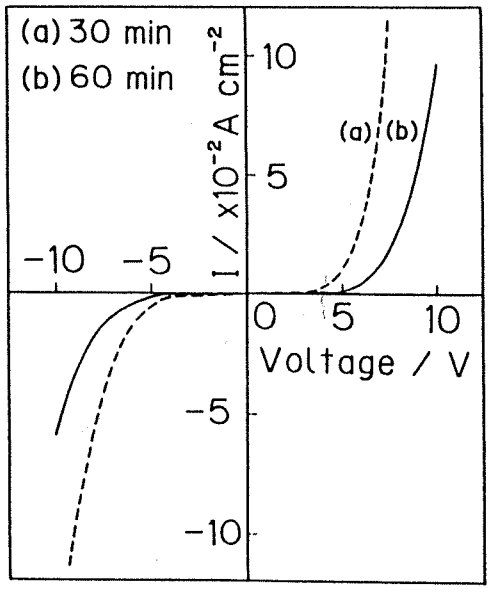

Fig. 8. I-V characteristics of the MIM device using PPy films deposited for (a) 30 min and (b) 60 min.

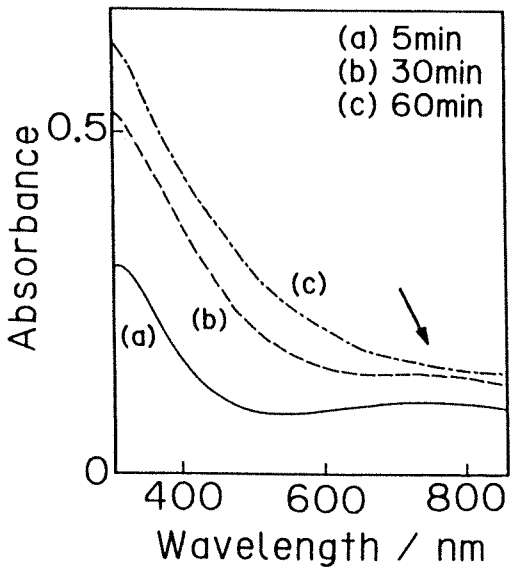

Fig. 10. Vis spectra of the PPy films as a function of polymerization time: (a) 5 min, (b) 30 min, (c) 60 min.

at 760 nm, becomes smaller, and disappears completely at more than 45 min polymerization. This may be due to the attack of hydroxide anion to the positive site of the bipolaron leading to the destruction of it. Thus the improvement of the resistance value probably is due to both the increase of the film thickness and the proceeding overoxidation reaction.

4 CONCLUSION

The electroinactive and nonconducting PPy films were able to be electropolymerized from NaOH aqueous solution at highly anodic potential electrolysis. Their electroinactivity and less conductivity were for the most part caused by the overoxidation reaction. The concentration of NaOH affected not only the electroactivity but the morphology of the PPy film. The ITO/PPy/ITO type MIM device using the electroinactive PPy showed stable nonlinear I-V responses, and the possibility of its practical use was demonstrated. The dependence of the I-V characteristics on polymerization time was explained by the increase in film thickness and structural changes of the PPy film.

The authors would like to acknowledge the experimental support and valuable discussion of Prof. Sadako NAKAMURA and Miss Keiko OIKE, Japan Women's University, and financial support from the Japanese Ministry of Education, Science and Culture.

5 REFERENCES

1) H. Koezuka and S. Etoh, J. Appl. Phys., 54, 2551 (1983).
2) H. Koezuka and A. Tsumura, Synth. Met., 28, C753 (1989).
3) T. Osaka, K. Ueyama, and K. Ouchi, Chem. Lett., 1989, 1543.
4) T. Osaka, K. Ouchi, and T. Fukuda, Chem. Lett., 1990, 1535.
5) D. E. Baraff, J. B. Long, C. J. Miner, and R. W. Streater, Conf. Record. of 1980 Biennial Display Resarch Conf., IEEE, 107, (1980).
6) H. Maeda, Y. Otobe, and S. Kobayashi, IEICEJ Tech. Rep., OME-89-43, 19, (1989).
7) P. K. Abraham, and K. Sathianandan, Thin Solid Films, 164, 353, (1988).
8) C. A. Hogarth, and M. Zor, phys. stat. sol. (a), 98, 611, (1986).
9) A. S. N. Murthy, and S. K. S. Reddy, J. Mater. Sci. Lett., 3, 745, (1984).
10) T. Ohsaka, Y. Ohnuki, and N. Oyama, J. Electroanal. Chem., 161, 399, (1984).
11) Y. Ohnuki, H. Matsuda, T. Ohsaka, and N.Oyama, J. Electroanal Chem., 158, 55, (1983).
12) Y. Li, and R. Qian, Synth. Met., 26, 139, (1988).
13) J. L. Bredas, J. C. Scott, K. Yakushi, and G. B. Street, Phys. Rev. B, 30, 1023, (1983).
14) F. Beck, P. Braun, and M. Oberst, Ber. Bunsenges. Phys. Chem., 61, 967, (1987).
15) S. Wang, K. Tanaka and T. Yamabe, Synth. Met., 32, 141, (1989).

– Communication –

LCD Driving Characteristics of MIM Diode Using Electropolymerized Polypyrrole Thin Film as an Insulator

Toshiki NAKAJIMA*, Fumiaki MATSUSHIMA, Toshihiro FUKUDA† and Tetsuya OSAKA†

Received July 1, 1991; Accepted September 12, 1991

1 INTRODUCTION

An MIM type non-linear resistance device is used as a switching device for active matrix LCD of the high display quality[1]. So far, the Ta/TaO_x/Metal structure is known as for this device[1~3]. And an MIM device using organic insulating film prepared by LB (Langmuir-Blodgett) technique is studied by Maeda *et al*[4].

We have reported an electropolymerized thin organic film that is applicable to an insulator for the MIM device[5~7]. Electropolymerization can easily form an organic thin film and can produce a large-size LCD at a low cost. Especially, the polypyrrole(PPy) film electropolymerized in the alkali solution (e.g. pH12) has high resistance (10^{10} ohm cm) in as-prepared conditions, and the MIM device which uses this PPy film as an insulator shows non-linear and symmetrical I-V characteristics stably as is previously reported[6,7].

In this report, we describe the results of the multiplexing drive simulation of TN-LC cell connected to the MIM device on the basis of the basic results of Refs. 6 and 7, and discuss the possibility of active-matrix LCD driven by this MIM device.

2 EXPERIMENT

The MIM device consisted of the ITO/PPy/ITO structure. The fabrication process was similar to the previous experiments[5,6]. A 1 μm thick photoresist film (OMR-83, Tokyo Ohka Kogyo Co., Ltd.) was formed over the ITO/glass electrode, and 300 μm diameter contact holes for the deposited PPy were prepared by photolithographic technique. PPy films were electropolymerized in aqueous solution containing 0.25M Py and 0.01M NaOH at the constant potential of 1.5V vs. Ag/AgCl for 60 minutes. The film thickness of the PPy film was 0.1 μm. PPy films were first rinsed in water, next dried in atmosphere for 24 hours, and then dried at 160°C for 60 minutes. Then sputtered ITO films were formed on the each PPy film having a 2mm×3mm area.

Figure 1a) shows the schematic measurement circuit of the TN-LC cell switching behavior by this MIM device. The TN-LC cell had an area of 5 mm × 5 mm and a capacitance of 135 pF. The MIM device had a capacitance of 155 pF. Figure 1b) shows MIM-LC driving waveforms applied to on-state and off-state LC cell. Driving voltage is defined as on-state waveform pulse voltage (V_a). Typical transmittance (T) – V_a characteristics were investigated at a frame frequency of 32 Hz, duty ratio $T_r/T_f = 1/64$ or 1/256, and bias ratio $V_b/V_a = 1/4$. The V_b was fluctuated in the actual multiplexing driven LCD, however, in this experiment V_b was at a constant level for simple evaluation.

In an MIM driven LCD, in order to get high contrast ratio between on-off waveforms, large C_{LC}/C_{MIM} ratio(e.g. 10) is better[2]. For example in an MIM-LCD using TaO_x as MIM's insulator, the C_{LC}/C_{MIM} ratio was 3.5. In this experiment, this ratio had not been optimized ($C_{LC}/C_{MIM} = 0.9$) because the MIM of larger area was easy to construct and evaluate the performance properties.

Production Engineering Department, SEIKO EPSON Corporation, (1-17-1 Tsukahara, Chino City, Nagano, 391)
†Department of Applied Chemistry, Waseda University, (3-4-1 Okubo, Shinjuku-ku, Tokyo, 169)
Key Words: MIM, Polypyrrole, Active Matrix LCD, Eletropolymerization

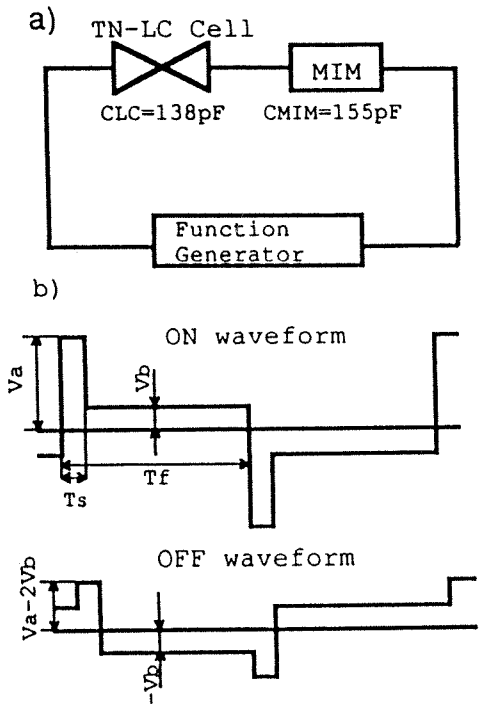

Fig. 1 MIM-LC driving circuit diagram and waveforms.

3 RESULTS AND DISCUSSION

As is already reported[5,6], this MIM device has a symmetrical non-linear I-V characteristic, and has threshold voltages at $\pm 5V$[6].

Figure 2 shows a T-V_a characteristics of TN-LC cell with and without the MIM device at duty ratio 1/64. Without MIM, there is scarcely a difference of T-V_a curves between on-off waveforms, so that multiplexing drive is impossible. With an MIM device, threshold voltages of the LC cell are obviously different between on-off waveforms. And the T-V_a curve at on-waveform improves steeper than that without the MIM because the charge on the on-state LC cell is maintained by the switching effect of MIM device. Therefore the contrast ratio between on-off waveforms at the same V_a became obviously high. When a condenser was inserted into the circuit instead of the MIM device, T-V_a curves improved weak slope and threshold voltages of the LC cell were scarcely different between on-off waveforms. It explains that this MIM diode actually works as a

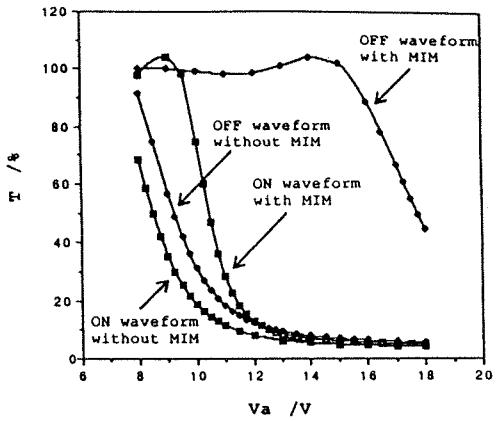

Fig. 2 T-Va characteristics of TN-LC cell with and without MIM diode at 1/64 duty ratio.

switching device, and that does not work as a voltage divider by the capacitance of the MIM device.

Figure 3 shows T-V_a characteristics of LC cell driven at 1/256 duty ratio. By the switching effect of the MIM device, a sufficient contrast was obtained even at 1/256 duty ratio. Because actual pocket TVs with MIM-LCD are operated at 1/256 duty ratio[3], the MIM is able to be used for a pocket TV.

Maximum contrast ratios were about 17 at 1/64 duty ratio and 8 at 1/256 duty ratio. In this experimental, capacitance ratio of C_{LC}/C_{MIM} had not been optimized, so that higher contrast ratio would become possible by making C_{MIM} smaller, i.e. using smaller size MIM device.

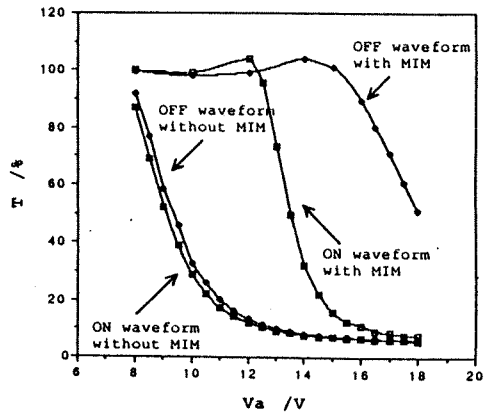

Fig. 3 T-Va characteristics of TN-LC cell with and without MIM diode at 1/256 duty ratio.

In conclusion, the MIM device of ITO/PPy/ITO construction works as the switching device for active matrix LCD of at least 1/256 duty ratio.

REFERENCES

1) D. R. Baraff, J. R. Long, B. K. MacLaurin, C. J. Miner, and R. W. Streater, Conf. Record. of 1980 Biennial Display Research Conf., IEEE, p.107 (1980).
2) S. Morozumi, T. Ohta, R. Araki, T. Sonehara, K. Kubota, Y. Ono, T. Nakazawa and H. Ohara, Japan Display '83 Proc. of the 3rd Int'l Display Res. Conf., 404 (1983).
3) K. Oguchi, S. Maezawa, K. Niwa, Y. Wakai, and H. Baba, *Nikkei Microdevices*, **7**, 121 (1987).
4) H. Maeda, Y. Otobe, and S. Kobayashi, *Proc. of the SID*, **31/2**, 79 (1990).
5) T. Osaka, K. Ueyama, and K. Ouchi, *Chem. Lett.*, **1989**, 1543.
6) T. Osaka, K. Ouchi, and T. Fukuda, *Chem. Lett.*, **1990**, 1535.
7) T. Osaka, T. Fukuda, K. Ouchi and T. Nakajima, *Denki Kagaku*, **59**, 1019 (1991).

測定法講座

最前線の電気化学－測定法の実際

ポリマー二次電池とその基礎特性評価法

逢坂哲彌
門間聰之

1　はじめに

1977年，ペルシルバニア大学のMacDiarmid教授らによってπ電子共役系ポリマーであるポリアセチレンがドナーあるいはアクセプターのドーピングによって高い導電性を示すことが発見され[1]，さらに1979年にはこのポリアセチレンが電解液中で電気化学的に可逆なイオンのドーピング，脱ドーピングを行うことが明らかとなった[2]．これを端緒に導電性高分子が二次電池の電極活物質となりうることが示され，特にリチウム負極と組み合わせた場合，高分子の持つ軽量，柔軟性という特徴を生かした高いエネルギー密度の二次電池の作製が可能であることが，各研究者によるこの分野の研究を加速してきた．現在では，ポリマー電池の可能性と限界がほぼ明らかになりつつある．ここではポリマー電池として最も可能性が高いリチウム/ポリマー電池における，ポリマーカソードの評価法，すなわち正極活物質である導電性高分子の特性評価法について紹介する．

2　リチウム/ポリマー二次電池の特性評価

二次電池電極材料の評価基準としては次のようなものが考えられる．①起電力/放電電圧（$\pi-\pi^*$準位），②充放電容量（ドーピングレベル），③エネルギー密度（①×②），④最大電流密度，⑤自己放電性，⑥サイクル特性，⑦材料の機械的強度，⑧材料コスト，⑨毒性，等々．このような評価基準をもとにしてリチウム/ポリマー二次電池の評価を行う必要がある．

リチウム/ポリマー二次電池の特性は正極であるポリマーの電気化学的特性によって大きく影響を受ける．このため電池の特性評価に際してはポリマー正極の電気化学的特性の評価は重要となる[3]．二次電池の特性評価および各測定法の理論は他の成書[4,5]に譲るとして，ここではポリマー正極の基礎特性およびその電池特性との関連性についての評価を，我々が研究を行ってきた電解重合導電性高分子を例に挙げて解説する．

2．1　サイクリックボルタンメトリー法

電気化学反応の初期診断法として有用なサイクリックボルタンメトリーはポリマー正極の基礎特性を評価する上でたいへん有効な手段である．以下に正極のサイクリックボルタモグラムから得られる情報を挙げる．

①ボルタモグラム波形から二次電池を組んだ際の充電および放電電圧が推測できる．
②電位窓から正極の過充電および過放電電圧がわかる．
③電流値の積分により正極の酸化還元容量がわかる．
④電流値より定電流電池充放電試験の際の適切な電流密度を予想できる．

以上の情報を得るためには電位の掃引は充分に遅い速度で行う必要がある．これは，速い掃引においては電極反応は拡散の影響を大きく受け，充分な酸化還元電流が流れず，またそのピーク電位がシフトするためである．このため，これらの測定を行う際には予備実験として電位掃引範囲および掃引速度を変えてボルタモグラムをとる必要がある．Fig. 1にポリアニリン，ポリピロール，ポリアズレンのサイクリックボルタモグラムの代表例を

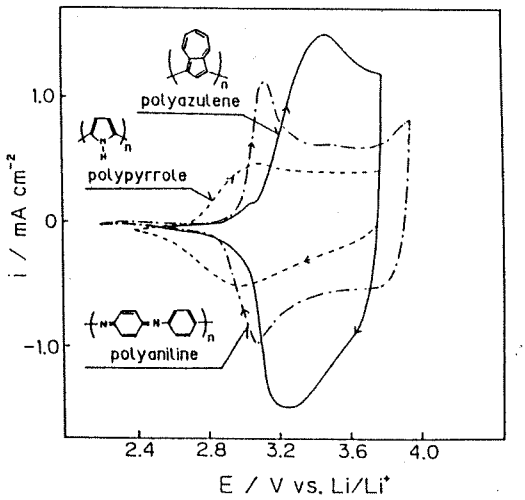

Fig. 1　Cyclic voltammograms of polyaniline (PAn), polyazulene (PAz), and polypyrrole (PPy) in 1.0 mol dm^{-3} $LiClO_4$/PC electrolyte. Films were formed with 1C cm^{-2}.

早稲田大学理工学部（〒169 東京都新宿区大久保3－4－1）

示す[6]．このボルタモグラムから得られるレドックス容量から，Table 1のように各高分子のドーピングレベルが計算できる[3]．また，Fig. 2には各種の支持電解質を重合時に用いたときの，重合電位，重合電気量を変えて得られたポリピロールのレドックス容量を示す[7]．明らかにレドックス容量の重合電位依存性は支持電解質に大きく依存することがわかる．このような正極の基礎的評価はリチウム二次電池を作成する上で有効である．

また，電位掃引速度を変えたボルタンメトリーから，電極反応の律速段階を推し量ることが可能である．一般に，電位掃引速度が大きくなるにつれ電流値は増加し，ピークはシフトしブロードになる．サイクリックボルタモグラムで，拡散が律速となる系においては，アノードピーク電流 i_{pa} は電位掃引速度 v の 1/2 乗に比例し，電荷移動反応が律速の系では i_{pa} は v に比例する．電極上のポリマーの酸化還元挙動が金属電極上における不均一反応と同様であると仮定すると，この関係を利用して i_{pa} vs. v プロットを両対数グラフに表せばその直線の傾きから v の指数 x を求められる．この x は 0.5 から 1 の間の値を示し，電極反応速度におけるイオンの拡散の影響を半定量的に推し量ることができる[6]．

また，サイクリックボルタモグラムを，電池の負極となるリチウム金属を Li/Li^+ 参照極として測定すると，電位－電池電圧の変換が容易となる．

Table 1 Maximum doping levels of electro polymerized conducting polymers.

	Maximum doping level (%)
Polyaniline	50～60
Polyazulene	30～45
Polypyrrole	25～45

2. 2 交流インピーダンス法[9]

電極反応の交流応答を測定する交流インピーダンス法は印加周波数を変えることで反応の素過程を分離することが可能で，精度の高い非定常法の一つとして反応速度の速い系の解析に有効であるため，電極反応や電池特性の評価に有効な手段である．ここでは，電池正極特性の評価を目的としたポリマー電極の解析例を示す．

インピーダンス測定結果は複素インピーダンスを複素平面上に描くコールコール（Cole-Cole）プロットがよく用いられる．結果の解析は，電極と溶液界面のモデルを電気回路モデルに表した等価回路を用いて行うことができる．等価回路は電荷移動抵抗 r と電気二重層容量 C_{dl} の並列回路として表された Randles 型の回路を基本とする種々の回路が提案されている[10,11]．この等価回路の設計および選択には反応の素過程を充分に吟味した上で理論的裏付けを持った対応が必要となる．

Fig. 3 に最も一般的な等価回路と，そのインピーダンス応答のコールコールプロットを挙げる[12]．コールコールプロットは複素平面の第 4 象限に現れる．高周波数側には r と C_{dl} の並列回路に相当する半円が現れ，その直径は r に相当する．電荷移動抵抗 r は反応のしやすさを表す速度論的パラメーターであり，r の値が小さなものほど電荷移動反応の過電圧が小さいことを示す．ポリマー電極の場合には，rC_{dl} で表される時定数 τ は一定の値ではなく，電極の形状や，高分子であることに起

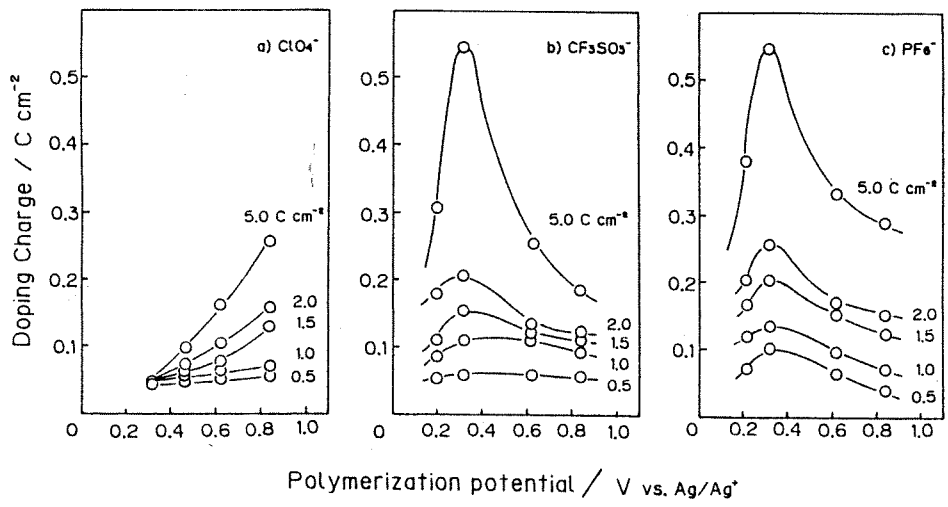

Fig. 2 Dependence of the doping charge of polypyrrole films on polymerization potential as a function of electrolyte anion.

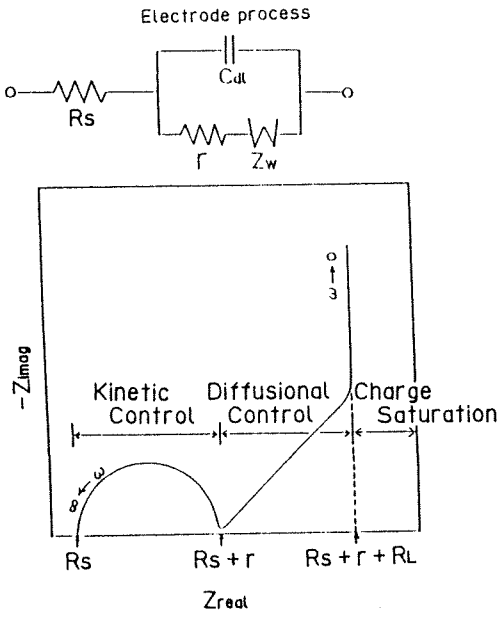

Fig. 3　The Randles equivalent circuit for the ac response of an electrochemical system and the schematic Cole-Cole plot of the system.

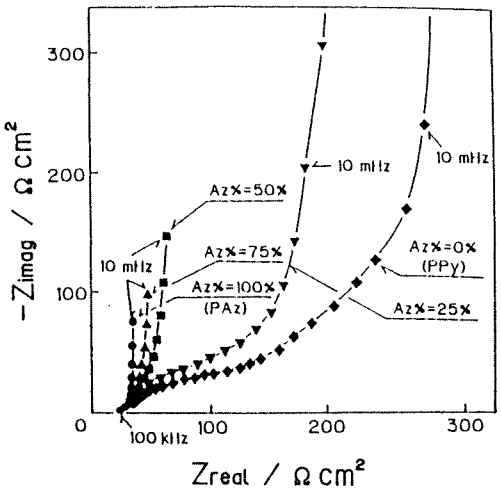

Fig. 4　Cole-Cole plots for various PPy-PAz composite films at anodic peak potentials.

因するレドックス電位の分布により，広がりを持った値となる．このためコールコールプロットにおける半円の中心は第1象限側にずれることが多い．低周波数側には拡散が支配的となる領域が現れる．半無限拡散に近似できる領域ではコールコールプロットは傾き45度の直線となり，さらに周波数が低くなり，溶液の対流の影響により拡散層の厚さが限界となる限界拡散領域では横軸に垂直な直線となる．ポリマー電極のレドックスの際にはドーパントイオンがポリマー中および電解液中に拡散層を形成するが，ポリマー膜内の拡散係数は溶液中での拡散係数に比較して3～6桁ほど小さな値を示すため，溶液中での拡散は無視でき，ここから求まる拡散係数はポリマー膜内の拡散係数Dと近似できる．Hunterら[13]によるとレドックスポリマーにおいて印加周波数が低く，コールコールプロットが横軸に垂直に並ぶ領域では，拡散層厚さLが充分に大きくなるため，角速度ωはL^2/Dより充分に小さいという条件が成立するようになる．この条件下で周波数を0に外挿したとき得られる容量（限界容量）C_Lは次式で表すことが出来る．

$$C_L^{-1}=d(-Z_{imag})/d(\omega^{-1}),\quad \omega \ll L^2/D \qquad (式1)$$

また，傾き45度の直線領域では次式が成り立つ．

$$|Z|=C_L L D^{-1/2}\omega^{-1/2} \qquad (式2)$$

通常は，正極膜厚を拡散層の厚さと仮定して用いる．この式より，$|Z|$ vs. $\omega^{-1/2}$プロットは直線となり，その傾きから式1より求めたC_Lを用いて拡散係数Dを求めることが出来る[13]．ただし，実際のポリマー膜の拡散層は膜厚よりも薄くなり，算出された拡散係数は実際よりも大きい値を示すことが多い．また，限界拡散領域の直線を横軸に外挿した値から限界抵抗（周波数を0に外挿したときに得られる抵抗）R_Lが算出される．rとR_Lの和は直流分極を行った際のポリマー電極の抵抗であり，限界容量C_Lはそのポリマー電極のレドックス容量と相関性を持っている．Fig. 4に組成を変えて作製したアズレンとピロールの共重合膜のコールコールプロットを示す[14]．この共重合膜はアズレンモノマーとピロールモノマーを含む重合液より得られ，元素分析から膜の組成比は重合液中のモノマーの比にほぼ等しい．このコールコールプロットはFig. 3の代表的なインピーダンス挙動の変化を典型的に表している．すなわちアズレン100%（ポリアズレン）膜は最も膜内の拡散が速く，ピロールの割合が増えるに従って膜内拡散が遅くなり，Fig. 3の型に近づくのがわかる．この図から求めた拡散係数および限界容量を重合液中アズレンユニット比で表したものがFig. 5である．この図からこの共重合膜は25%アズレン膜で急激な拡散係数の増加がみられ，75%アズレン膜で容量値の増大がみられる．この基礎特性は，電池特性に正確に対応し，前者の膜で急激な電池出力の増大，後者の膜で急激な電池容量の増大が確認されている[14]．

次にフィブリル状の膜形態を有するポリアニリン膜の各種有機電解液中のコールコールプロットをFig. 6に示す．明らかに溶媒による膜特性の差がインピーダンス結果で示されており，PC-DME>PC-EC>PCの順でドーパントイオンの膜内拡散が容易になっていることが

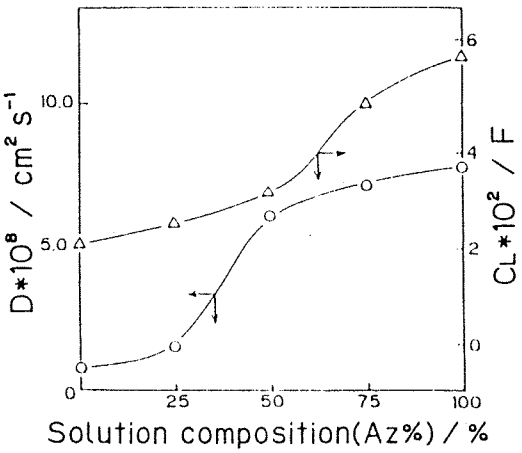

Fig. 5 Correlation between the diffusion coefficient (D) and redox capacitance (C_L) for various PPy-PAz composite films against Az%.

わかる．ここでPC，DME，ECはそれぞれプロピレンカーボネート，ジメトキシエタン，エチレンカーボネートである．Fig. 6から求めた拡散係数等の各因子はTable 2のように算出され，電解液の特性評価が可能である[15]．ただし，ポリアニリンのようなラフネスの高い膜での拡散層厚の見積りはアニリン膜厚では大きすぎ，フィブリル径を拡散層厚とすることが妥当である[15]．

Fig. 7に膜厚の異なるポリピロール電極のコールコールプロットと，その解析に用いた等価回路を示す[16]．ここでは，ポリピロールの膜厚が厚い場合には，ポリピロール膜自身の抵抗および容量が電極反応系とともに測定できるようになり，図中右側では第2円が現れている．すなわち，左図では電極反応系に対応するFig. 3のモデルのみで説明できるが，右図では膜自身の電子伝導系が電極反応の電荷移動反応系およびイオン伝導系に加わって2つの半円が現れている．

2. 3 ポテンシャルステップ・クロノアンペロメトリー（PSCA）法[17]

実際のイオンの拡散係数を求めるには印加電位をステップさせたときの電流値の変化を測定するPSCA法を用いるのが一般的である．ポリマー膜中のドーパントイオンの拡散が溶液内拡散より遅く，律速になるという仮定から，この方法による拡散係数がポリマー膜内拡散過程のものとして得ることが出来る．Fig. 8 a）にポリピロールおよびポリピロールにNBRゴムを複合させて膜を疎にしたポリピロール電極にこのPSCA法を適用した例を示す[8]．印加電位をステップさせた後の電流は式3のコットレル（Cottrell）式を満たす．

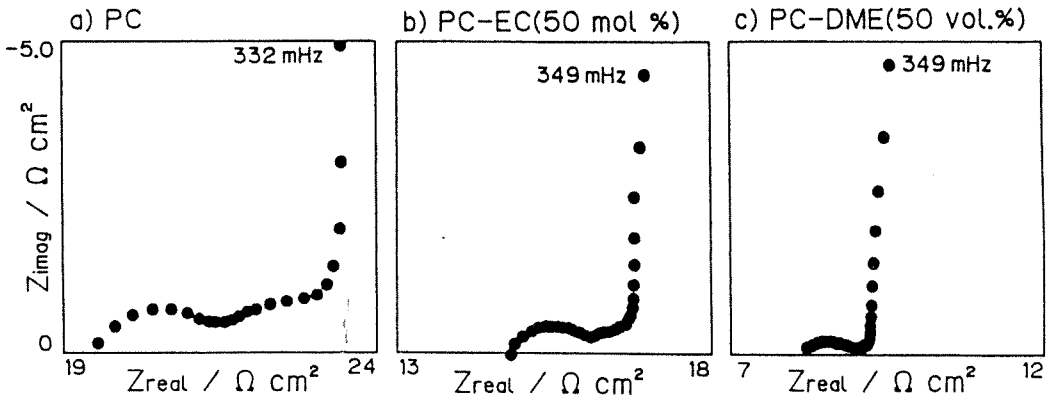

Fig. 6 Cole-Cole plots of PAn films measured in various electrolyte solutions containing $LiClO_4$ and blended solvents.

Table 2 Experimentally determined values from the rate-determining region of the charge-transfer and the finite diffusion region for PAn films (1 C cm^{-2}) deposited from PC polymerization solution, measured at various electrolyte solutions.

Polymerization solutions	Electrolyte solutions	$R_s/\Omega\ cm^2$	$r/\Omega\ cm^2$	$C_L \cdot 10^2/F\ cm^{-2}$	$R_1/\Omega\ cm^2$	$D \cdot 10^9/cm^2\ s^{-1}$
PC	PC	19.6	2.24	10.5	2.66	7.64
PC	PC-EC	14.7	1.60	10.9	0.90	21.7
PC	PC-DME	8.10	1.04	11.6	0.56	32.8

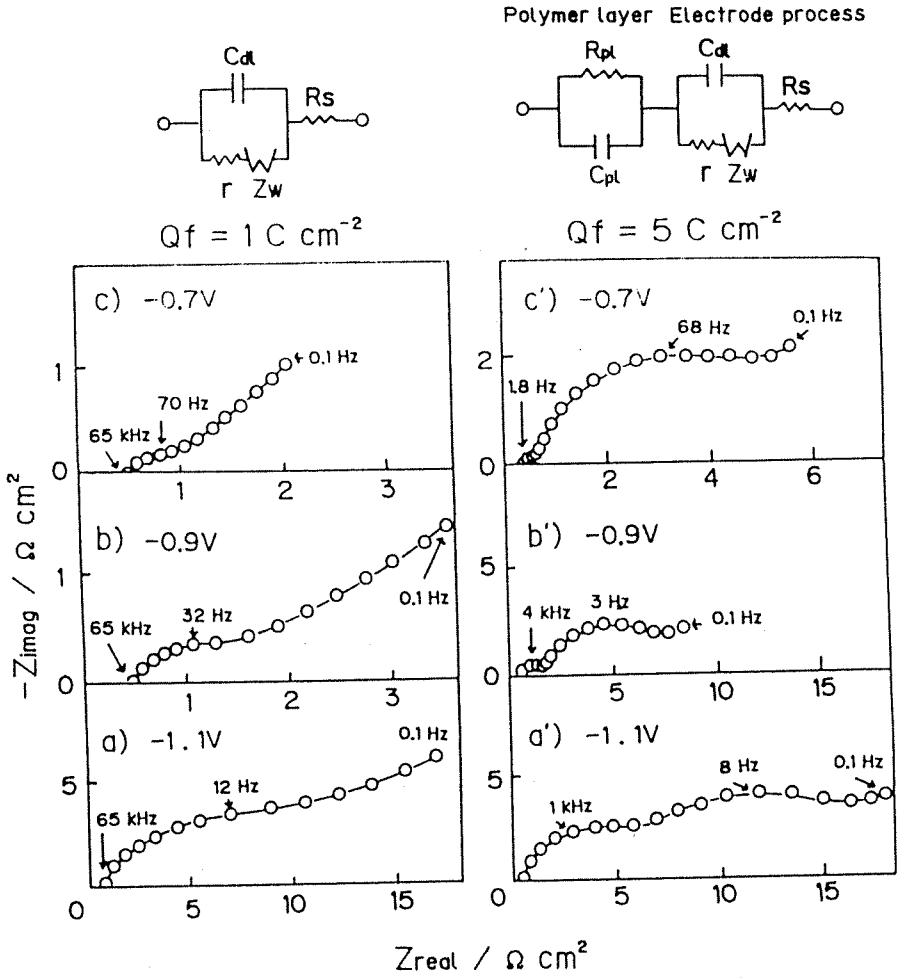

Fig. 7 Cole-Cole plots of PPy electrodes at various potentials. The film formation potentials (vs. Ag/Ag^+). are indicated in the figures. Q_f is the film formation charge.

$$i(t)=nFD^{1/2}C^{1/2}\pi^{-1/2}t^{-1/2} \qquad (式3)$$

電流の経時変化を i vs. $t^{-1/2}$プロット (Cottrell Plot) で表すと，Fig. 8 b) のように原点を通る直線が得られ，この直線の勾配よりポリマー膜内のドーパントイオンの拡散係数の算出が可能である．この場合，NBR/PPy の方が明らかに傾きが大きく，この膜の方が拡散係数 D が大きいことは明らかである[8]．

2. 4 電池充放電試験

二次電池の電池充放電特性を評価する際の，充電および放電のモードにはそれぞれ定電圧充電，定電流充電，定負荷放電，定電流放電などがある．これらのモードは評価しようとする目的に応じて選択する必要がある．それぞれのモードの特徴を以下に述べる．定電圧充電は電極反応において副反応を抑制することができ，電池容量の評価には便利な方法である．また，電池と抵抗で閉回路を形成する定負荷放電は実用に近い放電様式となるため，製品化する際に有効である．これに対して定電流による充放電では時間を制御することにより充放電深度が制御できる．このため基礎特性を評価する手段としては他の方法よりすぐれている．

ここでは定電流充放電について基礎特性評価を行った一例を示す．通常，充電量は電池電圧が一定の値に達したところ，あるいは充電時間により制御し，放電は時間あるいは電極の過放電を避けるため電圧がある値に達したところで停止させる．この際の電池電圧の変化を充放電時間に対してとると，Fig. 9 のような定電流充放電曲線が得られる[16]．左図は低い電位で重合した密なポリピロールを正極にした例で，右図は高い電位で重合した疎な膜の例である．明らかに右の方が充放電特性が向上していることがわかる．ここで充電時間，あるいは充

放電時の電流値を変化させ，その際の放電時間すなわち放電量をプロットすると Fig. 10 に示すように電極の充電容量および充放電速度依存性がわかる[6]．また，サイクルを重ねて充放電を行えば，サイクル特性が評価できる[6]．この様な充放電試験の際には，前もってサイクリックボルタンメトリーなどの電気化学的手法により，酸化還元電位や拡散が支配的とならない電流密度，酸化還元容量などを見積っておく必要がある．

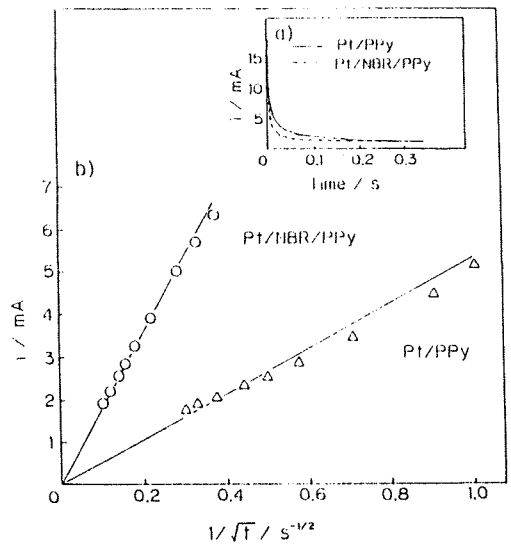

Fig. 8 Potential step chronoamperometry for PPy and NBR/PPy electrodes. a) Decay curves, b) Cottrell plots.

2. 5 その他の測定法

ポリマー膜の基礎特性評価を行う上で電気化学的測定以外の測定法による評価も重要である．電解重合導電性高分子はその作成方法により種々の特性の膜が作成可能で，得られたポリマー膜の特性はその膜形態に大きく依存する．従って形状の観察は重要で，光学顕微鏡や走査型電子顕微鏡（SEM）による観察は，膜形状を把握する上で有効な手段である．この二つを比較すると，光学顕微鏡は簡便で非破壊測定であり，顕微鏡観察した後で他の測定が可能であるという利点を持つ．これに対して SEM は高倍率でしかも焦点深度が深いといった特徴を持つ反面，電子線による表面損傷が生じ，また真空中での観察のため破壊測定となる．電解重合導電性高分子は一般に表面の凹凸が大きいため，SEM がよく用いられている．

さらに，最近では膜内のイオンの出入りを *in situ* で測定する QCM 法や PDIM 法が膜の評価に利用されだしており[19]，今後，いくつかの *in situ* 測定も有効に利用されるようになるであろう．

3 おわりに

リチウム/ポリマー電池に限らず高エネルギー密度の二次電池の需要が今後ますます高まるのは必至である．二次電池の基礎的評価は電極反応解析が主である．多く

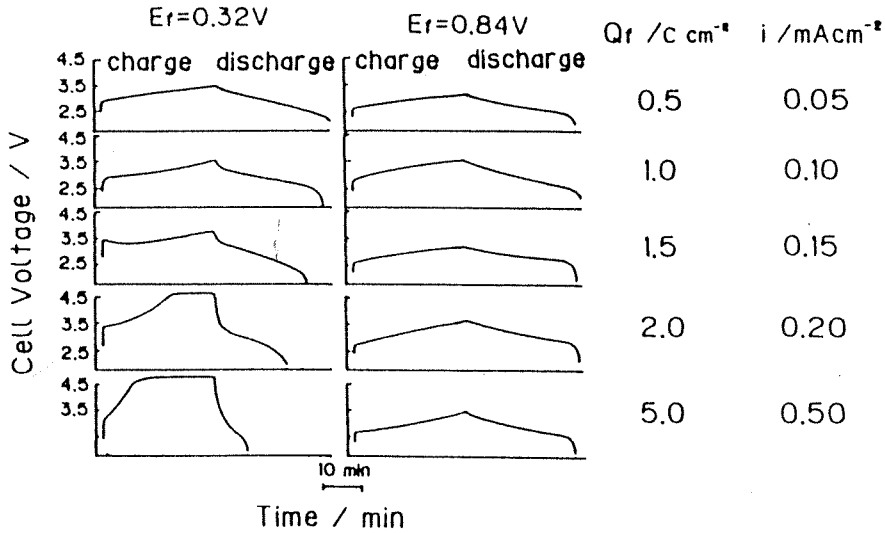

Fig. 9 Charging-discharging curves for Li/PPy batteries with various thickness PPy cathodes. The film formation charge Q_f and potential E_f (V vs. Ag/Ag^+) and charging-discharging current density i are indicated in the figure.

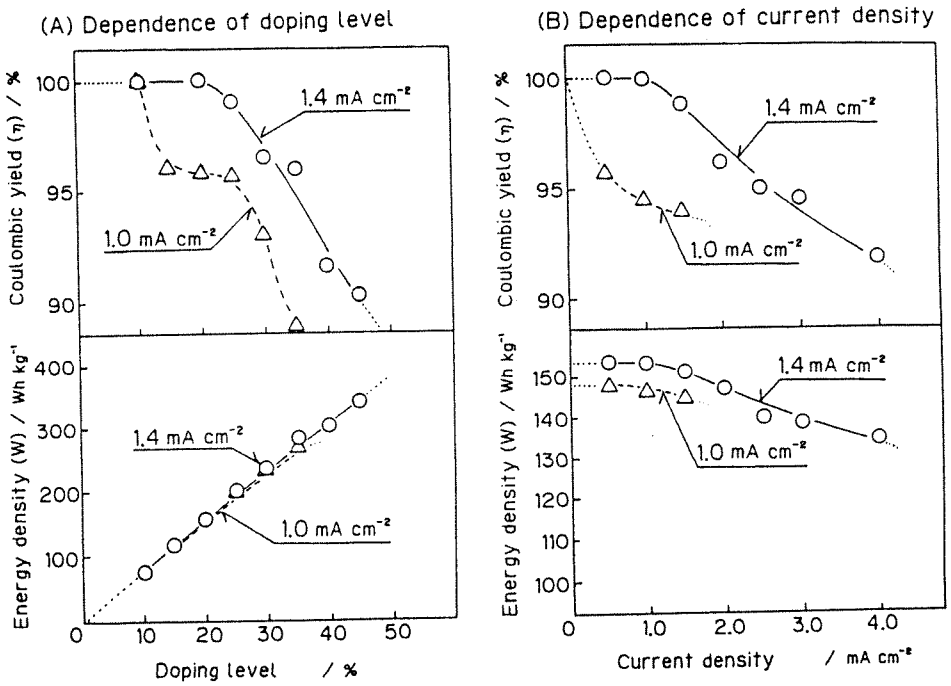

Fig. 10 The dependence of Li/PAz battery performances on doping level and current density as a function of the film formation current. The charging-discharging current density was 0.5 mA cm^{-2} for (A) and the doping level was 20% for (B).

の素反応および副反応を含む電極反応は，一つの測定法のみで得られる情報だけでは充分な評価が出来ないため，今後は反応機構を鑑み，電気化学的測定のみならず多角的な測定法を複合させた解析が行われるようになってくるであろう．

文　献

1) H. Shirakawa, E. J. Louis, and A. G. MacDiarmid, *JCS Chem. Commun.*, 1977, 578 (1977).
2) P. J. Nigrey, A. G. MacDiarmid, and A. J. Heeger, *JCS Chem. Commun.*, 1979, 574 (1979).
3) 逢坂哲彌，直井勝彦，金属表面技術，39，486 (1988).
4) 吉澤四郎，“電池”，講談社 (1982)；高村　勉，佐藤祐一，“ユーザーのための電池読本”，電子情報通信学会 (1988)；逢坂哲彌，小山　昇，“電気化学法－応用測定マニュアル”，講談社サイエンティフィク (1990)；藤島　昭，相澤益男，井上　徹，“電気化学測定法”，技報堂出版 (1984)；外島　忍，佐々木英夫，“電気化学”，電気学会 (1976)；等々．
5) 逢坂哲彌，小山　昇，大坂武男，“電気化学法－基礎マニュアル”，講談社サンエンティフィク (1989).
6) K. Naoi, K. Ueyama, and T. Osaka, *J. Electrochem. Soc.*, 136, 2444 (1989).
7) T. Osaka, K. Naoi, and S. Ogano, *J. Electrochem. Soc.*, 135, 1071 (1988).
8) K. Naoi and T. Osaka, *J. Electrochem. Soc.*, 134, 2479 (1987).
9) 参考文献5) の p.157.
10) J. E. B. Randles, *Disc. Faraday Soc.*, 1, 11 (1947).
11) 直井勝彦，永瀬幸雄，逢坂哲彌，金属表面技術，36，404 (1985).
12) R. M. Penner, L. S. Van Dyke, and C. R. Martin, *J. Phys. Chem.*, 92, 5274 (1988).
13) T. B. Hunter, P. S. Tyler, W. H. Smyrl, and H. S. White, *J. Electrochem. Soc.*, 134, 2198 (1987).
14) K. Naoi, K. Ueyama, T. Osaka, and W. H. Smyrl, *J. Electrochem. Soc.*, 137, 494 (1990).
15) T. Osaka, T. Nakajima, K. Shiota, and T. Momma, *J. Electrochem. Soc.*, 138, 2853 (1991).
16) T. Osaka, K. Naoi, and S. Ogano, *J. Electrochem. Soc.*, 134, 2096 (1987).
17) 文献5) の p.126.
18) T. Osaka, K. Naoi, H. Sakai, and S. Ogano, *J. Electrochem. Soc.*, 134, 285 (1987).
19) 逢坂哲彌，電気化学，58，218 (1990).

Electrochimica Acta, Vol. 37, No. 6, pp. 989–995, 1992
Printed in Great Britain.

0013-4686/92 $5.00 + 0.00

REVIEW ARTICLE

ELECTROCHEMICAL ASPECTS OF ADVANCED ELECTRONIC MATERIALS

TETSUYA OSAKA
Department of Applied Chemistry, Waseda University Okubo, Shinjuku-ku, Tokyo 169, Japan

(*Received* 27 *August* 1991)

Abstract—Electrochemical ideas and techniques are widely used in advanced electronic materials. As one of the most representative types of highly functional materials, magnetic recording materials are introduced and reviewed to illustrate the potential of electrochemical techniques.

Key words: electronic material; electroless-plating, functional thin film, high density magnetic recording media, thin film heads.

INTRODUCTION

During past decades the electronics industry has gone through a very rapid evolution towards the use of thinner films, in which electrochemical techniques have often played an important role[1]. The technologies used in advanced electronic materials including the plating of Co alloys with a very thin, homogeneous thickness distribution and the plating of NiP amorphous underlayers for high density magnetic rigid disks, the plating of the NiFe alloys with extremely tight compositional control in narrow places and the plating of Cu with fine coil patterns for thin film heads, the plating of Ni alloys of heating resistors with higher thermal stability for thermal printing heads or thin film resistors for hybrid ICs, and the plating of Cu or precious metal alloys with highly reliable contacts, connectors, and conductors for widely-used printed wiring boards. Figures 1, 2 and 3 are photographs of high aspect ratio (*ca* 20) through hole Cu plating of a 42 multi-layer printed wiring board (Fujitsu Ltd)[2], fine coil pattern (3.0 μm coil, 1.3 μm gap, 5 μm height) Cu plating of a thin film head (NEC Corp.)[3], and NiWP plating of heating resistors for a thermal printing head[4]. In 1990, multi-layer printed wiring boards of more than 50–60 layers were shipped by Fujitsu Ltd and NEC Corp. Typical examples of plating used in electronic materials, including both electrolytic and electroless plating, are listed in Table 1. Development of such new, high-level techniques is a tremendous challenge for electrochemical scientists and engineers.

When the features of electrochemical (wet) processes and vacuum (dry) processes are compared, the advantages of wet processes are mass-productivity and cost performance of the apparatus as is seen in Table 2. The disadvantages are limitations on the deposited metal elements and complicated systems that are not familiar to and are often avoided by electrical engineers. In the advanced electronic materials field, electrochemical ideas and techniques will often give us the solution to the challenges we face, if we attempt to utilize new, high-level techniques with consideration of these features.

HIGH DENSITY MAGNETIC RECORDING APPLICATIONS

Electrochemical plating of magnetic recording layers

Highly functional magnetic recording materials are one of the most typical examples of materials formed by highly controlled techniques. Figure 4 shows the progress towards higher storage of magnetic recording density for rigid disks, in particular. In this field, thin film heads constructed of an electroplated NiFe core and a Cu coil and thin film rigid disks using electroless-plated CoNiP and amorphous NiP alloy films have been adopted as practical means for making the density higher.

Region I indicates conventional combinations of a coated disk and a bulk head. Region II is the area of transition to region III, where the combination of a thin film disk and a thin film head is adopted. The combination of a thin film head and a thin film disk at region III was made a reality in 1989. Recently, IBM (in 1990[5]) and Hitachi (in 1991[6]) announced prototype machines with area densities of 1 and 2 Gbits in^{-2}, respectively. In these machines, a thin film disk and an inductive-write MR-read composite head of 120 kBPI, 8.5 kTPI are used by IBM and one of 120–150 kBPI and 17 kTPI are used by Hitachi. Why is a thinner film disk used in order to increase recording density? The main reason is to decrease demagnetization. Fortunately, the use of an electroless plating method is advantageous in the formation of a homogeneous film even over a large disk area as well as advantageous in terms of mass-productivity.

A perpendicular magnetic recording system, which is a promising future system for high density recording, has been proposed by Iwasaki[7, 8]. This system has very high resolution, comparable to the size of

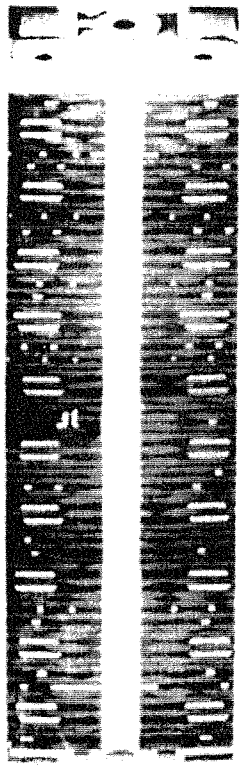

Fig. 1. Photographs of cross-sectional view of high aspect ratio through hole copper electroplating for printed wiring board with 42 layers (Fujitsu Ltd). Aspect ratio = *ca* 20.

micro-crystalline particles of the recording medium, and with its use, achievement of high density of Tera bits in^{-2} is theoretically foreseen[9]. The first

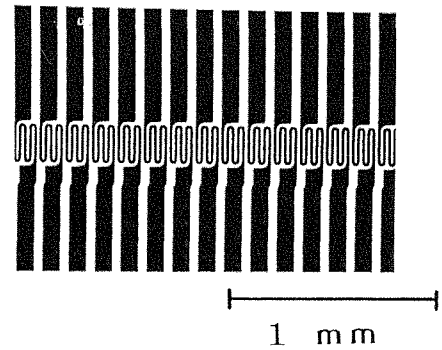

Fig. 3. Photograph of heating resistor of NiWP electroless plating for thermal printing head (OKI Electric Industry Ltd). 8 dots mm^{-1} (13 μm, gap 12 μm).

successful results for a perpendicular magnetic recording medium were obtained with a sputtered CoCr film[10]. Perpendicular magnetic recording media usually require the condition of Hk (anisotropy field) $> 4\pi Ms$ (saturation magnetization). Many kinds of perpendicular media have been proposed that satisfy this condition. Moreover even for perpendicular media, it is desirable for the saturation magnetization, Ms, and perpendicular coercivity, $Hc(\perp)$, to be higher in order to make the signal higher. The schematic drawing of the relation between Ms and $Hc(\perp)$ in Fig. 5 is a modification of one originally reported by Ouchi[11]. Electroless-plated alloy films have been applied to perpendicular magnetic recording media by our group[12, 13]. Figure 6 is a schematic graph of how we have developed our electroless-plated magnetic recording media. Our latest developments are simplified CoNiReP[14] and CoNiP[15, 16] alloys. The Ms of

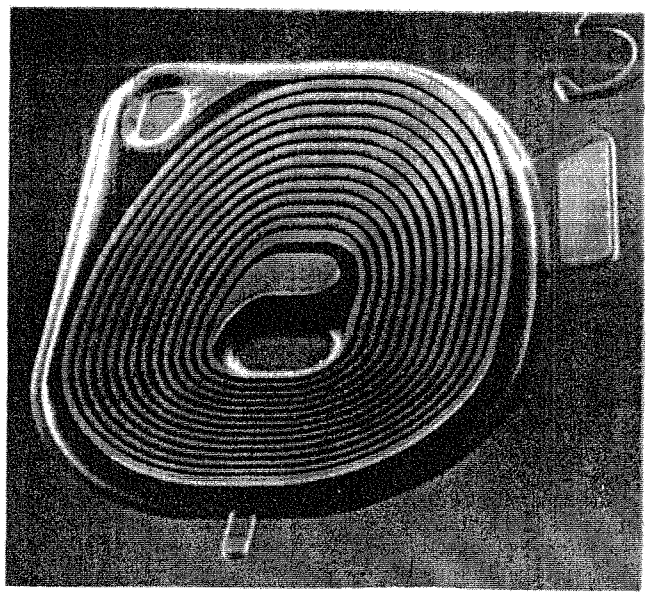

Fig. 2. Photograph of fine coil pattern of copper electroplating for thin film head (NEC Corp.). Cu coil 3.0 μm, gap 1.3 μm, height 5 μm.

Table 1. Application of electrolytic or electroless-plating to electronic components

Item	Application
Printed wiring board	Conductors subtractive method semi-additive method fully-additive method Resistors (NiP) hybrid IC Contacts (Au, Ag, PdNi)
Magnetic materials	Magnetic disks (CoNiP, CoP) Underlayer for magnetic disks (NiP) Thin film magnetic heads (NiFe)
Video disk	Stampers (Ag, NiP, Ni) Initial thin film of stamper master
Contact material	Connector bumps (Au, Ag, Ni) Lead frames (Ag)
High frequency material	Microwave waveguide (Cu, Ni, Au, Ag)
Electromagnetic wave shielded materials	EMI shield (Cu, Ni)
Si device	Via holes for electrodes (NiB) Connectors for solar cells (NiP)

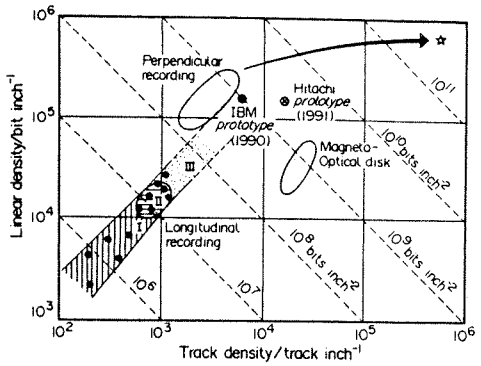

Fig. 4. Recent trends in recording density for magnetic disks. I: coated disk + bulk head, II: coated disk + thin film head, or thin film disk + bulk head, III: thin film disk + thin film head, x: inductive (write)/MR (read) composite head.

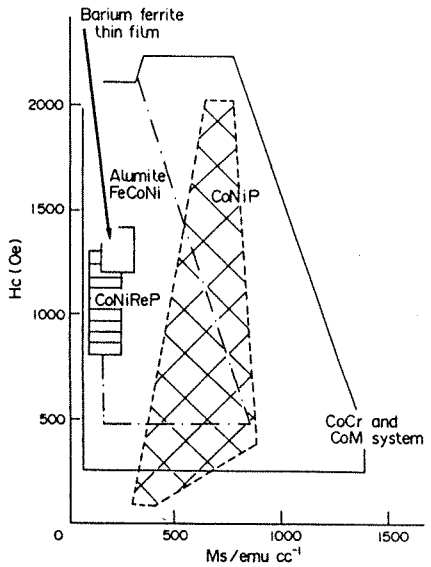

Fig. 5. Relation between *Ms* and *Hc*(⊥) of candidate media for perpendicular magnetic recording.

CoNiReP is lower, but the CoNiP has a higher value of *Ms*. We recently confirmed an extremely high recording density of $D_{50} = 172$ kFRPI and a higher 300 kFRPI output signal for a CoNiReP/NiWP flexible medium combined with a 0.2 μm gap Sendust ring-type head[17] and a density of $D_{50} = 134$ kFRPI using a CoNiReP/NiFeP rigid disk combined with a MIG head with less than 0.1 μm of spacing[18]. This was achieved through the two effects of underlayer, *ie* the so-called "double layer effect", in which reproduced voltage is enlarged due to stabilization of the recording magnetization by the soft magnetic underlayer, and the "underlayer effect", in which the crystallinity and crystal orientation of the magnetic medium is improved by the surface structure of the underlayer[19]. Examples of microstructural analysis are shown in Fig. 7, including a RHEED pattern of the surface and TEM bright and dark field images of a cross-section of the CoNiReP film[20]. The RHEED pattern indicates that the *c*-axis of the hcp Co crystal is strongly oriented normal to the film plane. Since the *c*-axis of hcp Co is an easy axis direction of magnetization, the film satisfies the needs of perpendicular medium. From the TEM images, it can be seen that columns of hcp Co within a diameter of 30 nm are clearly formed. Since the linear density corresponding to 30 nm is 833 kBPI, the magnetic recording density would be limited by the physical structure of the film if one magnetic bit area is assumed to exactly correspond to the column size. However, from wet etching analysis, we have concluded that the CoNiReP film has a microstructure consisting of magnetically isolated fine Co alloy

Table 2. Comparison of dry vacuum and wet plating methods

Item	Dry method	Wet method
System	vacuum, simple	open, complicated
Cost	high	low
Mass productivity	low	high
Waste water treatment	none	needed
Elements to be deposited	almost unlimited	limited
Shape of film	relatively small area	relatively large area
Deposition temperature	relatively high	relatively low
Substrate	conducting and non-conducting materials	conducting and non-conducting materials

particles dispersed in a non-magnetic NiP amorphous region[21]. Moreover, it has been shown that the 30 nm columns are composed of fine, more precise particles, suggesting the possibility that the density will be limited not by the column size but by this more precise, minute physical structure[21].

We have pointed out that in a perpendicular recording system with a ring-type head a very thin quasi-soft magnetic underlayer effectively supports the enhancement of output voltage[19]. Recently, we proposed an interesting medium system using the CoNiReP/NiMoP medium, where a non-magnetic NiMoP underlayer controls the microstructure of a CoNiReP upperlayer. The magnetic upperlayer automatically becomes two component layers comprising a quasi-soft magnetic initial layer and a perpendicular anisotropy layer, and the initial layer thickness can be controlled by the underlayer plating conditions[22, 23]. Such a system is preferable to investigating what combination of upper- and under-layers will be the best for a certain system.

Electrochemical plating of soft magnetic layers

The first commercial thin film head was mounted on the IBM 3370 disk drive in 1979, in which an

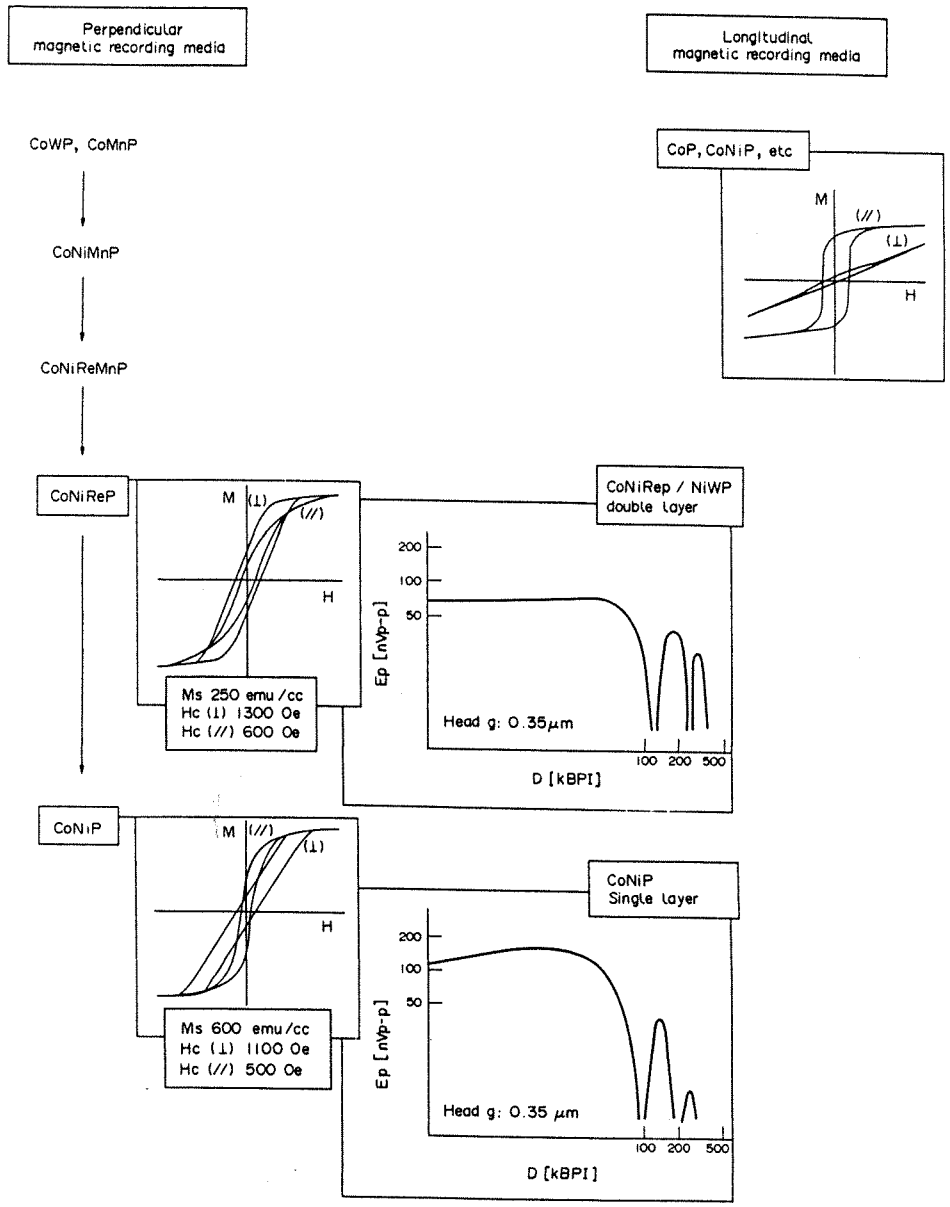

Fig. 6. Electroless-plated magnetic recording media developed through our research.

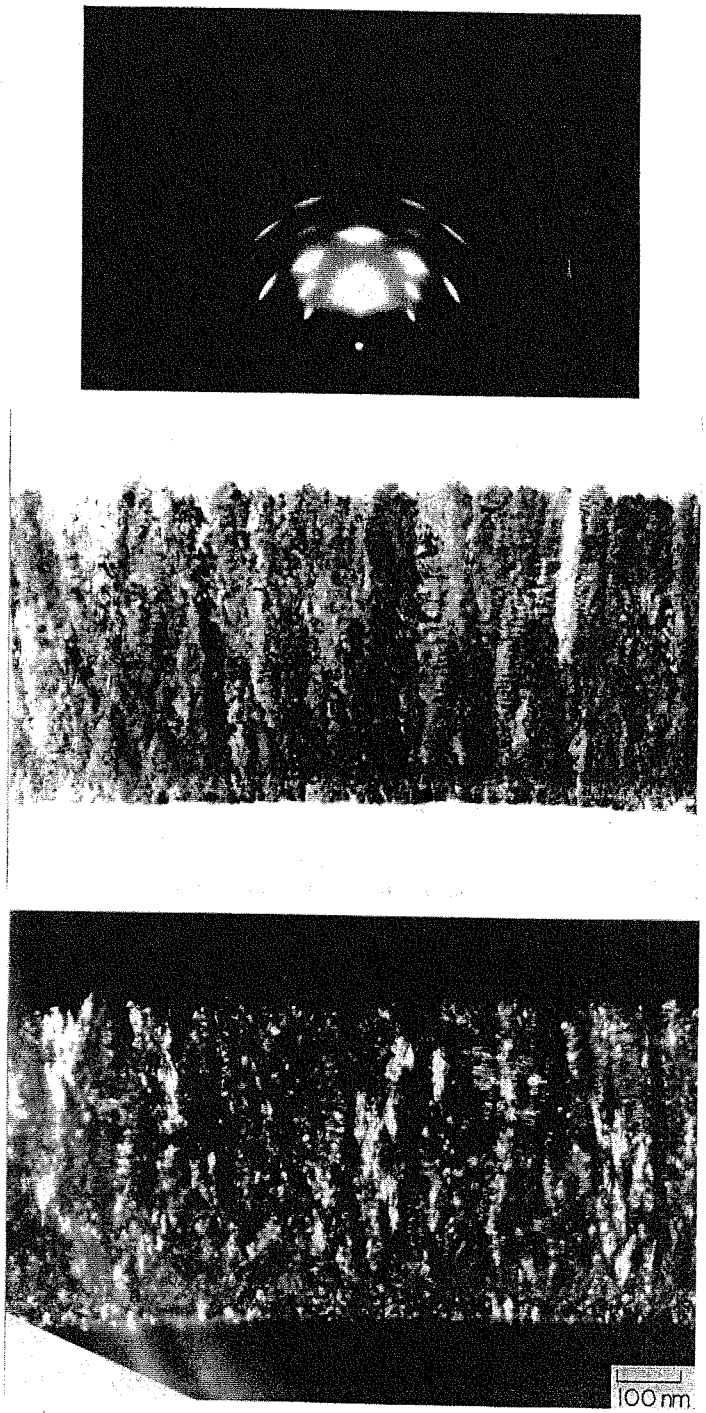

Fig. 7. Typical example of structural analysis by RHEED and TEM (bright and dark field) for electroless-plated CoNiReP media.

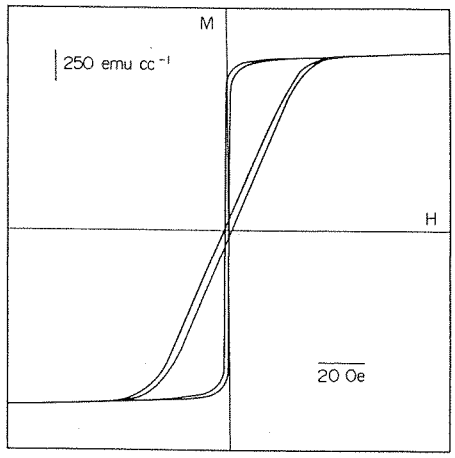

Fig. 8. Electroless-plated soft magnetic thin films developed through our research.

electroplated NiFe film of *ca* 80 wt% Ni possessing almost zero magnetostriction, λs, was used[24]. The thin film head with an electroplated soft magnetic film provided higher read efficiency due to the higher permeability and thickness uniformity of the plated NiFe. Electroplated CoFe films with a high saturation flux density of $Bs = 1.9$ Tesla, almost twice that of permalloy, have recently been reported and a prototype thin film head using CoFe had overwrite characteristics 10 dB higher than those of a permalloy head[25].

We have attempted to fabricate electroless-plated soft magnetic thin films using DMAB (dimethylamineborane) as a reducing agent[26]. Figure 8 represents the hysteresis loop of a CoB film formed with an external magnetic field of 560 Gauss[27] (see also Table 3). The particles of CoB apparently are quite fine as is seen in Fig. 9. It works as a soft magnetic film even when containing a high Co content (Co 96 at%), and its saturation flux density is $Bs = 1.76$ Tesla. The addition of Fe improves the permeability and its saturation flux density becomes $Bs = 1.86$ Tesla. This film may have great possibilities as a thin film head, due to its high saturation flux density and almost zero magnetostriction[27].

Table 3.

	$Co_{96}B_4$ (Hext)	CoB
Ms (emu cc^{-1})	1400	1400
Hc (Oe)	0.64	1.20
Hk (Oe)	40	40
μ (5 MHz)	520	—
λs	-4.2×10^{-7}	—

CONCLUSIONS

The high potential capabilities of electrochemically formed thin films for advanced electronic materials is being demonstrated through research and development. Also, new attempts at electrochemically forming polymers into functional electronic materials are progressing in the organic materials field[28–30]. New, highly advanced electronic materials will result from developments in electrochemical methods, when approaches are made on the basis of their merits, *ie* cost performance, mass-productivity, uniformity of thin film formation over large areas, and so on. At the same time, research in this field should be done in order to clarify the relationships between film properties and the atomic level microstructures of films[31, 32]. The results of such research will help us understand how to control and create the film properties of highly functional materials.

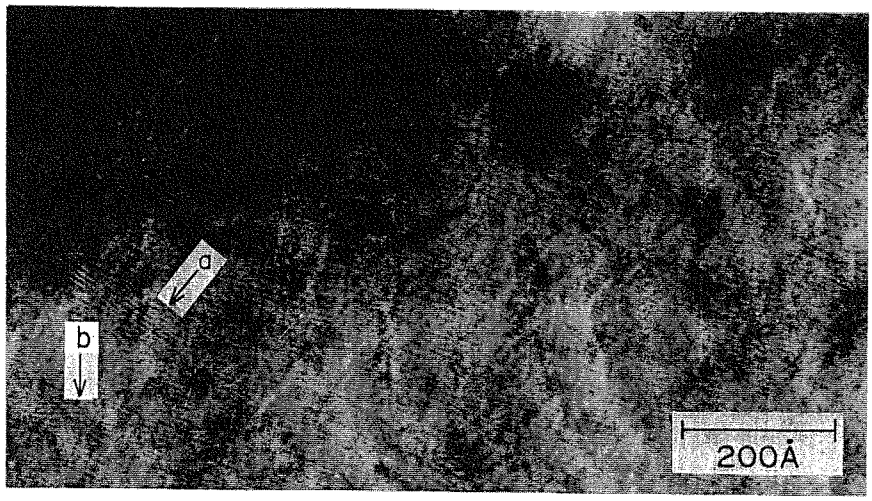

Fig. 9. Typical example of TEM bright field image for electroless-plated CoB film of 50 nm thick. (a) Region of moire's junction; (b) region of moire's disappearance.

REFERENCES

1. *Proc. Symp. on Electrochemical Technology in Electronics*, Vol. 88–23 (Edited by L. T. Romankiw and T. Osaka). Electrochem. Soc. Inc., Proc. (1988).
2. K. Takagi, *Denshi Gijutsu (Electronic Technology)*, **32**(12), 80 (1990).
3. K. Ohashi, M. Ito and M. Watanabe, in *Proc. Symp. on Electrochemical Technology in Electronics*, Vol. 88–23 (Edited by L. T. Romankiw and T. Osaka) p. 525, Electrochem. Soc. Inc., Proc. (1988).
4. H. Sawai, T. Kanamori, I. Koiwa, S. Shibata, K. Nihei and T. Osaka, *J. electrochem. Soc.* **137,** 3653 (1990).
5. T. Yogi, C. Tsang, T. A. Nguyen, K. Ju, G. L. Gorman and G. Castillo, *IEEE Trans. Magn.* **26,** 2271 (1990).
6. M. Futamoto, F. Kugiya, M. Suzuki, H. Takano, Y. Matsuda, N. Inaba, Y. Miyamura, K. Akagi, T. Nakao and H. Sawaguchi, *IEEE Trans. Magn.* **27** (1991).
7. S. Iwasaki and Y. Nakamura, *IEEE Trans. Magn* **MAG-13,** 1272 (1977).
8. *Perpendicular Magnetic Recording* (Edited by S. Iwasaki and J. Hokkyo). Ohmsha (1991).
9. Y. Nakamura, *J. Magn. Soc. Jpn* **14,** 593 (1990).
10. S. Iwasaki and K. Ouchi, *IEEE Trans. Magn* **MAG-14,** 849 (1978)
11. K. Ouchi, 10th Takei Seminar Text, (1990).
12. T. Osaka, N. Kasai, I. Koiwa, F. Goto and Y. Suganuma, *J. electrochem. Soc.* **130,** 568 (1983).
13. I. Koiwa, H. Matsubara, T. Osaka, Y. Yamazaki and T. Namikawa, *J. electrochem. Soc.* **133,** 685 (1986).
14. I. Koiwa, M. Toda and T. Osaka, *J. electrochem. Soc.* **133,** 597 (1986).
15. T. Osaka, T. Homma, K. Inoue and K. Saga, *Denki Kagaku* **58,** 661 (1990).
16. T. Homma, K. Inoue, H. Asai, K. Ohrui, T. Osaka, Y. Yamazaki and T. Namikawa, *J. Magn. Soc. Jpn* **15,** 113 (1991).
17. H. Matsubara, S. Mitamura, K. Noda and T. Osaka, *J. Magn. Soc. Jpn* **13,** 679 (1989).
18. T. Osaka, T. Homma, K. Saito, K. Noda, F. Goto, N. Shiota and T. Yamamoto, *IECE Tech. Group Meeting of Magnetic Recording* **MR90-10,** 1 (1990).
19. H. Matsubara, K. Yamanishi, K. Mizutani and T. Osaka, *J. Metal Finishing Soc. Jpn* **37,** 708 (1986).
20. T. Osaka, T. Homma, K. Inoue, Y. Yamazaki and T. Namikawa, *J. Magn. Soc. Jpn* **13,** 85 (1989).
21. T. Osaka, T. Homma, K. Inoue, Y. Yamazaki and T. Namikawa, *J. Magn. Soc. Jpn* **13**(S1), 779 (1989).
22. H. Matsubara, H. Mizutani, S. Mitamura and T. Osaka, *Jpn. J. Appl. Phys.* **27,** 1895 (1988).
23. H. Matsubara, S. Mitamura, K. Noda and T. Osaka, *J. Magn. Soc. Jpn* **13**(S1), 679 (1989).
24. R. E. Jones, *IBM Disk Storage Technology*, 3 (1980).
25. S. H. Liao, *IEEE Trans. Magn* **MAG-23,** 2981 (1987).
26. T. Osaka, T. Homma, N. Masubuchi, K. Saito, M. Yoshino, Y. Yamazaki and T. Namikawa, *J. Magn. Soc. Jpn* **14,** 309 (1990).
27. T. Osaka, T. Homma, K. Saito, A. Takekoshi and H. Shimura, *Proc. Surf. Finishing Soc. Jpn* 27B-6 (1991).
28. T. Osaka, T. Nakajima, K. Shiota and B. B. Owens, *Proc. Symp. on Rechargeable Lithium Batteries*, Vol. 90-5, p. 170. Electrochem. Soc. Inc., Proc. (1990).
29. T. Osaka, K. Ouchi and T. Fukuda, *Chem. Lett.* 1535 (1990).
30. T. Osaka, T. Fukuda, K. Ouchi and T. Nakajima, *Denki Kagaku* **59**(12) (1991) in press.
31. T. Homma, T. Yamazaki, T. Kubota and T. Osaka, *Jpn J. appl. Phys.* **29,** L2114 (1990).
32. T. Homma, K. Naito, M. Takai, T. Osaka, Y. Yamazaki and T. Namikawa, *J. electrochem. Soc.* **138,** 1269 (1991).

Thin Solid Films, *215* (1992) 200-202

Conduction mechanism in indium tin oxide/electroinactive polypyrrole/indium tin oxide sandwich structures

Tetsuya Osaka, Toshihiro Fukuda, Kiyoshi Ouchi and Toshiyuki Momma

Department of Applied Chemistry, School of Science and Engineering, Waseda University, 3-4-1 Okubo, Shinjuku-ku, Tokyo 169 (Japan)

(Received January 16, 1992; accepted March 3, 1992)

Abstract

The electrical conduction mechanism for the indium tin oxide (ITO)/polypyrrole (PPy)/ITO sandwich type of metal-insulator-metal element was investigated, where electroinactive PPy polymerized in aqueous NaOH solution was used as an insulator. The ITO/PPy/Au element demonstrated a non-linear $J-V$ response exactly the same as that of the ITO/PPy/ITO element, indicating that the carriers do not come from the interface but the bulk of an insulator. For the temperature dependence of the $J-V$ responses of the ITO/PPy/ITO element, Poole-Frenkel emission is confirmed to be a dominant conduction mechanism. The activation energy of PPy electropolymerized for 60 min was calculated to be 0.46 eV on the basis of Poole-Frenkel emission. The activation energy and the conductivity of the PPy film were dependent on polymerization time.

1. Introduction

In recent years the preparation and application of polymeric thin films have been extensively investigated in terms of mechanical, electric and electrochemical properties [1-5]. Among them, electropolymerization methods have attracted attention because of their simple preparation process and varying film characteristics depending on polymerization conditions. We have investigated the fabrication of metal-insulator-metal (MIM) devices using electropolymerized films as the insulator [6-9], and have already reported the non-linear current density-voltage $J-V$ responses of the indium tin oxide (ITO)/electroinactive polypyrrole (PPy)/ITO element, as shown in Fig. 1 [7, 8], on the basis of its possible use as a diode for an active matrix type of liquid crystal display [9].

The definition of conduction mechanisms of polymeric material is very important for basic research as well as its practical use. Some electrical conduction mechanisms in dielectrics at high fields have been suggested, namely tunnelling [10], space-charge-limited current (SCLC) [11], Schottky emission [12], and Poole-Frenkel emission [13]. In this paper we analyse and discuss the conduction mechanism of the MIM element using electroinactive PPy as an insulator, which gives non-linear $J-V$ properties as shown in Fig. 1.

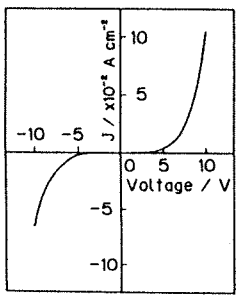

Fig. 1. $J-V$ response of an ITO/PPy/ITO element, where PPy is electropolymerized at 1.5 V (Ag/AgCl) for 60 min.

2. Experimental details

The fabrication process of the MIM elements and measurement of the $J-V$ responses were the same as previously reported [7, 8]. An aqueous solution containing 0.25 mol pyrrole dm^{-3} and 0.01 mol NaOH dm^{-3} was deaerated with argon gas. Electroinactive PPy films were electropolymerized at 1.5 V (Ag/AgCl) onto ITO (0.4 μm thick) glass substrates with various polymerization times. The MIM element's structure was an ITO/PPy/ITO or ITO/PPy/Au sandwich type. The upper ITO or gold (0.1 μm thick) electrode was prepared by a d.c. magnetron sputtering method. $J-V$ characteristics of MIM devices were measured in the range from 223 K to 283 K in a thermostat using a calibrated thermocouple which was set near the sample.

3. Results and discussion

Electrical conduction mechanisms of non-linear current density-voltage characteristics similar to those in

0040-6090/92/$5.00

Fig. 1 are usually suggested as "metal–polymer–interface limited" Schottky emission and "polymer-bulk-limited" Poole–Frenkel emission [14] or SCLC [15]. In order to determine the conduction mechanism for this element we fabricated an ITO/PPy/Au type of cell using the metal with a different work function as the upper electrode. Figure 2 shows the $J-V$ characteristics of the ITO/PPy/ITO and ITO/PPy/Au elements using PPy films electropolymerized for 60 min. The non-linear and symmetric $J-V$ responses are the same in both the symmetrical and the asymmetrical elements. Concerning the electrical conduction mechanism of the MIM devices, it is considered that polymer-bulk-limited current is predominant because the difference in the work function scarcely affects the responses.

When SCLC is dominant, one expects linearity on a plot of $\log J$ *vs.* $\log V$ with a slope of 2 [15]. The measured $J-V$ characteristics did not give the straight line and the slope of *ca.* 4 was rather larger than the value of 2. Thus the electrical conduction mechanism is not governed by the interface-limited current, but there is a significant possibility of bulk-limited Poole–Frenkel emission for an ITO/PPy/ITO element. In order to confirm the electrical conduction mechanism, we next examined the equation based on Poole–Frenkel emission [14]:

$$J/V = (J/V)_0 \exp[\beta_{PF}(V/d)^{1/2}/kT] \quad (1)$$

with

$$(J/V)_0 = en\mu d^{-1} \exp(-\phi/kT) \quad (2)$$

and

$$\beta_{PF} = (e^3/\pi\epsilon\epsilon_0)^{1/2} \quad (3)$$

where d, e, n, μ, and ϕ are the film thickness, the charge on an electron, the concentration of free carriers for an intrinsic material, the mobility and the energy difference between the emission site and the bottom of the conduction band respectively. $(J/V)_0$ is the extrapolated intercept of the linear relation of $\log(J/V)$ *vs.* $V^{1/2}$ plots. ϵ and ϵ_0 are the high frequency relative dielectric constant and the permitivity of free space respectively. Equation (1) is expressed as follows:

$$\log(J/V) = \log(J/V)_0 + (0.434\beta_{PF}d^{-1/2}/kT)V^{1/2} \quad (4)$$

For Poole–Frenkel emission, the logarithm of the conductivity varies linearly with the square root of the applied voltage. Moreover, the temperature dependence of the $(J/V)_0$ value can be obtained from the plots of $\log(J/V)_0$ *vs.* T^{-1} as follows from eqn. (2). Figure 3 shows the temperature dependence of the $\log(J/V)$ *vs.* $V^{1/2}$ relation for the typical ITO/PPy/ITO element when the electroinactive PPy formed by 60 min of electrolysis is used. In the range between 223 K and 303 K, the plots of $\log(J/V)$ *vs.* $V^{1/2}$ nearly give straight lines at applied voltages more than 1.0 V, and the current decreases with decreasing temperature. This indicates that the electrical conduction mechanism is related to the thermally emitted carriers. Furthermore, the relation between $(J/V)_0$ and the reciprocal T^{-1} of the temperature is plotted in Fig. 4, where the value of $(J/V)_0$ is the intercept in the $\log(J/V)$ *vs.* $V^{1/2}$ plots in Fig. 3. The plots in Fig. 4 exhibit excellent linearity in this temperature range. From the results of the linearity of both of the plots we confirm that Poole–Frenkel emission dominates the electrical conduction mechanism of ITO/electroinactive PPy/ITO elements. The activation energy ϕ of Poole–Frenkel emission can be estimated to be 0.46 eV from eqn. (2).

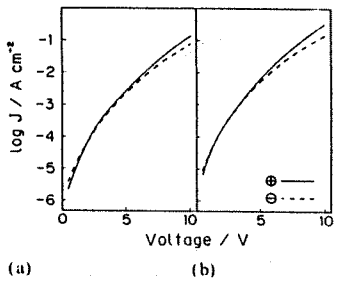

Fig. 2. $\log J-V$ characteristics of (a) ITO/PPy/ITO and (b) ITO/PPy/Au elements, where PPy is electropolymerized for 60 min.

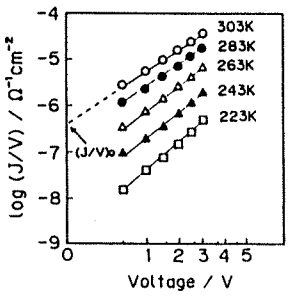

Fig. 3. The temperature dependence of $\log(J/V)$ – $V^{1/2}$ responses of a ITO/PPy/ITO elements. PPy is electropolymerized for 60 min.

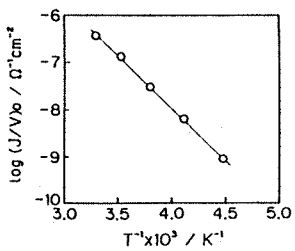

Fig. 4. The relationship between $\log(J/V)_0$ and T^{-1} for an ITO/PPy/ITO element. PPy is electropolymerized for 60 min.

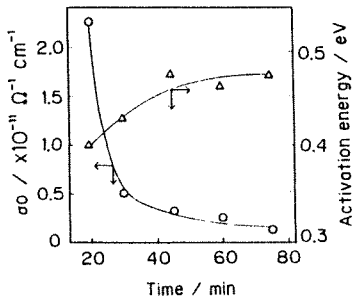

Fig. 5. The dependence of the conductivity and activation energy of the electroinactive PPy films on deposition time.

Next, we investigated the relation between film characteristics and deposition time of PPy on the basis of the Poole–Frenkel emission. The threshold voltage of the $J-V$ characteristics decreased with shortening deposition time as previously reported [8]. We assumed in the previous paper [8] that the change in threshold voltage is caused by the decrease in electric field with increasing film thickness and by the structural change of PPy degraded by an overoxidation reaction. In particular, the latter introduces carbonyl groups (–C–O) in PPy chains, which influences the band structure. Figure 5 exhibits the conductivity σ_0, calculated from $(J/V)_0$ at 283 K, and the activation energy ϕ against the deposition time. With increasing deposition time, the conductivity decreases and the activation energy rises. This indicates that the trap centres of PPy changed with deposition time. The electroinactive PPy is expected to be of low crystallinity because the carbonyl groups exist irregularly in the PPy chains and its absorption edge in the visible spectrum is not clear [8], similar to amorphous solids. Therefore, in the PPy film localized orbits may lie continuously below the non-localized band, similar to amorphous solids [16]. The band gap of conducting PPy is *ca.* 3.0 eV in the literature [17]; however, the activation energy of these non-conducting PPy films is obviously lower, less than 0.5 eV. Such a lower activation energy suggests that the non-conducting PPy possesses localizing trap centres and that the carriers of the Poole–Frenkel emission come from the localized orbits. Consequently, the decrease in the conductivity and the increase in the activation energy may be caused by broadening of the localized part with increasing deposition time.

4. Conclusions

The electrical conduction mechanism of the MIM element using an electropolymerized electroinactive PPy film is governed by Poole–Frenkel emission. The activation energy of PPy electropolymerized for 60 min was found to be 0.46 eV as determined by the temperature dependence of the $J-V$ characteristics. The conductivity and activation energy of PPy film varied with polymerization time, this being caused by the proceeding overoxidation reaction.

Acknowledgment

We would like to thank Miss K. Oike, Nippon Women's University, for her experimental support for this research.

References

1 M. Satoh, K. Kaneto and K. Yoshino, *Synth. Met.*, *14* (1986) 286.
2 B. F. Cvetko, M. P. Brungs, R. P. Burford and M. Skyllas-Kazacos, *J. Mater. Sci.*, *23* (1988) 2102.
3 G. Schiavon, S. Sitran and G. Zotti, *Synth. Met.*, *32* (1989) 209.
4 T. Osaka and K. Ueyama, *Denki Kagaku*, *57* (6) (1989) 572.
5 T. Osaka, K. Naoi and S. Ogano, *J. Electrochem. Soc.*, *135* (5) (1988) 1071.
6 T. Osaka, K. Ueyama and K. Ouchi, *Chem. Lett.*, (1989) 1543.
7 T. Osaka, K. Ouchi and T. Fukuda, *Chem. Lett.*, (1990) 1535.
8 T. Osaka, T. Fukuda, K. Ouchi and T. Nakajima, *Denki Kagaku*, *59* (12) (1991) 1019.
9 T. Nakajima, F. Matsushima, T. Fukuda and T. Osaka, *Denki Kagaku*, *59* (12) (1991) 1074.
10 B. Mann and H. Kuhn, *J. Appl. Phys.*, *42* (11) (1971) 4398.
11 A. K. Kalkar, S. Kundagol, S. Chand and S. Chandra, *Thin Solid Films*, *196* (1991) 361.
12 K. Suzuki, K. Matsumoto and S. Sakamoto, *J. Vac. Sci. Technol. B*, *7* (6) (1989) 2062.
13 C. A. Hogarth and M. Zor, *Phys. Status Solidi A*, *98* (1986) 611.
14 J. R. Yeargan and H. L. Taylor, *J. Appl. Phys.*, *39* (12) (1968) 5600.
15 D. R. Lamb, *Electrical Conduction Mechanisms in Thin Insulating Films*, Methuen, London, 1967.
16 N. F. Mott and E. A. Davis, *Electronic Processes in Non-Crystalline Materials*, Clarendon Press, Oxford, 2nd edn., 1979.
17 J. L. Bredas, J. C. Scott, K. Yakushi and G. B. Street, *Phys. Rev. B*, *30* (1983) 1023.

CHEMISTRY LETTERS, pp. 1787 1790, 1992.

Electroactivity Change of Electropolymerized Polypyrrole/ Polystyrenesulfonate Composite Film in Some Organic Electrolytes

Tetsuya OSAKA,* Toshiyuki MOMMA, and Ken NISHIMURA
Department of Applied Chemistry, School of Science and Engineering,
Waseda University, 3-4-1 Okubo, Shinjuku-ku, Tokyo 169

Electroactivity of polypyrrole/polystyrenesulfonate composite film obtained from an aqueous solution was examined in various organic electrolytes. The composite film worked like electroinactive film in electrolyte using propylene carbonate or some solvents except in the case of DMF or DMSO electrolytes, however, the film changed from electroinactive to electroactive even in propylene carbonate and some organic electrolytes after an electrochemical potential application to the film while in DMF or DMSO electrolytes.

In recent years, electropolymerized conducting polymers show promise for various kinds of applications, such as battery cathodes, electrocatalysts, etc.[1] Most electropolymerized conducting polymers are p-type materials which are oxidized or reduced through the insertion or removal of anion to compensate the film charges. Shimidzu *et al.* have indicated that the p-type polymer film with fixing polyanion works as an n-type polymer in appearance because cation penetrated from the electrolyte compensates the electroneutrality of the film.[2] When using this composite material as a cathode, the lithium secondary battery does not need a large volume electrolyte solution due to the fact that there is no change of electrolyte concentration during charging and discharging.[3]

Since metal salts of polyanion are usually able to dissolve only in aqueous electrolyte, not in organic ones, the polypyrrole composite film with polystyrenesulfonate (PPy/PSS) could be formed only from an aqueous solution containing pyrrole and poly(sodium 4-styrenesulfonate) by electro-oxidation onto a Pt substrate. For the purpose of applying the film to a lithium battery cathode, we have to use organic electrolytes with a process to exchange the electrolyte and remove the water solvated in the

film. The composite film showed good electroactivity in an aqueous electrolyte containing $LiClO_4$ as shown in Fig. 1a; however in the propylene carbonate (PC) electrolyte, the composite film became electro-inactive as shown in Fig. 1b.

On the contrary, in the organic electrolyte of 1.0 mol dm^{-3} $LiClO_4$ / dimethylfolmamide (DMF) electrolyte, the film showed high electroactivity after applying 2.0 V vs. Li/Li^+ potential to the film. When the 2.0 V was applied, cathodic current was observed initially, and it disappeared in a few seconds as shown in Fig. 2a. Figure 2b shows the cyclic voltammograms after 2.0 V application, where high-reversibly faradaic waves appear at around *ca.* 3.0 V vs. Li/Li^+. The reversible currents are attributed to the redox reactions of polypyrrole with ion doping-undoping in the composite film.

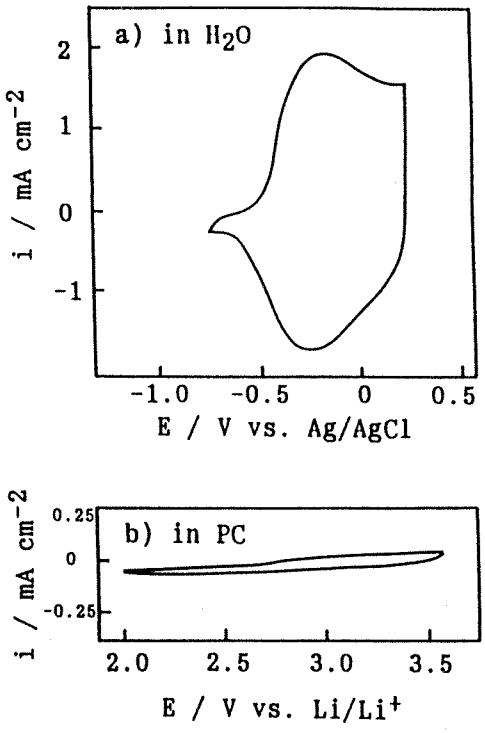

Fig. 1. Cyclic voltammograms of PPy/PSS composite films at 20 mV s^{-1}. Electrolytes were a) H_2O and b) PC containing 1.0 mol dm^{-3} $LiClO_4$. The films were prepared from 0.25 mol dm^{-3} pyrrole and 0.5 mol dm^{-3} SO_3^- unit of PSS-Na / H_2O at 0.75 V vs. Ag/AgCl with 0.5 C cm^{-2}.

Such a phenomenon is observed not only with the PPy/PSS composite film but also with small anion-doped polypyrrole film such as PPy/ClO_4^-, which is prepared from an aqueous solution containing pyrrole monomer and $LiClO_4$. In order to investigate the effect of such electrolyte solvents on the electroactivity of the PPy/PSS film, the electrochemical behavior of the PPy/PSS film obtained from an aqueous solution was examined in various organic electrolytes. Sulfolane (SL) (acceptor number AN=19.3), dimethylsulfoxide (DMSO) (donor number DN=29.8) and dimethylacetoamide (DMA) having physical properties similar to those of DMF (AN=16.0), were selected as electrolyte solvents. In the electrolytes using DMA and SL, the composite film showed electroinactivity, but in the DMSO electrolyte the film showed a particular phenomenon which is exhibited in Fig. 3a. The faradaic currents due to the reversible redox reaction of polypyrrole gradually grew

with potential cycling and reached a stable state as shown in the figure. In Fig. 3a, low cathodic current at the lower potential region under 2.5 V vs. Li/Li^+ decreases with cycling and finally disappears. At the same time the reversible redox currents of polypyrrole, at the potential of around 3.0 V, reach a stable state. In the cyclic voltammograms obtained in the DMF electrolyte a similar phenomenon occuring in the DMSO electrolyte was observed when the potential was cycled between 2.75 V and 3.55 V vs. Li/Li^+. Figure 3b shows a current-potential curve of Pt electrode in the DMSO electrolyte containing a small amount of H_2O, where the potential is scanned to a negative direction. In Fig. 3b, the cathodic current is observed in the potential range under 2.5 V vs. Li/Li^+ and usually the current does not appear in the DMSO electrolyte. Therefore the cathodic current observed under 2.5 V in Fig. 3a is assigned to the reduction of H_2O in the film. When considering the growth of polypyrrole electroactivity with the disappearing cathodic current, electroactivity of polypyrrole in the organic electrolytes may be enhanced by removing the solvated H_2O in the film where the active site is surrounded by an H_2O molecule. From these results, it is suggested that the DMSO electrolyte has an intermediate performance against PPy/PSS film between PC and DMF electrolytes.

Similar enlargement of redox

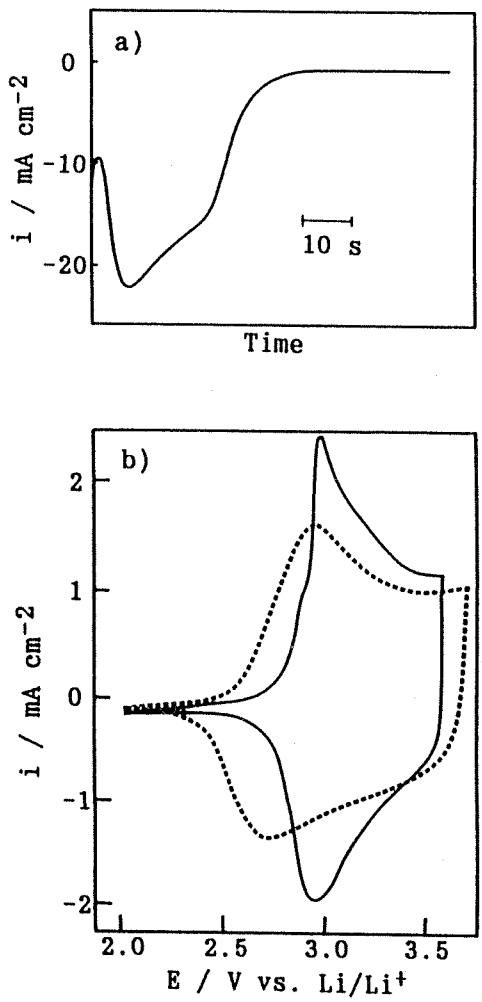

Fig. 2. a) Cathodic current change on PPy/PSS film while applying 2.0 V vs. Li/Li^+ in DMF electrolyte.
b) Cyclic voltammograms of PPy/PSS film at 20 mV s^{-1} in organic electrolyte containing 1.0 mol dm^{-3} $LiClO_4$. The solid and dotted lines are obtained in DMF and PC electrolytes, respectively. The composite films were formed at 0.55 V vs. Ag/AgCl with 0.5 C cm^{-2} from 0.1 mol dm^{-3} SO_3^- unit of PSS-Na polymerization solution.

currents in the cyclic voltammetry of polymer coated electrode, where redox active species is involved, was reported by Anson *et al.*[4] In such a case, the enhanced electroactivity of the thin film coated electrode was caused by increasing electroactive species penetrated. However in the case of polypyrrole, the electroactive species were located on the electrode substrate and only the environment of the electroactive sites could be altered.

In conclusion, the electroactivity of the PPy/PSS films deposited by aqueous solutions is electroinactive in PC electrolyte as-deposited state. After reducing H_2O, while applying cathodic potential in suitable organic electrolytes, the film shows good electroactivity. Such an electrochemical method of exchanging solvent in the film may be useful in the organic solution for the use of electropolymerized film obtained from an aqueous solution.

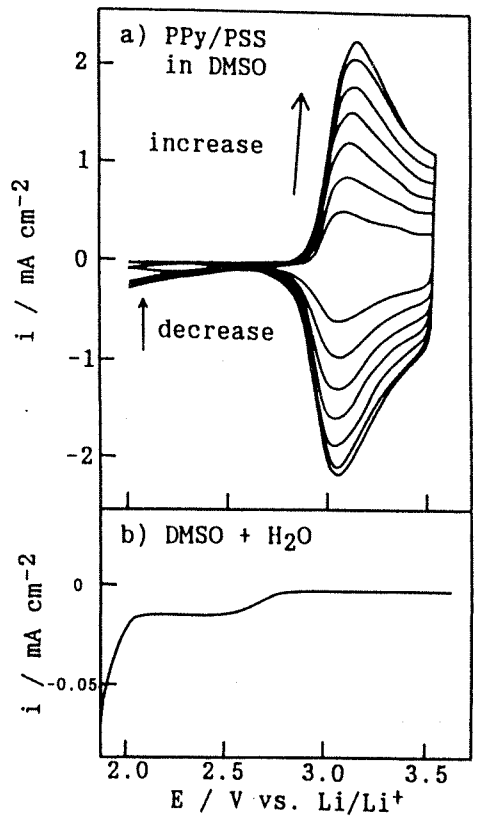

Fig. 3. a) Cyclic voltammograms of PPy/PSS composite film at 20 mV s^{-1} in DMSO electrolyte containing 1.0 mol dm^{-3} $LiClO_4$. The composite films were formed at 0.55 V vs. Ag/AgCl with 0.5 C cm^{-2} from 0.1 mol dm^{-3} SO_3^- unit of PSS-Na polymerization solution.
b) Current vs. potential curve of Pt at 10 mV s^{-1} in DMSO electrolyte with an addition of 1 v/o water.

References

1) T. Osaka, *Denki Kagaku*, 58, 218(1990).
2) T. Shimidzu, A. Ohtani, T. Iyoda, and K. Honda, *J. Electroanal. Chem.*, 224, 123(1987).
3) A. Shimizu, K. Yamataka, and M. Kohno, *Bull. Chem. Soc. Jpn.*, 61, 4401(1988).
4) K. Shigehara, N. Oyama, and F. C. Anson, *J. Am. Chem. Soc.*, 103, 2552(1981).

(Received June 18, 1992)